

Studies toward Developing Chemical Tools for  
Protein Arginine Methyltransferase 4 and 6

by

Lingyan Du

Department of Chemistry  
Duke University

Date: \_\_\_\_\_

Approved:

\_\_\_\_\_  
Qiu Wang, Supervisor

\_\_\_\_\_  
Michael C. Fitzgerald

\_\_\_\_\_  
Dewey G. McCafferty

Thesis submitted in partial fulfillment of  
the requirements for the degree of Master of Science  
in the Department of Chemistry  
in the Graduate School of Duke University

2019

ABSTRACT

Studies toward Developing Chemical Tools for  
Protein Arginine Methyltransferase 4 and 6

by

Lingyan Du

Department of Chemistry  
Duke University

Date: \_\_\_\_\_

Approved:

\_\_\_\_\_  
Qiu Wang, Supervisor

\_\_\_\_\_  
Michael C. Fitzgerald

\_\_\_\_\_  
Dewey G. McCafferty

An abstract of a thesis submitted in partial fulfillment of  
the requirements for the degree of Master of Science  
in the Department of Chemistry  
in the Graduate School of Duke University

2019

Copyright by  
Lingyan Du  
2019

## Abstract

The Protein Arginine Methyltransferases (PRMTs) are a family of proteins that play important roles in epigenetic modification of genes. They have been found to have crucial roles in various diseases, most notably in cancer. In order to probe their functions and potentials in cancer therapy, we have undertaken efforts to design and discover small-molecule compounds that specifically target PRMT4 and PRMT6. We have also developed a series of functional assays to assess the effects of potential lead compounds on enzymatic activities of PRMT4 and PRMT6 proteins.

We took a computation-facilitated *in silico* approach to identify small-molecule binders of PRMT4 and an empirical facilitated structure-based design for PRMT6. From these efforts, a few lead compounds have been identified for future studies.

We have established multiple-mode assays for characterizing small molecule's effects on enzymatic activities of PRMT4 and PRMT6, including biochemical activity assays, cellular activity assay, and downstream-gene regulatory assay. The reliability of all assays has been validated. However, further validation of the downstream gene assay for PRMT4 is needed.

Our efforts also involved the development of a fluorescence probe for fluorescence polarization (FP) assay of PRMT6.

# Contents

Abstract .....	iv
List of Schemes and Tables.....	viii
List of Figures .....	ix
Acknowledgements .....	xi
1. Introduction .....	1
1.1 Epigenetic Regulation of Chromatin Remodeling.....	1
1.1.1 Significance of Epigenetic Machinery.....	1
1.1.2 Epigenetic Modifying Enzymes and the Histone Codes .....	2
1.1.3 Epigenetic Modifiers as Anti-cancer Drug Targets .....	6
1.2 The Protein Arginine Methyltransferases (PRMTs) .....	7
1.2.1 Classification of PRMTs Based on Product Generated .....	7
1.2.2 Structure and Methylation Mechanism of PRMTs .....	8
1.2.3 Kinetic Mechanism of PRMTs .....	10
1.2.4 Substrate Scope and Biological Relevance of PRMTs.....	12
1.2.5 PRMTs as Potential Anti-cancer Therapeutic Targets.....	13
1.2.6 Development of PRMT Inhibitors.....	14
1.3 Research Objective of this Thesis .....	18
2. A CARM1 Inhibitor with Novel Structure from Computational Facilitated Structural Diversifying Virtual Screening.....	20
2.1 Introduction: Target of Interest – PRMT4 (CARM1).....	20
2.1.1 Biological Functions of CARM1 and its Relation to Diseases .....	20

2.1.2 Current Status of Small Molecule Inhibitor Development towards CARM1 ...	22
2.1.3 The Work of This Thesis towards Design and Development of Cellular Active CARM1 Small-molecule Inhibitors .....	26
2.2 Establishment and Validation of Multiple-mode Assays for Characterization of CARM1 Inhibitors .....	27
2.2.1 Validation of CARM1 <i>in vitro</i> Biochemical Assay .....	27
2.2.2 Expression and Purification of Human CARM1-FALG with Mammalian cell 293T and Determination of its Enzymatic Activity .....	29
2.2.3 Development and Validation of Direct Cellular Assay for CARM1 Enzymatic Activity.....	31
2.2.4 Attempts to Develop Cell-based Assays for CARM1 Downstream Effect.....	34
2.3 Design Rationales of CARM1 Inhibitors, Computational Facilitated Structural Diversification and <i>in silico</i> Screening, Empirical Structural Optimization.....	40
2.4 Conclusions and Future Plans .....	48
3. Potential PRMT6 Small Molecule Regulators Targeting SAM-substrate Bi-pockets ....	49
3.1 Introduction: Target of Interest – PRMT6.....	49
3.1.1 Biological Functions of PRMT6 and its Relation to Diseases .....	49
3.1.2 Current Gap on Small Molecule Inhibitor Development towards PRMT6 and the Work of This Thesis .....	51
3.2 Establishment and Validation of Multiple-mode Assays for Characterization of PRMT6 Inhibitors .....	53
3.2.1 Validation of PRMT6 <i>in vitro</i> Biochemical Assay .....	53
3.2.2 Expression and Purification of Human PRMT6-His with Insect Cell Sf9 and Determination of its Enzymatic Activity .....	55
3.2.3 Development and Validation of Direct PRMT6 Enzymatic Activity Cellular Assay and Downstream Gene Regulatory Effect Assay .....	57

3.3 Design Rationales of Potential PRMT6 Small Molecule Regulator Targeting SAM-substrate Bi-pockets .....	61
3.4 Conclusions and Future Plans .....	63
4. Design of a Small Molecule Fluorescence Polarization (FP) Probe for Quantitative Analysis of PRMT6 .....	65
4.1 Introduction: Fluorescence Polarization, Basic Principle and Current Applications in Drug Discovery .....	65
4.1.1 Fluorescence Polarization Assay is a Good Tool for Assessing Macromolecule–small Molecule Interaction.....	65
4.1.2 Considerations in Development of FP assay: Strengths and Drawbacks.....	67
4.1.3 Application of FP in Drug Discovery .....	69
4.1.4 Emerging Applications of FP in Epigenetic Field: Meeting the Unmet Needs	70
4.2 FP Probe Design and Synthesis .....	73
4.3 Optimization of Experimental Conditions for FP Assay by Quantitative Analysis of PRMT6 Binding .....	74
4.3.1 Inhibitory Effect of Fluoro-tagged Probe against PRMT6 in Biochemical Assay .....	74
4.3.2 ITC Determination of PRMT6 and Fluoro-tagged Probe Binding Affinity.....	75
4.3.3 FP Binding Assay for PRMT6 .....	77
4.4 Conclusions and Future Plans .....	78
5. Conclusions.....	79
Appendix A.....	80
References .....	85

## List of Schemes and Tables

Scheme 1.1: Biological reaction catalyzed by PRMTs. PRMTs can be classified into Type I, II and III based on the product they generated.....	8.
Scheme 1.2: Proposed methylation mechanism for PRMT1. ....	10.
Table 1.1: Representative substrates of PRMTs.....	12.

## List of Figures

Figure 1.1: Epigenetic machinery ‘writer’, ‘eraser’ and ‘reader’ integrally regulate transcription by chromatin remodeling.....	2.
Figure 1.2: Representative post-translational modifications on histone tails.....	4.
Figure 1.3: Conserved domains in PRMTs structure .....	9.
Figure 1.4: Selective small molecule inhibitors towards PRMT family members .....	17.
Figure 2.1: Substrates and biological functions of CARM1.....	21.
Figure 2.2: Current selective inhibitors towards CARM1.....	23.
Figure 2.3: Biochemical validation of CARM1 methyltransferase activity.....	28.
Figure 2.4: Expression, purification and activity determination of recombinant FLAG-CARM1 protein.....	30.
Figure 2.5: Cellular CARM1 methyltransferase activity assay establishment with substrate PABP1.....	33.
Figure 2.6: PSA-luc assay establishment in LNCaP cells.....	35
Figure 2.7: A representative qPCR result for the randomness of the Wnt3A CM activation of downstream gene levels in RKO cells .....	38.
Figure 2.8: A representative qPCR result for the no co-relation between CARM1 knockdown and RAR $\beta$ 2 gene down regulation.....	40.
Figure 2.9: ASCESS Algorithm Flowchart (adapted from ref <sup>118</sup> ) and Docking/MMGBSA/Molecular Dynamic Scoring Flowchart.....	41.
Figure 2.10: Selective SAM mimics (BI compounds) with different level of CARM1 inhibitory effect in benchmarking of CARM1 computational model.....	44.
Figure 2.11: CARM1 small molecule binder <i>in silico</i> screening and structural optimization generated 14-compound library for future synthesis .....	47.

Figure 3.1: Substrates and biological functions of PRMT6.....	50
Figure 3.2: Current Type I PRMTs inhibitors with the display of IC <sub>50</sub> towards PRMT6.....	51
Figure 3.3: Biochemical validation of PRMT6 methyltransferase activity.....	54
Figure 3.4: Expression, purification and activity determination of recombinant His-PRMT6 protein.....	56
Figure 3.5: Description of p21 downstream effect assay reporting PRMT6 cellular function.....	58
Figure 3.6: Cellular PRMT6 direct activity assay establishment with H3R2.....	59
Figure 3.7: PRMT6 downstream gene regulatory assay establishment with p21 mRNA.....	60
Figure 3.8: PRMT6 empirical designed benchmarking controls, bisubstrate binders and literature reference compounds.....	63.
Figure 4.1: Description of fluorescence polarization binding small fluorophores that change polarization between bound and unbound status.....	67.
Figure 4.2: The design of PRMT6 FP probe.....	74.
Figure 4.3: IC <sub>50</sub> of MS023 and derivatives with PRMT6.....	75.
Figure 4.4: Determination of affinity constant (K <sub>d</sub> ) between PRMT6/MS023 and PRMT6/MS023-CC-F with ITC titration.....	76.
Figure 4.5: Optimization of binding conditions for MS023-CC-F and PRMT6 in FP assay format.....	77.

## Acknowledgements

First of all, I would like to express my heartfelt gratitude to my advisor, Dr. Qiu Wang for her great guidance, care and support through the years of my graduate study, which has led me in the right direction and inspired me to overcome difficult hurdles. I would like to thank my thesis committee members, Dr. Michael C. Fitzgerald and Dr. Dewey G. McCafferty for their kindly guiding me through this process and providing invaluable discussions and feedbacks.

I would have to also thank my fantastic lab members, fellow graduate students and church friends for their generous support, love and friendship, which has become an integral part of my graduate life.

Most importantly, I would like to thank my beloved family members, especially my parents, my grandma, aunts, uncles, and cousins. I will not be able to achieve this without their love, support and constant encouragement over the years and through my hard times.

And last but not least, may all the glories be to my Father in Heaven, for all these hills and valleys You have walked me through were all out of your blessings.

# 1. Introduction

A wide variety of human diseases that are traditionally seen as a genetic disease, which is caused by alteration or mutation of the gene sequence, are found to be associated with epigenetic abnormalities. Furthermore, epigenetic aberrations are nowadays considered as hallmarks for many of those diseases, including cancers, inflammatory diseases, and neurodegenerative diseases, to name a few.<sup>1</sup> This thesis aims at discovering small-molecule tool compounds targeting a subfamily of epigenetic modifiers, protein arginine methyltransferases (PRMTs), for better understanding of their unique biological functions and their roles in diseases and potential therapy development.

## ***1.1 Epigenetic Regulation of Chromatin Remodeling***

### **1.1.1 Significance of Epigenetic Machinery**

Epigenetics is the study of regulation of gene expression by EPI-genetic (epi-, above or upon, referred to post-transcriptional/translational) modifications rather than alteration of the genetic sequence itself. While genetic mutations are considered permanent, epigenetic changes may be reversible, however, inheritable under certain circumstances.<sup>2</sup> The concept of 'epigenotype' was first introduced by Waddington<sup>3</sup> in 1942 describing the gap between genotype and phenotype, however did not attract enough attention until the 21<sup>st</sup> century, when a variety of diseases were found not related to alterations of gene sequence but rather associated with stable alterations in

gene expression. This inheritable stable alteration in gene expression, now known as epigenetic regulations, is achieved by numerous kinds of covalent modifications on DNA, RNA or histones, catalyzed and recognized by the epigenetic family members, resulting in the high plasticity of transcriptional activation or repression.

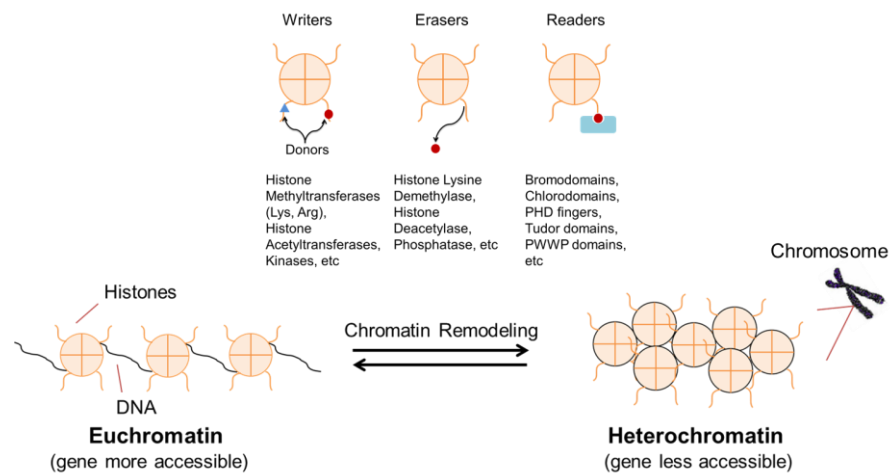


**Figure 1.1: Epigenetic machinery ‘writer’, ‘eraser’ and ‘reader’ integrally regulate transcription by chromatin remodeling**

The influence of epigenetic regulation on gene transcription leads to cellular reprogramming which may be caused by environmental changes, diseases or early life experiences, and can be passed on to decedents. Therefore, epigenetic members have become the emerging targets for cancers, inflammatory diseases, viral infections and cardiovascular diseases drug development in the past two decades.<sup>4</sup>

### 1.1.2 Epigenetic Modifying Enzymes and the Histone Codes

The dynamic of epigenetic modifications is much more rapid than genetic alterations and is under a complex regulation mechanism of epigenetic “writer”,

“eraser” and “reader” (Figure 1.1).<sup>5</sup> The “writers” are enzymes catalyzing the appending of a marker to their substrate, such as DNA methyltransferases (DNMTs), protein lysine methyltransferases (PKMTs), protein arginine methyltransferases (PRMTs), protein arginine deiminases (PADs, catalyzing the citrullination of arginine residues) and histone acetyltransferases (HATs). The “erasers” are enzymes that remove the markers appended by the “writers”, including lysine (K)-specific demethylase (KDMs), histone deacetylases (HDACs). The “readers” are proteins that recognize and bind to the markers and trigger responses resulting in transcriptional activation or repression.<sup>6</sup> The major substrates that are associated with gene regulations resulting from epigenetic modifications are DNA, RNA, RNA-binding proteins and histones.<sup>4</sup>

Cellular DNA is stored in the form of chromosome, which is packed by 147 base pairs of DNA wrapped around a histone octamer consisting of the duplicate of four core histones H2A, H2B, H3 and H4 and connected by linker histone H1.<sup>7</sup> Direct modifications on DNA, mostly identified as DNA methylation by DNA methyltransferases (DNMTs) on cytosine’s 5-position, largely results in transcriptional silencing.<sup>8</sup> Recent studies revealed that RNA can also be methylated on adenosine’s N<sup>6</sup>. However, the modifiers and consequences still remain unknown.<sup>9</sup> The most abundant epigenetic modification occurs on the “tail” regions on histones that linger on the octamers. The markers generated or removed by the epigenetic modifiers, “writers” and “erasers”, on the four core histones’ tail can influence the chromatin remodeling

between heterochromatin (DNA tightly bound region) and euchromatin (DNA loosely bound region), therefore resulting in the genes in the less or more accessible form and regulation of transcription (Figure 1.1). The delicate pattern of histone post translational modification (Figure 1.2) is now referred as “the histone code”<sup>10</sup> which contains more than 60 different kinds of modulations, including methylation, acetylation, phosphorylation, citrullination, sumoylation, ubiquitination, etc..<sup>11</sup>

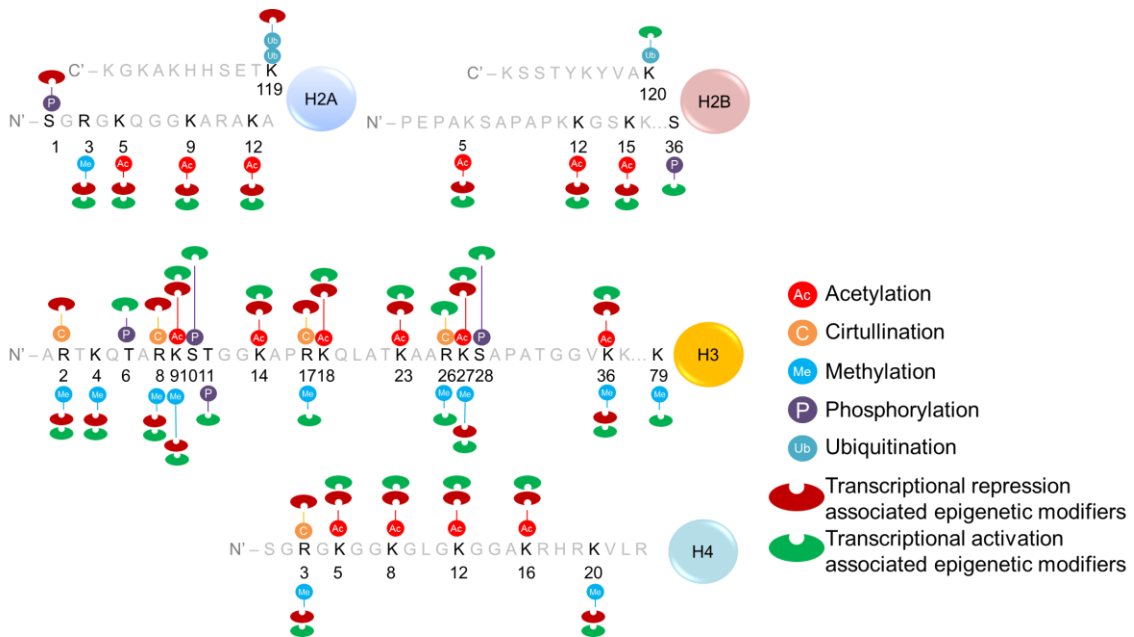


**Figure 1.2: Representative post-translational modifications on histone tails**

Post-translational modifications on arginine (R), lysine (K), serine (S) and threonine (T) are shown with selected respective modifying enzymes. Note that the transcriptional activation or repression modifying enzymes indicated may be multiples. Based on data from uniprot.org for Homo Sapiens H2A (P04908), H2B (P62807), H3 (P68431) and H4 (P62805) ; December 2017 and a summary by Huynh *et al*<sup>12</sup>.

Among the histone codes, the most well-studied and most abundant modifications are acetylation and methylation.<sup>5</sup> The acetylation only occurs on the lysine (K) residues and is catalyzed by histone acetyltransferases (HATs) with acetyl-CoA as

the acetyl-donor.<sup>5</sup> The histone deacetylases (HDACs) catalyze the reversion of this process. The acetyl group neutralizes the positive charge on lysine residue and therefore may affect histone-DNA interaction. The functional outcome of HATs usually results in transcriptional activation and that of HDACs results in transcriptional repression,<sup>12</sup> which is highly cell-type specific, indicating their intrinsic roles in dynamic regulation of gene expression.

Histone methylation presents a more complex regulation process with various functional outputs, associated with the different amino acid substrates as well as the number and the pattern of methyl groups added. Comparing to acetylation, methylation is more site-specific and more stable. The methyl marker, donated by *S*-adenosylmethionine (SAM), can be added to lysine (K) and arginine (R) residues of histone tails. Methylation upon lysine or arginine would not change the overall charge and can lead to either transcriptional activation or repression. Protein lysine methyltransferases (PKMTs) and lysine (K)-specific demethylase (KDMs) lysine (K)-specific demethylase (KDMs) work cooperatively to control the lysine methylation status, ranging from unmethylated, to mono-, di- and tri- methylated. The PKMT family is the current largest family among epigenetic regulators with more than 50 members identified, which mostly shared a SET-domain except one outlier, DOT1L.<sup>13</sup> Compared to PKMT family, the PRMT family is rather small with nine PRMTs which can catalyze the mono-, asymmetrical di- and symmetrical di-methylation on arginine residues. To date, there is

no demethylation enzyme identified for methylated arginine, however, protein arginine deiminases (PADs) somehow antagonize PRMTs' activity by transforming arginine into citrulline.<sup>14</sup>

### **1.1.3 Epigenetic Modifiers as Anti-cancer Drug Targets**

Due to the intrinsic regulatory roles in gene transcription, dysregulation of epigenetic functionalities have become a well-recognized hall mark for cancerous cells.<sup>15</sup> This reversible nature of epigenetic changes has led to great opportunities for the development of therapeutic strategies targeting chromatin-modifying enzymes. The FDA has approved the histone deacetylases (HDACs) inhibitor Vorinostat for treatment of cutaneous T-cell lymphoma, and the DNA methyltransferases (DNMTs) inhibitors 5-azacitidine and Decitabine for treatment of myelodysplastic syndrome (MDS).<sup>1</sup> PKMTs and KDMs, as the second generation of anti-cancer epigenetic targets, also attracted great attention in drug development with several candidates in clinic trials: 1) Pinometostat, a DOT1L (PKMT family member) selective inhibitor entering phase I clinical trial for rearranged MLL gene bearing relapsed/refractory leukemias; 2) CPI-1205, a EZH2 (PKMT family member) inhibitor in phase I clinical trial for B cell lymphomas, and 3) four inhibitors of LSD1 (KDM family member) in clinical trials for acute myeloid leukemia or small-cell lung cancer.<sup>13</sup>

The expansion capacity of epigenetic modifiers as potential anti-cancer therapeutics remains huge and in this work PRMTs is chosen as primary targets as they

play an indispensable role in regulation of gene regulation and possess significant diseases relevance, though far less extensively studied comparing to DNMTs, HDACs, PKMTs and KMDs. Detailed review on PRMTs is elaborated in section 1.2.

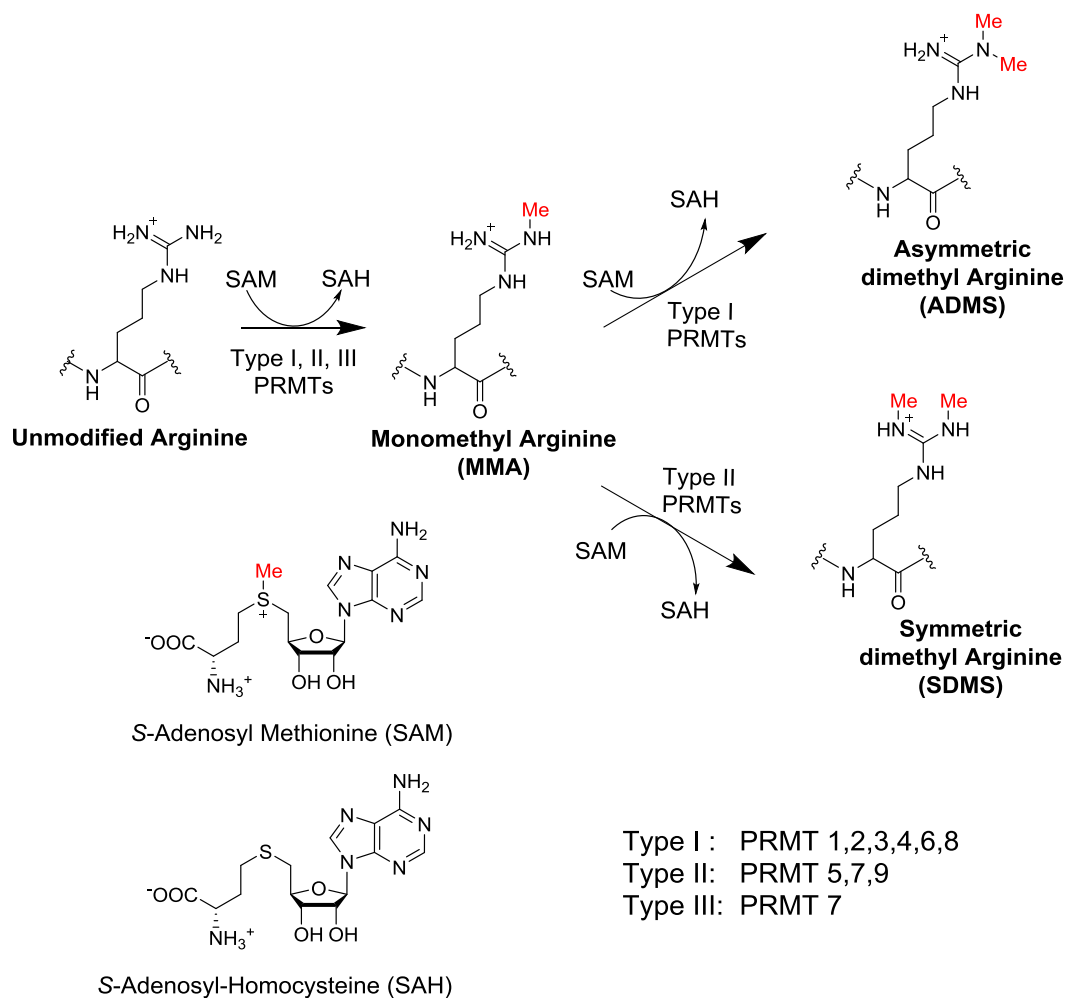
## **1.2 The Protein Arginine Methyltransferases (PRMTs)**

Post-translational methylation on arginine residues is a ubiquitous marker in eukaryotic cells which impact numerous crucial cellular processes such as gene regulation, RNA processing, DNA repair and nuclear receptor mediated signaling by methylating their histones and non-histone substrates.<sup>16</sup>

### **1.2.1 Classification of PRMTs Based on Product Generated**

In humans, there are 9 family members of PRMTs have been identified so far and chemogenetic analysis indicated up to 44 PRMTs existed in human proteome.<sup>17</sup> By transferring the methyl group from the biological methyl-donor *S*-adenosyl-methionine (SAM) to their protein/peptide substrate generating methylated product and by product *S*-adenosyl-*L*-homocysteine (SAH), PRMTs can be classified to three types based on the product they generate (Scheme 1.1). Type I PRMTs includes PRMT 1, 2, 3, 4, 6 and 8, all of which catalyze the formation of asymmetric  $N^{\omega},N'^{\omega}$ -dimethyl Arginine (ADMS); Type II PRMTs includes PRMT 5, 7 and 9 generating the symmetric  $N^{\omega},N'^{\omega}$ -dimethyl arginine (SDMS) and Type III PRMT only include PRMT 7, generating the  $N^{\omega}$ -monomethyl arginine.

**Scheme 1.1: Biological reaction catalyzed by PRMTs. PRMTs can be classified into Type I, II and III based on the product they generated**



### 1.2.2 Structure and Methylation Mechanism of PRMTs

In the past decades, great efforts have been dedicated to understanding the structural information of PRMTs. So far, X-ray crystal structures are available for 8 members of PRMTs except PRMT9.<sup>18-26</sup> The PRMTs all contain conserved core region consisted with a Rossmann fold harboring the SAM-binding site and a  $\beta$ -barrel

important for substrate binding (Figure 1.3). Six PRMTs contain a dimerization arm and an  $\alpha$ -helix which may also facilitate the SAM and substrate binding.

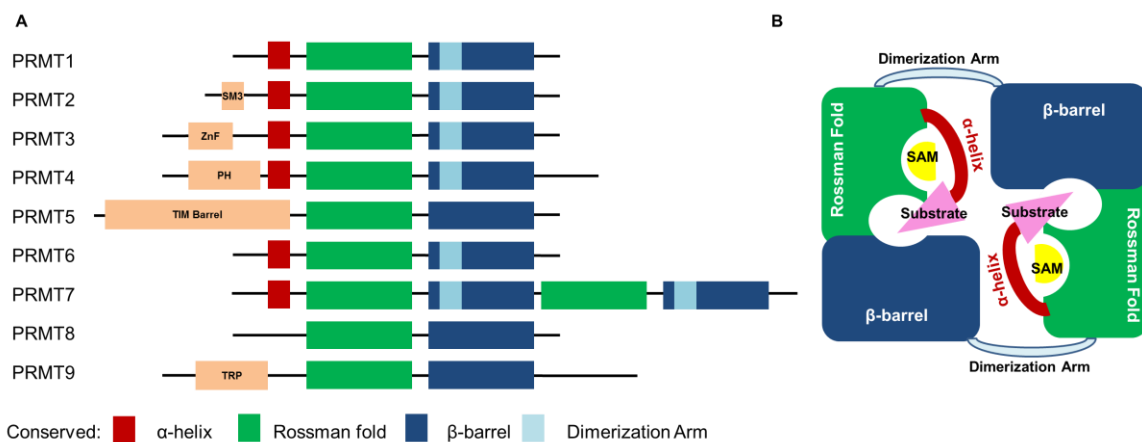
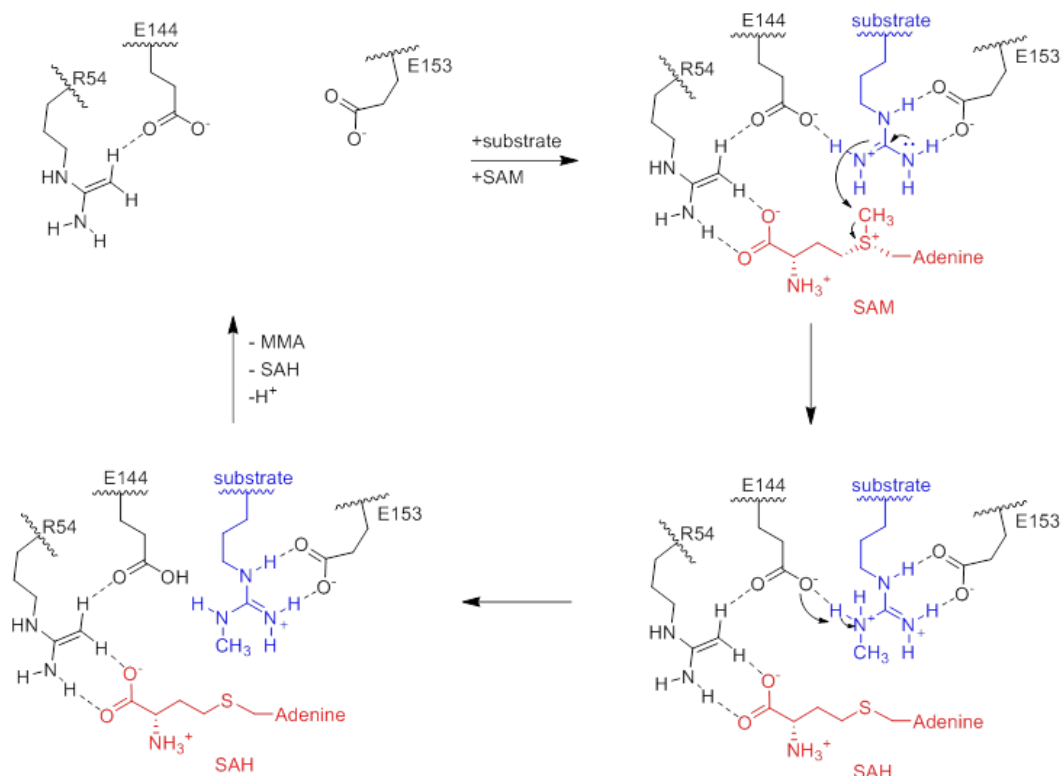


**Figure 1.3: Conserved domains in PRMTs structure**

(A) The SAM-binding site harboring Rossmann fold and substrate loop containing  $\beta$ -barrel is conserved among all PRMTs and many PRMTs contain  $\alpha$ -helix and dimerization arm. (B) Type I PRMT folding cartoon. Adapted from Schapira *et al* <sup>21</sup>.

Within the Rossmann fold, a “double E-loop” consisted by two conserved glutamic acid (E) (i.e. E144 and E153 in PRMT1;<sup>20</sup> E257 and E266 in PRMT4;<sup>27</sup> E155 and E164 in PRMT6 <sup>28</sup>) is crucial for the arginine containing substrate aligning to the proper orientation in order to make the  $S_N2$  attack to the methyl group on SAM. Another conserved arginine (R) group (i.e. R54 in PRMT1, R169 in PRMT4, R66 in PRMT6) is in charge of SAM binding through H-bonding interaction with the carboxylic acid group of the amino acid moiety within the SAM structure. The methylation mechanism of PRMT1 has been proposed by two individual labs in the same way by either theoretical calculation <sup>29</sup> or mutagenesis studies <sup>30</sup>. List below (Scheme 1.2) is the proposed PRMT1 catalytical mechanism as a representative for the PRMT family.

**Scheme 1.2: Proposed methylation mechanism for PRMT1**  
 Conserved double-E loop and R residues were shown. Adapted from  
 Zhang *et al* <sup>29</sup> and Heather *et al* <sup>30</sup>.



### 1.2.3 Kinetic Mechanism of PRMTs

The kinetic mechanism studies towards PRMTs have been performed with PRMT1 <sup>31</sup>, PRMT5 <sup>32</sup> and PRMT6 <sup>33</sup>. Due to the nature of generating di-methylated product, the substrate and co-factor binding mechanism for producing the MMA product is either sequential ordered or rapid equilibrium random ordered, and the mechanism for producing the ADMA/SDMA product is either distributive (releasing of MMA product before rebinding) or processive (non-releasing of MMA product).

The current kinetic studies on PRMT1, 5 and 6 with dead-end analogue inhibition all suggested that the formation of MMA products possessed a rapid equilibrium random ordered mechanism.<sup>31-33</sup> However, a crystallography study with CARM1 indicated that upon SAM binding, a conformational change occurred to the catalytic site leading to stabilization of the conserved  $\alpha$ -helix<sup>34</sup> suggesting that sequential ordered mechanism may also be possible and the random ordered mechanism may not apply to all members in PRMT family.

The kinetic mechanism for the second methyltransfer reaction was only reported with PRMT1 and PRMT5.<sup>31,32,35</sup> The formation of SDMA catalyzed by PRMT5 (*C. elegans*) was found to be distributive while the formation of ADMA catalyzed by PRMT1 (human) was suggested to be partially processive. A distributive mechanism will result in the accumulation of MMA product due to product release and a processive mechanism will obligatorily generate DMA product. In the case of PRMT1, the partially processive mechanism was caused by the MMA product may or may not be released due to the random ordered release of products from the first step. This result was confirmed with the measurement of catalytic efficiency (defined by  $k_{cat}/K_m$ ) of PRMT1 towards several histone and non-histone peptide substrates that MMA peptides possess increased efficacy compared to non-methylated peptide, however the degree varied between different peptide substrates.<sup>35</sup>

## 1.2.4 Substrate Scope and Biological Relevance of PRMTs

The fine-tuned catalytic sites of PRMTs resulted in high substrate selectivity. Although certain histone markers can be modulated by several PRMTs *in vitro*, the PRMTs are likely to have distinct functions and substrates *in vivo* and cannot be replaced by other family members.<sup>36</sup> Although PRMT1 and PRMT5 are the major producers of cellular ADMA and SDMA, the knockout of PRMT4, 6, or 8 would also be either embryonically or postnatally lethal, indicating their indispensable roles in development.<sup>36-38</sup>

**Table 1.1: Representative substrates of PRMTs**  
The substrate scope of PRMTs reveals their major biological relevance.  
Information summarized from Wei *et al* <sup>39</sup>.

PRMT (Type)	Histone Substrate	Non-histone Substrate			
	(Epigenetic control of transcription)	RNA Metabolism and Splicing	DNA repair and Apoptosis	Transcription Factors	Signal Transduction Components
PRMT1 (I)	H4R3 (activation)	SAM68, SPT5, TAF15	MRE11, 53BP1	PGC1 $\alpha$	ER $\alpha$ , IFN $\alpha/\beta$
PRMT2 (I)	H3R8				ER $\alpha$
PRMT3 (I)		RPS2	p53		
PRMT4 (I)	H3R17 (activation), H3R26	RNA Pol II CTD, PABP1		CBP/p300, SRC3	
PRMT5 (II)	H4R3 (repression)	Sm D1/3	p53, RAD9	E2F1	EGFR
PRMT6 (I)	H3R2 (repression), H2AR29	HMGA1a	DNA Pol $\beta$		PRMT6
PRMT7 (II/III)	H4R3, H2AR3, H3R2				
PRMT8 (I)	H2A , H4			MBP (CNS-specific)	PRMT8
PRMT9 (II)		SAP145			

Most of the PRMTs possess histone substrates and have been confirmed to have the function of controlling gene transcription (Table 1.1).<sup>39</sup> PRMTs are often found as crucial components in the complexes of transcription factors, which may complicate their effects on gene transcription upon methylation. Moreover, the PRMTs also methylate a broad scope of non-histone substrate including RNA binding or slicing

factors, ribonucleic proteins, DNA repair complexes components, transcription regulators and signal transducers.<sup>39</sup> By methylating the diverse range of substrate, PRMTs demonstrate their versatility and significance in biological relevance. Except the aforementioned commonly identified substrates, certain PRMTs possess unique substrates and demonstrate vital functionalities in related biological pathways, e.g., the methylation of PRMT6 towards HIV Tat protein results in restriction of HIV production in cellular assays.<sup>40</sup>

The scope of the substrate and biological relevance of PRMTs is still expanding. Therefore, chemical tool compounds selectively targeting PRMTs are greatly desired for the understanding of the biological functions of PRMTs under different circumstances.

### **1.2.5 PRMTs as Potential Anti-cancer Therapeutic Targets**

Due to the significant involvement in numerous oncogenic related biological pathways, PRMTs' dysregulation of PRMTs has been found to be associated with numerous cancers.<sup>41</sup> Overexpression of PRMT1,<sup>42</sup> 2,<sup>43</sup> 3,<sup>44,45</sup> 4,<sup>46</sup> 6,<sup>47</sup> 7<sup>48</sup> have been indicated in breast cancer, which may contribute to aberrant expression of estrogen receptors (ER). Another type of hormone sensitive cancer, prostate cancer, has been well documented to be associated with overexpression of PRMT1<sup>49</sup>, 4<sup>50-52</sup> and 6<sup>53</sup>, which may be involved in regulation of gene expression of androgen receptors. PRMT1,<sup>54</sup> and 4<sup>55</sup> are associated with colorectal cancer through Wnt/ $\beta$ -catenin signaling pathway, while PRMT5 is involved in colorectal cancer by direct methylation of several oncogenes.<sup>56</sup> Lung cancer

has been reported to be related to overexpression of PRMT1,<sup>57</sup> 4,<sup>58</sup> 5<sup>59</sup> and 6<sup>57</sup>. Leukemia is associated with PRMT1<sup>60,61</sup> and 5<sup>62,63</sup>, bladder cancer is associated with PRMT1 and 6<sup>57</sup>, and lymphoma is exclusively associated with PRMT5<sup>63,64</sup>.

Therefore, development of chemical tools selectively targeting individual PRMTs is of great importance for further understanding of the roles PRMTs in cancer development, and selective PRMT inhibitors may serve as good candidates for potential anti-cancer therapies.

### **1.2.6 Development of PRMT Inhibitors**

For almost two decades, tremendous efforts have been spent in development of small molecule compounds targeting PRMTs for (Figure 1.4). To date, small-molecule inhibitors for PRMT1, PRMT3, PRMT4 and PRMT5 have been reported to have fairly adequate selectivity, while inhibitors for PRMT6, PRMT7 and PRMT8 were not very selective, with cross-reaction with other members in the PRMT family.<sup>65</sup> No small molecule probes for PRMT2 or 9 have been identified due to lack of specific substrates.<sup>23</sup>

In the work of this thesis, PRMT4 and PRMT6 has been chosen as the targets of interest and the small molecule inhibitor review for these two enzymes can be found in the corresponding chapters. In this section, small molecule inhibitor discovery towards the other PRMTs is summarized and can be categorized into pan-inhibitors, specific inhibitors and bi-substrate inhibitors. The approaches towards PRMTs inhibitor discovery include computational facilitated *in silico* screening, *in vitro* compound library

screening, rational design/improvement based on structure of previous inhibitors and crystal structure of the enzymes.<sup>65</sup>

The inhibition of PRMTs can be tracked back to the development of pan-methyltransferase-inhibition probes, which usually were designed as SAM mimics. Sinefungin (SFG, **1.1**) a structural mimic of SAM is the most widely used pan-methyltransferase inhibitor and is a naturally occurring antibiotic originally found within *Streptomyces* species.<sup>66</sup> The cellular application of SFG is limited due to the inhibition of all SAM utilizing enzymes, but SFG has been widely used in co-crystallization studies.<sup>21</sup> A non-structurally-alike SAM mimic pan-methyltransferase inhibitor BIX-01338 (**1.2**)<sup>67</sup> was reported in 2010 from a screening of PKMT inhibitors. More recently, MS023 (**1.3**),<sup>28</sup> which contains the diamine moiety mimicking the arginine residue within the substrate, has been reported as a potent Type I PRMT inhibitor from the rational design approach based on previous inhibitors from large scale screening, as well as a fragment inhibitor **1.4**<sup>68</sup> harboring the similar pharmacophore from a fragment-based screening. The same group also reported a Type II PRMT inhibitor, DS437 (**1.5**)<sup>69</sup> from a PRMT5 crystal structure-based design which a urea containing group substituted the amino acid side chain of SAH. The aforementioned three inhibitors were all reported with cellular activities by reducing the corresponding endogenous histone tail site-specific arginine methylation levels.

AMI-1 (**1.6**)<sup>70</sup>, the first selective inhibitor towards PRMT1, reported in 2004, inhibits cellular PRMT1 activities and is still the most widely used PRMT1 chemical probe. It was later determined that the selectivity resulted from the binding of histone substrate rather than PRMT1.<sup>71</sup> Much further effort has been dedicated to developing selective PRMT1 inhibitors. Many symmetric dye-like compounds, inspired by the structures of AMI series, were reported. However none achieved significant higher potency or better selectivity than AIM-I (**1.6**).<sup>72-77</sup> A virtual screening approach toward PRMT1 inhibitor discovery was later undertaken, yielding novel structures which potentially have some selectivity over other Type I PRMTs and show inhibition on cancer cell lines proliferation effects.<sup>78</sup>

The only allosteric inhibitor reported towards PRMT is SGC707 (**1.7**) which is highly selective for PRMT3, due to the binding at the dimerizing interface, and is potent *in vitro* and under cellular condition.<sup>18</sup> The study towards developing PRMT5 selective inhibitor is boosted by the successful expression of PRMT5:MEP50 complex, of which MEP50 is the regulator of PRMT5 and is important for maintaining PRMT5 *in vitro* activity.<sup>24</sup> A potent and selective PRMT5 inhibitor over other PRMTs and 14 selective PKMTs, EPZ015666 (**1.8**)<sup>79</sup> was yielded from a screening of a library containing 370,000 compounds and further SAR improvement, which presented promising *in vivo* anti-tumor activity in mantle cell lymphoma (MCL) xenograph mouse model.

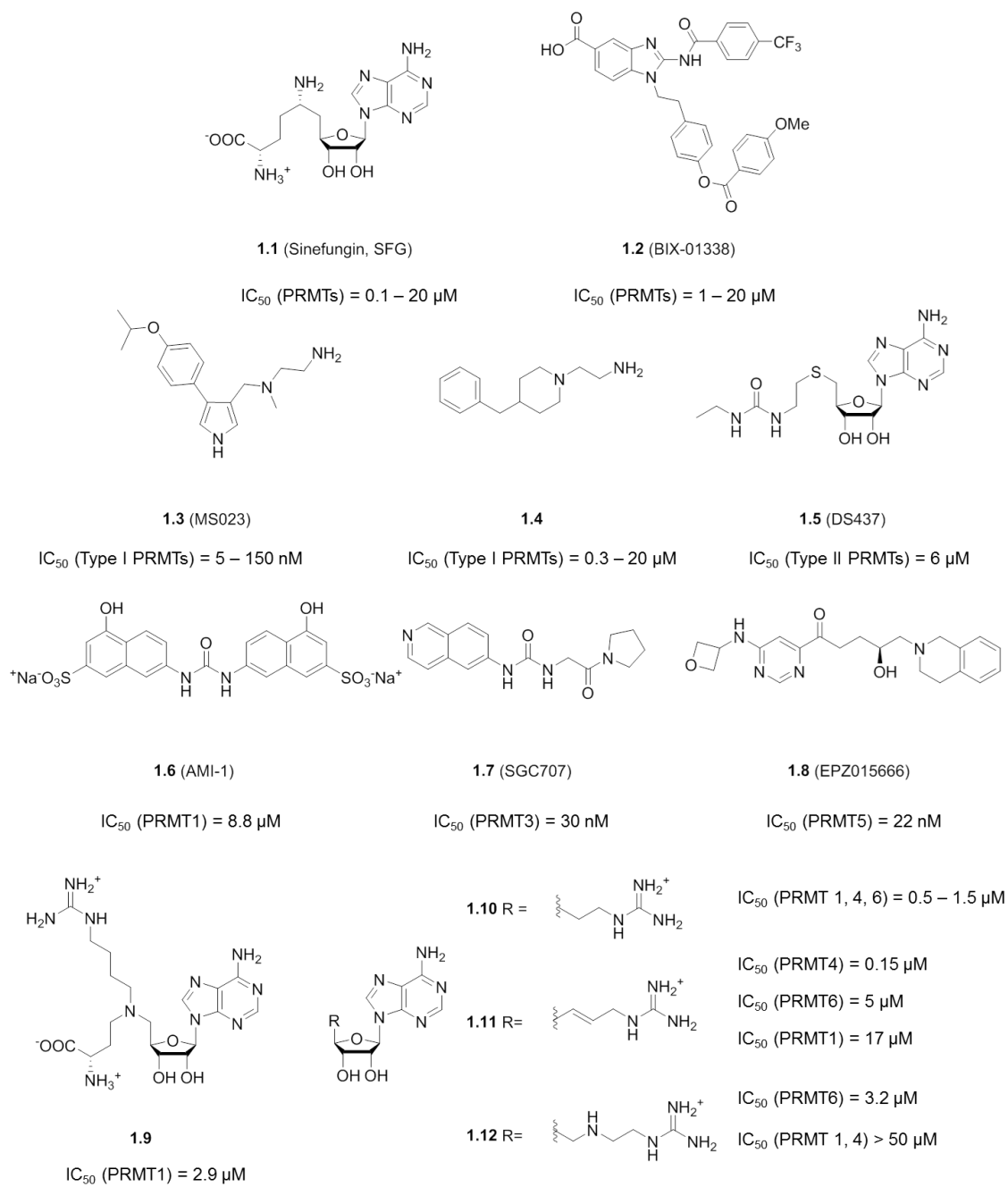


**Figure 1.4: Selective small molecule inhibitors towards PRMT family members**

The idea of resemble co-factor and substrate moieties into a “bisubstrate” inhibitor aims to achieve higher selectivity towards individual family member in an enzyme family, which has been found successful in targeting kinases<sup>80</sup> or KDMs<sup>81</sup>. Several groups have explored the conjugation of SAM analogues and guanidine group with viable linkers. Compound **1.9** possess micromolar inhibition towards PRMT1 and selective over PRMT4 and SET7 (a PKMT).<sup>82,83</sup> Compounds **1.10** – **1.12** presented higher potency and some selectivity among different members of the PRMT family.<sup>84</sup> This evidence suggests further improvement upon bisubstrate inhibitor is a promising direction for the development of potent and selective inhibitors towards PRMTs.

### **1.3 Research Objective of this Thesis**

Based on the evidence from the previous sections, PRMTs are promising targets in cancers. Development of small-molecule probes is important to further understand their intrinsic roles under physiological/diseases conditions and develop novel anti-cancer therapeutics. Our study in this thesis focuses on PRMT4 and PRMT6 as selective and cellular active small molecule inhibitors towards these enzymes are highly desired yet unavailable. The thesis comprises three components as follows:

- 1) Establishment of the multi-layered screening system towards the target enzymes consisting of *in vitro* biochemical activity assay; direct cellular activity assay detecting endogenous corresponding histone marker methylation level or other cellular

substrate level; downstream gene regulatory assay measuring the mRNA level of downstream genes indicating the regulation effects and potential therapeutic relations.

2) Rational design of small molecule inhibitors towards the targets of interest based on protein crystal structures and previous reported inhibitors and facilitated by collaborative computational *in silico* preliminary screening effort.

3) Rational design of a fluorophore-tagged PRMT6 small molecule probe and establishing of a fluorescence polarization (FP) based assay for cheaper and simpler screening of novel PRMT6 binders.

## **2. A CARM1 Inhibitor with Novel Structure from Computational Facilitated Structural Diversifying Virtual Screening**

### ***2.1 Introduction: Target of Interest – PRMT4 (CARM1)***

#### **2.1.1 Biological Functions of CARM1 and its Relation to Diseases**

Coactivator-associated arginine methyltransferase 1 (CARM1, also known as PRMT4), was the first PRMT that was originally identified as a transcriptional regulator.<sup>85</sup> It has recently drawn increasing interests due to the emergence of its gene regulating role in multiple biological processes.<sup>86</sup> As a Type I PRMT, CARM1 catalyzes the asymmetric demethylation of the arginine residues on its substrates, including histone substrate, epigenetic related transcriptional factors, and RNA regulators. CARM1 methylates the histone substrate histone H3 arginine 17 (H3R17) and transcriptional cofactors CREB-binding proteins (CBP) and p300, which co-activates the gene transcription. The gene activation is then mediated by transcription factors, such as nuclear hormone receptors (NHRs),<sup>87</sup> NF- $\kappa$ B,<sup>85,88-92</sup>  $\beta$ -catenin<sup>55</sup> and p53<sup>85,88-92</sup>. These transcription factors and their related biological pathways relate CARM1 with DNA damage response<sup>93</sup> and cell cycle progression<sup>87</sup>(Figure 2.1A). In addition, CARM1 methylates mRNA-stabilizing proteins<sup>94-96</sup>, RNA splicing factors,<sup>97</sup> and RNA polymerase II,<sup>98</sup> which results in mediating gene regulation in cell growth, development and differentiation (Figure 2.1B).<sup>96,97,99</sup> Researchers have also reported the affiliation of CARM1 with multiple types of cancers.<sup>50,51,87,100</sup> For example, CARM1 regulates *in vitro*

estrogen-stimulated cancer cell growth and elevated CARM1 mRNA level has been observed in grade-3 breast cancer,<sup>87,100</sup> indicating its involvement in estrogen-regulated cancer growth. Moreover, modulation of CARM1 level was found to be correlated with prostate cancer growth and progression of castration-resistance prostate cancer and gene silencing of CARM1 also induced the apoptosis of androgen-sensitive LNCaP prostate cancer cells.<sup>50,51</sup> More recently, CARM1 was found in co-activating Wnt/ $\beta$ -catenin regulated gene which was mostly found dysregulated in colorectal cancers.<sup>55</sup>

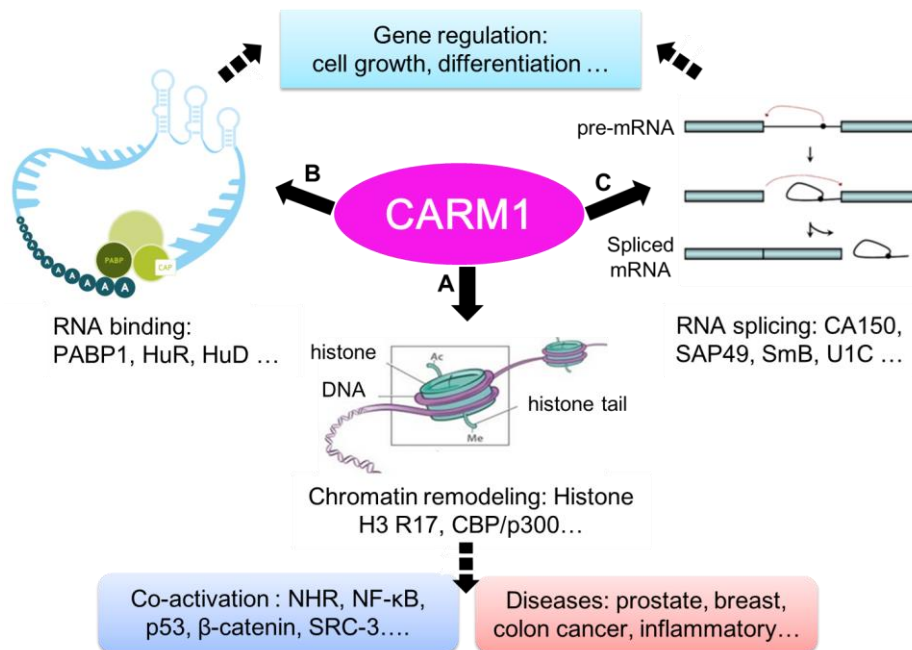


**Figure 2.1: Substrates and biological functions of CARM1**

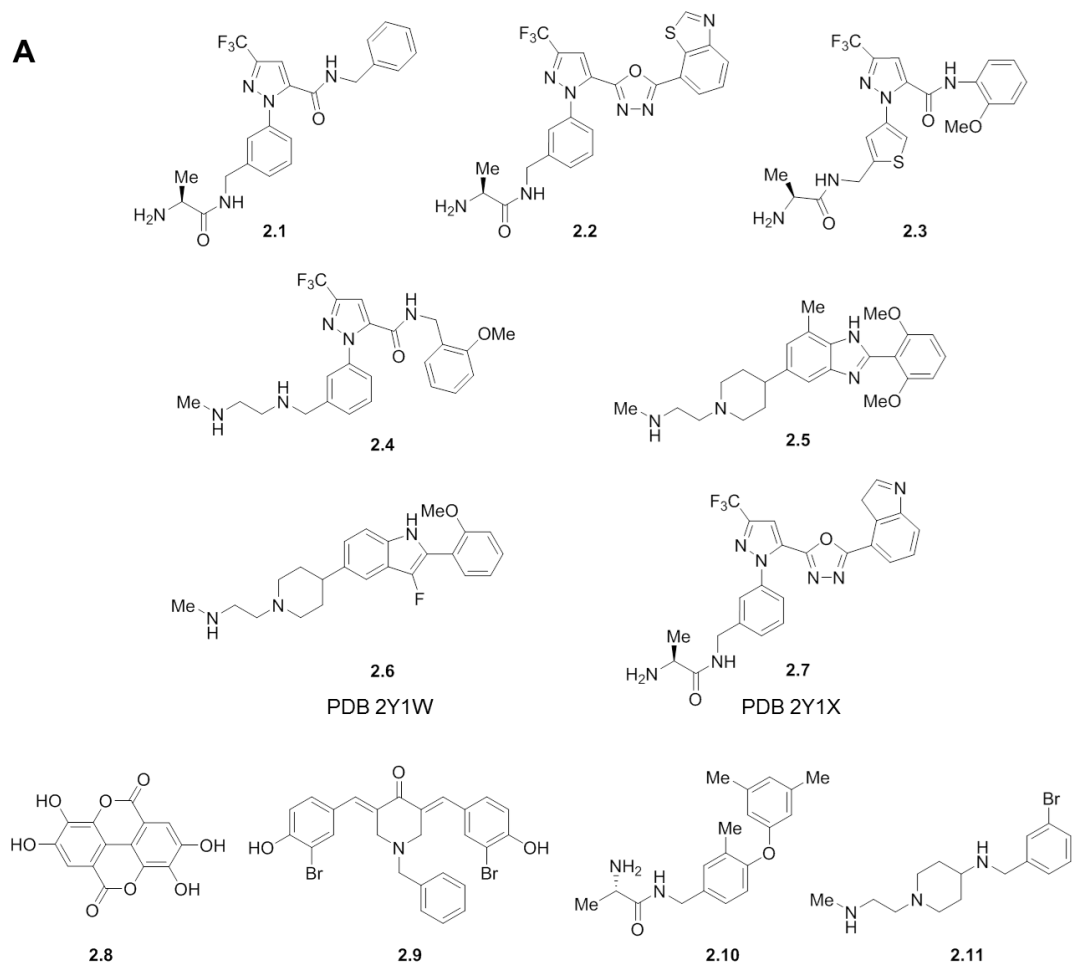
(A) Methylation of histone H3 Arg 17 and CBP/p300 by CARM1 co-activates gene activation mediated by nuclear factors and co-relates with diseases such as hormone-sensitive cancers. (B) (C)Methylation of non-histone substrates, RNA binding proteins and RNA splicing proteins relates CARM1 with cell growth, differentiation and development.

Additionally, CARM1 participates in inflammation signaling through co-activating NF- $\kappa$ B mediated gene regulation, which was known to be involved in immune and inflammatory responses that were fundamental responses in cancer development.<sup>90</sup> These emerging studies suggest CARM1 as a potential cancer therapeutic target.

### **2.1.2 Current Status of Small Molecule Inhibitor Development towards CARM1**

The search for CARM1 inhibitors has been going on for almost two decades. In 2008 and 2009, 5 hallmark papers were published towards the development of selective small-molecule inhibitors of CARM1.<sup>101-105</sup> Until then, no inhibitor had shown selectivity against CARM1 over PRMT1. The Purandare lab reported the first CARM1 selective inhibitor which was found through high-through-put screening (HTS) method with radioactive filter-binding assay. The pyrazole containing inhibitor, compound **2.1**,<sup>101</sup> was their best hit after a preliminary SAR study. It was the first compound shown inactive to PRMT1 and PRMT3 ( $IC_{50} > 25 \mu M$ ), the only two PRMTs with quantitative radioactive assays at that time. However, due to compound **2.1** did not behave well in the PAMPA (parallel artificial membrane permeability assay), they further optimized the structure and obtained compound **2.2**<sup>102</sup> with better  $IC_{50}$ , improved activity against PAMPA, while maintaining its selectivity.

Inspired by the structure of compound **2.1**, the Wahhab lab reported compound **2.3** which pushed the selectivity against PRMT1 and SET7/9 to  $IC_{50} > 100 \mu M$ .



**B**

IC <sub>50</sub> (μM)	2.1	2.2	2.3	2.4	2.5	2.8	2.9	2.10	2.11
PRMT1	>25	>25	>100		>25		>600	>100	>50
PRMT3								>100	>50
PRMT4/CARM1	0.08	0.04	0.06	0.2	0.07	25	8	0.05	0.09
PRMT5								>100	>50
PRMT6								5.2	
PRMT7								>100	>50
PRMT8								>50	9.2

**Figure 2.2: Current selective inhibitors towards CARM1<sup>101-110</sup>**  
 (A) Structures of selective inhibitors of CARM1. (B) IC<sub>50</sub> of these inhibitors towards different PRMTs.

Compound **2.3** was the first CARM1 selective inhibitor that was subjected to cellular studies. However, neither cellular H3R26 methylation level inhibition nor hormone dependent activity inhibition was observed.<sup>103</sup> They also reported compound **2.4** where the left end of the previous compound was simplified to 1,2-diamine. Although the potency of compound **2.4** dropped with a 3-fold increase of IC<sub>50</sub>, compared to **2.3**, but the pharmacokinetic profile was shown to be improved. However, no cellular activity was observed.

In the meanwhile, the Purandare lab reported compound **2.5**,<sup>105</sup> a benzoimidazole based inhibitor, which is also identified from the previous HTS and coincidentally has the similar 1,2- diamine tail as compound **2.4**. Unfortunately, no cellular activity was reported. This group and their collaborators also reported 2 co-crystallization structures of hCARM1 with compound **2.6** and **2.7**. The X-ray structures showed that the ligand occupies the arginine containing substrate binding pocket while the diamine containing moiety leans towards where the methyl locates in the SAM pocket which strongly mimics the position of the guanidine residue on the arginine containing substrates.<sup>108</sup> Yet, no cellular activity was reported on this series of compounds and no further follow-up studies were reported.

In 2010, a plant derived compound, ellagic acid (**2.8**) was reported to selectively inhibit CARM1's methylation on cellular H3R17 histone substrate with rather high IC<sub>50</sub>.<sup>106</sup> The mechanism of the inhibitory effect was elaborated as the ellagic acid

preferentially bound to the “KAPRK” motif on the histone 3 tail and the P16 contribute significantly to the binding. Therefore, although ellagic acid can inhibit CARM1’s methylation on H3R17, it is not a CARM1 binder, and the potency of the small molecule was insufficient.

In 2011, the Bedford group, which reported the first PRMTs selective inhibitor AMI-1(**1.6**), reported another symmetric dye-like compound **2.9** which possessed certain selectivity over PRMT1,3,5,6 and SET7 (a PKMT).<sup>107</sup> Compound **2.9** was shown to inhibit the methylation level of transfected FLAG-tagged PABP1 (mRNA binding protein, CARM1 cellular substrate) <sup>111</sup> and the luciferase signal controlled by androgen-driven cellular assay. However, it also shown pleiotropic effects under cellular conditions while the toxicity threshold and activity threshold were too close to be separated.

In 2016, the Bedford group and their collaborators published compound **2.10** <sup>109</sup> by virtual screening on the library of ~0.1 million commercial available compounds all of which contain basic amine tail, as well as compound **2.11** <sup>110</sup> by rational design based on structural information from compounds **2.6**, **2.7**. Compound **2.10** and **2.11** were highly selective towards CARM1 respectively in 100-fold and 20-fold, over all other PRMTs except PRMT6. These two compounds are the current best characterized CARM1 selective compounds. Compound **2.10** was subjected to cellular studies for inhibiting endogenous BAF155 R1064 methylation but was proved to be inactive while no cellular study of **2.11** was reported.

The current selective inhibitors against CARM1 and their IC<sub>50</sub> are summarized in Figure 2.2.

### **2.1.3 The Work of This Thesis towards Design and Development of Cellular Active CARM1 Small-molecule Inhibitors**

CARM1 is an important regulatory factor involved in many cellular processes and disease conditions. Therefore, selective and cellular active CARM1 inhibitors are highly desired to understand the complex physiological roles of CARM1 and to serve as potential therapeutic leads. Although the work shown in section 2.1.2 suggested the selectivity towards CARM1 has been realized in biochemical assays, cellular active CARM1 selective inhibitors remain unavailable.

The research in this thesis aims to address this challenge. We established multiple-mode systems for screening of CARM1 inhibitors, including *in silico* CARM1 binder evolution/diversification/virtual screening, *in vitro* biochemical activity assay, direct cellular activity assay for assessing methylation level of H3R17 or other cellular CARM1 substrates, and downstream effect assay for measuring the mRNA level of downstream genes.

The following sections will further discuss the rationales behind the *in silico* screening, validation of CARM1 *in vitro* assays and direct cellular activity assay with transfected recombinant PABP1. However, there was no significant correlation found between CARM1 siRNA knockdown and the downstream gene level downregulation for the three different downstream pathways tested, which is actually consistent with

recent literature reports<sup>112,113</sup>, in which knockdown of 90% cellular CARM1 can only achieve slight decrease in methylation level of endogenous PABP1 and the remaining amount of cellular CARM1 is still capable to maintain almost full cellular activity, indicating that CARM1 cellular inhibition may not have sufficient inhibitory effect to achieve any downstream effects.

## **2.2 Establishment and Validation of Multiple-mode Assays for Characterization of CARM1 Inhibitors**

### **2.2.1 Validation of CARM1 *in vitro* Biochemical Assay**

To measure the *in vitro* CARM1 enzymatic activity, we started from the commercially available CARM1 direct activity assay (BPS Bioscience 52041L) to set up the biochemical functional assay. In this assay, immobilized CARM1 histone H3 peptide substrate is incubated with the reaction mixture containing CARM1 and the methyl donor *S*-adenosyl-methionine (SAM). The methylated peptide was then detected with specific anti-methylated histone arginine antibody. The authenticity of the Flag-tagged CARM1 enzyme was verified by western blotting with specific anti-CARM1 and anti-FLAG antibodies (Figure 2.3C). To characterize the assay, the methylation reaction was performed with the treatment of the known methyltransferase inhibitor *S*-adenosyl-*L*-homocysteine (SAH, also the byproduct of the reaction). As shown in Figure 2.3A, a dose-dependent inhibition of the CARM1 catalyzed methylation was observed, well reflecting the concentration-dependent effect of the small molecule treatment. Moreover, we observed two new peaks of histone peptide in the matrix-assisted laser

desorption/ionization (MALDI) mass spectrum after initiating the methylation by adding the methyl donor SAM and all the reaction component from the assay kit with the free H3 1-21 peptide (BPS Bioscience 52011), which were identified to be mono- [M+14 (+ methyl)] and di- methylated [M+28 (+ 2 methyl)] histone peptide (Figure 2.3B).

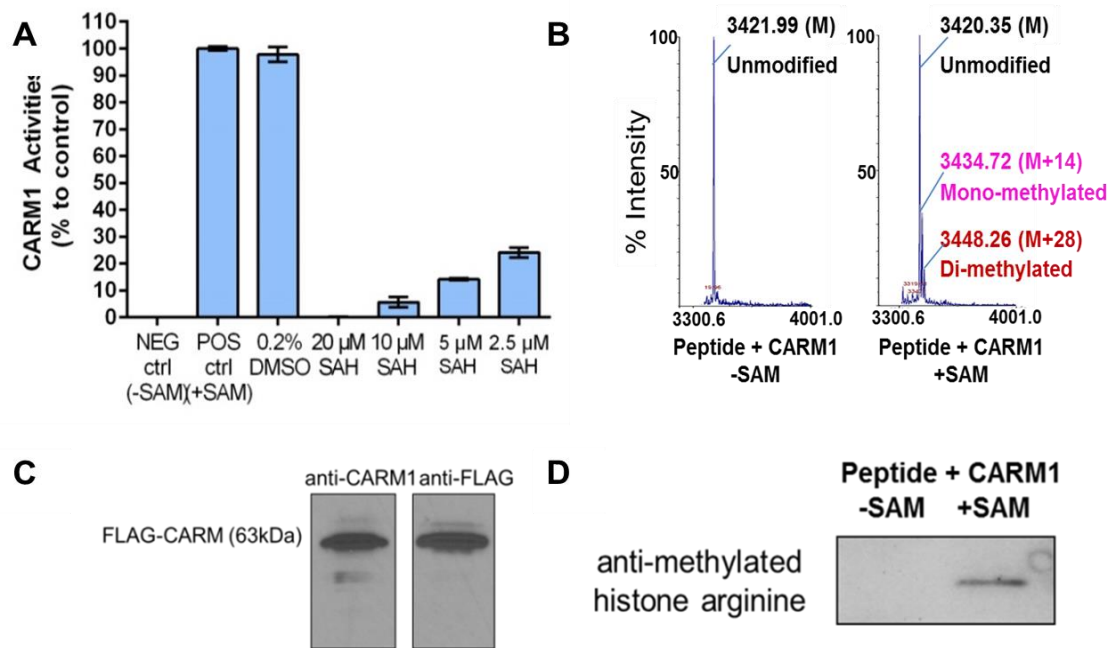


### Figure 2.3: Biochemical validation of CARM1 methyltransferase activity

(A) Commercial available CARM1 antibody-based biochemical assay detected CARM1 methyltransferase activity. Histone H3 substrate was immobilized on 96-well plate. Me-Arg substrate was recognized by specific anti-methylated primary antibody and signal was next produced by HRP-labeled secondary antibody. The CARM1 methyltransferase activity was inhibited by SAH in a dose dependent manner. See Appendix A.1 for assay details. (B) Mono- and di-methylated histone H3 substrate generated from CARM1 activity detected with MALDI proving methylation reaction happened in the commercial assay. See Appendix A.2 for MALDI details. (C) Western blotting of commercial Flag-CARM1 showing bands as expected. See Appendix A.11 for western blotting details. (D) Methylated histone H3 substrate generated from CARM1 activity detected by specific anti-methylated histone H3 antibody proving the signal from the commercial assay came from Me-Arg.

## **2.2.2 Expression and Purification of Human CARM1-FLAG with Mammalian cell 293T and Determination of its Enzymatic Activity**

Obtaining active CARM1 protein would be the first step for development of a scalable and robust CARM1 biochemical assay and MALDI confirmation assay, as well as for the follow-up test of thermodynamics of CARM1 inhibitors such as ITC (Isothermal Titration Calorimetry) and SAR (Surface Plasmon Resonance).

The plasmid of mammalian wild type recombinant CARM1-Flag-Myc was commercially purchased from Origene (RC217483). The CARM1 -FLAG-Myc plasmid was expressed in 293T cells, the expressed CARM1 was confirmed by Weston blot with anti-CARM1 antibody, and then purified with anti-FLAG antibody conjugated resin (Figure 2.4A). The expressed CARM1 was identified with anti-CARM1 antibody by western blot and can be comparable with the commercial BPS CARM1 (Figure 2.4B). The expressed CARM1 was confirmed to be functionally active by methylation assay of the histone H3 peptide used in 2.2.1 as detected by MALDI (Figure 2.4C), as well as by the CARM1 direct activity assay. The potency of our purified CARM1 was comparable to or even higher than that of the commercial BPS CARM1 (Figure 2.4B). We found that 50 ng of our in-house made CARM1 (5/20/14 batch) was as potent as 100 ng of commercially available BPS CARM1 (Lot# 110322) (Figure 2.4D), indicating that our in-house made CARM1 was twice as active as the commercial BPS CARM1. Successful purification of human, recombinant, N-terminal FLAG-tagged CARM1 protein has provided us an important tool for large scale assays and thermodynamic studies.

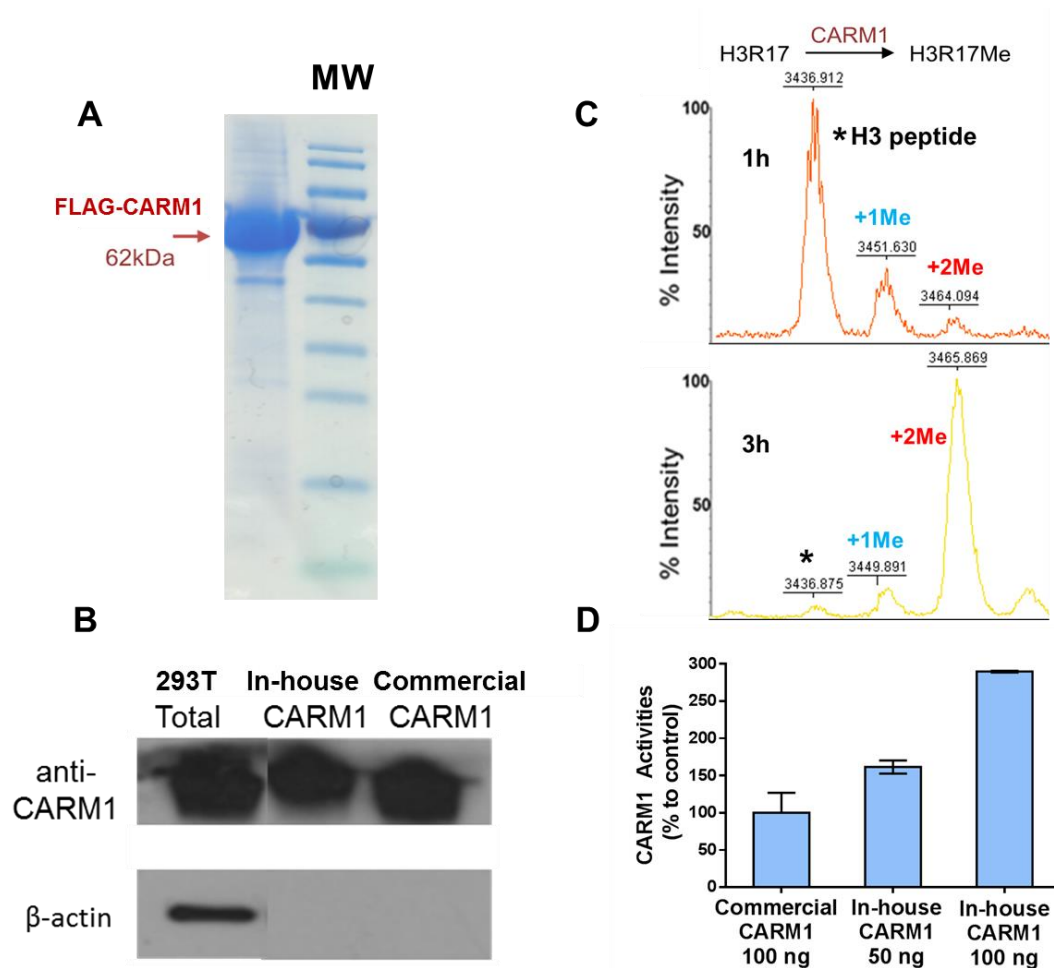


**Figure 2.4: Expression, purification and activity determination of recombinant FLAG-CARM1 protein**

(A) Coomassie stains of SDS-PAGE with partially purified recombinant FLAG-CARM1 from 293T cells and molecular weight markers. See Appendix A.3 for FLAG-CARM1 purification details. (B) Western Blot confirmation that in-house made CARM1 was as comparable with commercial CARM1. See Appendix A.11 for western blotting details. (C) In-house CARM1 methylated the H3 peptide substrate produced +1Me and +2Me product detected by MALDI, confirmed its methyltransferase activity. See Appendix A.2 for MALDI details. (D) Antibody-based direct activity assay showed the in-house CARM1 possessed higher activity than the commercial CARM1. See Appendix A.1 for assay details.

### **2.2.3 Development and Validation of Direct Cellular Assay for CARM1 Enzymatic Activity**

The direct cellular activity assay is a cellular system we developed for assessing substrate methylation by CARM1, which is a useful tool for identifying enzymatic activity of the hits from biochemical assays. This is an important step to screen out certain hits from the biochemical assay but cannot be cellular active.

We initially used the histone substrate H3R17me2 as the cellular substrate for CARM1, and we found that shRNA and siRNA knockdown of CARM1 did not interfere with the endogenous level of H3R17me2 in either embryonic kidney cell line 293T, or prostate cancer cell line LNCaP. The cellular substrates of CARM1 are not limited to H3R17. Other CARM1 substrates include Histone H3, acetyltransferase CBP/p300, RNA binding proteins such as PABP1 and RNA splicing factors such as CA150.<sup>97</sup> We then tested other CARM1 cellular substrates. The first one we tested was PABP1. The PABP1 expressing plasmid was kindly provided by Dr. Mark T. Bedford lab from the University of Texas MD Anderson Cancer Center, and anti-Me-PABP1 antibody was commercially purchased. The PABP1 plasmid was expressed in 293T cells, and then methylated PABP1 (Me-PABP1) level was measured after knockdown of CARM1.

We further optimized the experimental condition by balancing the toxicity of the transfection reagent (making the GFP level even) and the siRNA knockdown effect. The data we obtained was constantly reproducible. We found that the level of endogenous Me-PABP1 (Figure 2.5B) was not affected by knockdown of CARM1, which was the

same as our aforementioned finding with the endogenous H3R17me2. However, Me-PABP1 level of the co-expressed recombinant PABP1-GFP in the siCARM1 group was 30-50% lower than in the scramble siRNA group, though the GFP level showed no difference between the two groups (Figure 2.5B). This differential effect was most likely due to different cellular locations of the endogenous and recombinant PABP1 proteins. The endogenous PABP1 was located in the nucleus, whereas the recombinant PABP1-GFP was mostly located in the cytoplasm, which was where the siRNA knockdown effect mostly took place. We could then conclude that the recombinant Me-PABP1 level may serve as a reporter for CARM1 cellular activity.

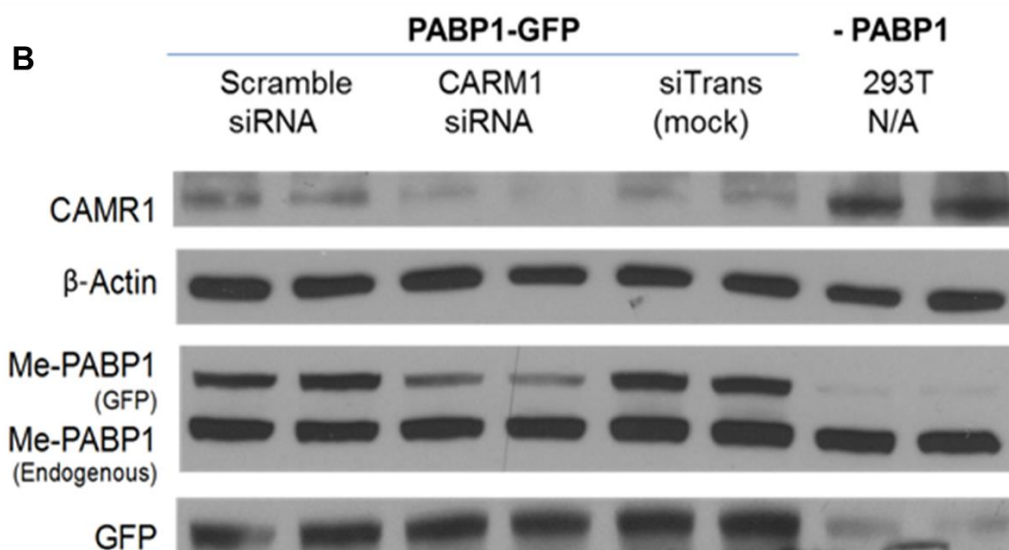
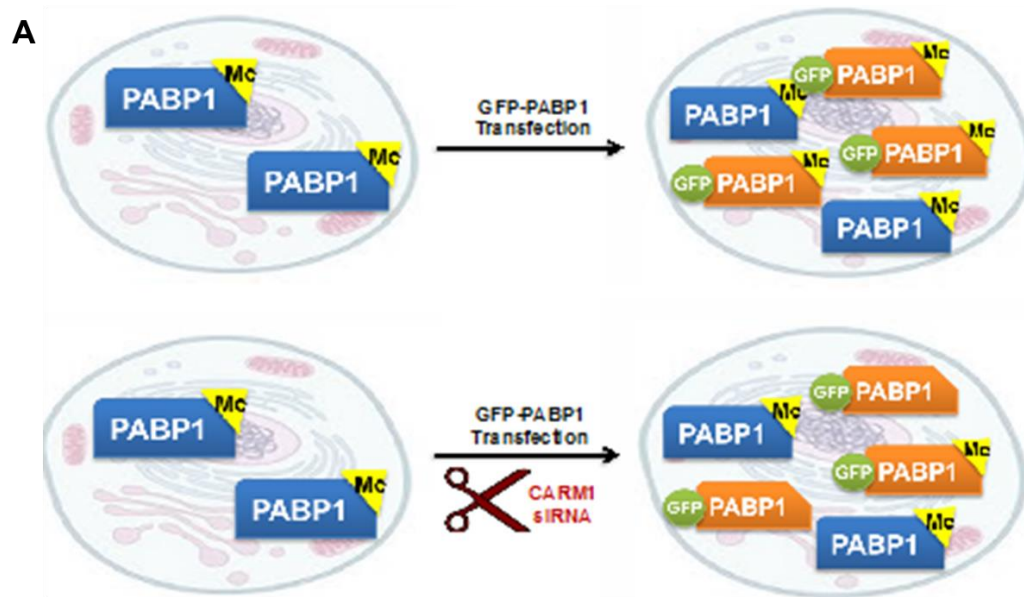


**Figure 2.5: Cellular CARM1 methyltransferase activity assay establishment with substrate PABP1**

(A) Cartoon representative of a cell-based assay for monitoring CARM1 activity based on recombinant Me-PABP1-GFP level. (B) Immunoblot of lane 1 showed successful knocking down CARM1 in 293T cell reduced the level of recombinant Me-PABP1-GFP showed in lane 3. GFP in lane 4 showed the PABP1-GFP expression was even.  $\beta$ -actin in lane 2 showed the loading was even. See Appendix A.4 for CARM1 knockdown details, A.11 for western blotting details.

## **2.2.4 Attempts to Develop Cell-based Assays for CARM1 Downstream Effect**

The ultimate goal of this project is to discover CARM1 probe with potential therapeutic effect. Therefore, after determining the probes that can interfere with CARM1's direct methylation activity under cellular condition, we need to further investigate the associated probe's capability of perturbing CARM1's downstream biological pathways, which may serve as the first screening step for potential therapeutic effect. However, much effort has been dedicated to set up the CARM1 downstream effect assay but all failed. We concluded it may be caused by the co-activator nature of CARM1 which knockdown of CARM1 will not totally inhibit its downstream signaling pathway. Here we list all the efforts we have made.

### *a) PSA-luc Reporter Gene Assay with in LNCaP Cell Failed to Determine CARM1 Level Changed Induced by SiRNA Knockdown*

Downstream effect assay to monitor CARM1's effect on downstream genes were attempted to establish by detecting the CARM1 downstream gene levels in the androgen-dependent prostate cancer cell line, LNCaP. In prostate cancer cells, CARM1 is involved in androgen receptor mediated gene expressions,<sup>50</sup> including the prostate-specific antigen (PSA) gene.<sup>112,113</sup> Therefore, a direct PSA-luciferase reporter system has been set-up to determine the CARM1 knockdown effect on downstream PSA regulation effect. However, repeatable experimental trials in LNCaP cells failed to determine the difference of PSA-luc level between control group and experimental group (Figure 2.6).

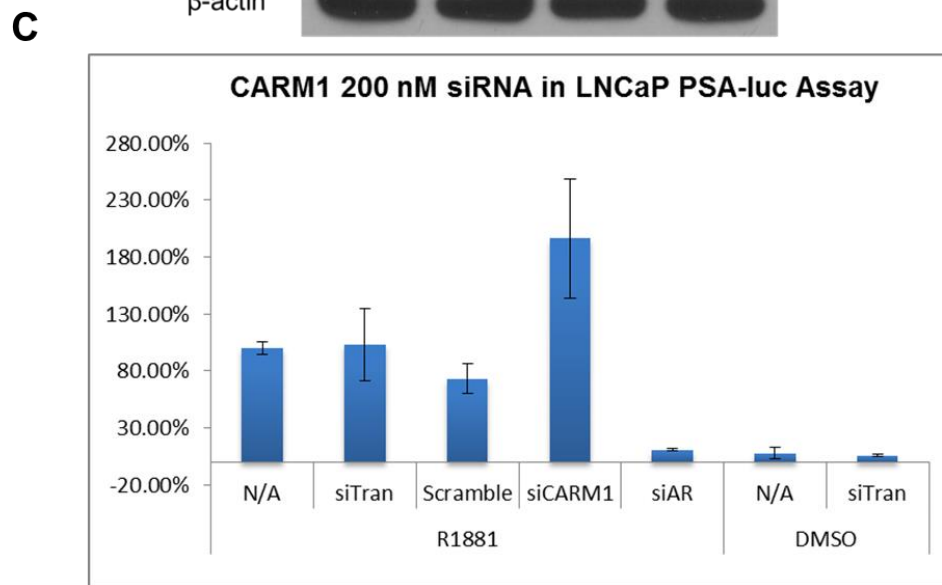
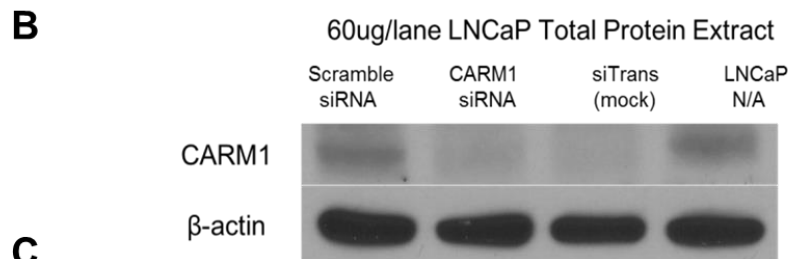
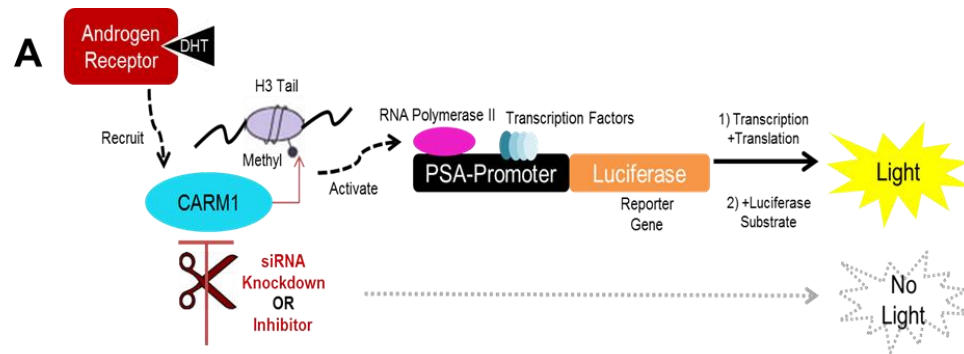


**Figure 2.6: PSA-luc assay establishment in LNCaP cells**

(A) Cartoon representative of the theoretical relation between CARM1 knockdown and PSA-luc reporter in LNCaP cells; (B) Western blotting confirmation that in LNCaP cells CARM1 knockdown did down regulate CARM1 level. See Appendix A.11 for western blotting details (C) Column 3 and 4 showed that between siScramble (siCTRL) and siCARM1, PSA-luc level did not down regulate, indicating that PSA-luc signal did not correlate with CARM1 knockdown. PSA-luc cannot report CARM1 cellular activity. The siAR (androgen reporter) served as the positive control for siRNA knockdown in this PSA-luc assay. See Appendix A.5 for PSA-luc assay details.

Figure 2.6B showed the CARM1 siRNA knockdown reduced the CARM1 level in LNCaP detected by CARM1 antibody, therefore eliminating the concern of the siRNA treatment in PSA-luc assay. From Figure 2.6C, we can see that the positive control N/A+R1881(DHT substitutive) to negative result N/A+DMSO ratio is 10:1, which marked the trustworthiness of the data. The transfection reagent siTrans did not lead to toxicity effect and scramble siRNA treatment led to 30% of signal reduction. The siCARM1 treatment led to increase of PSA-luc signal which might be a false positive read-out. The siAR (androgen) reduced up to 80% signal reduction, which suggested the siRNA transfection procedure was reliable. Overall, the information suggested that CARM1 knockdown would not reduce PSA-luc signal in the LNCaP cell, excluding the feasibility of using the PSA as a reporter of CARM1 cellular activity.

*b) RKO Cell Wnt/ $\beta$ -catenin Signaling Pathway Downstream Gene Affecting by CARM1 Activity — Failed Due to Low Level of mRNA Cannot be Accurately Detected*

In the conserved Wnt/ $\beta$ -Catenin pathway, on the off-state, with the absence of the Wnt signal,  $\beta$ -catenin, an integral *E*-cadherin cell-cell adhesion adaptor protein and transcriptional co-regulator, is targeted by intracellular ubiquitination system and go through the fate of degradation. On the contrary, in the presence of Wnt ligand (on-state), the stabilized  $\beta$ -catenin can be translocated to the nucleus where it binds to

LEF/TCF transcription factors, recruit other coactivators and activate Wnt target genes.

114

Wnt/ $\beta$ -catenin signaling was indispensable for the development of the gastrointestinal system, and aberrant activation of this pathway was implicated in disease, especially in colorectal cancer.<sup>55</sup> CARM1 was found to be directly recruited by  $\beta$ -catenin leading to  $\beta$ -catenin activated gene expression elevation. In RKO colon cancer cells, normal Wnt/ $\beta$ -catenin activity was found, and with Wnt3a ligand activation, accumulated  $\beta$ -catenin amount was observed from western as well as ChIP, by detecting the  $\beta$ -catenin downstream gene Axin2 and GRP49, with the antibody of  $\beta$ -catenin and H3R17me2.<sup>55</sup> CARM1 lentiviral shRNA treatment reduced the Wnt3a activated Axin2 and GRP49 mRNA level detected by qPCR comparing to the scramble shRNA treatment. With the aforementioned literature support, we thought we may establish the CARM1 downstream effect assay in the RKO colorectal cancer cells by detecting the Wnt/ $\beta$ -catenin downstream gene level.

To establish the RKO Wnt/ $\beta$ -catenin CARM1 downstream effect assay, multiple qPCR attempts have been performed to detect the elevation of GFP49 and Axin2 mRNA level upon different dosage of Wnt3A CM activation and CARM1 knockdown, however the result was random. We controlled the quality of the Wnt3A medium with a HEK293 cell line stably transfected with SuperTopFlash reporter incorporated of LEF1-regulated luciferase gene (STF cell), obtained from Dr. Michael Stallcup group from USC, using

purchased pure mouse Wnt3A as positive control. After the Wnt3A medium read-out was stabilized, we focused on the qPCR. However, the RNA levels of the downstream genes Axin2 and GRP49 upon siRNA treatment were still random upon multiple runs (Figure 2.7 as a representative).

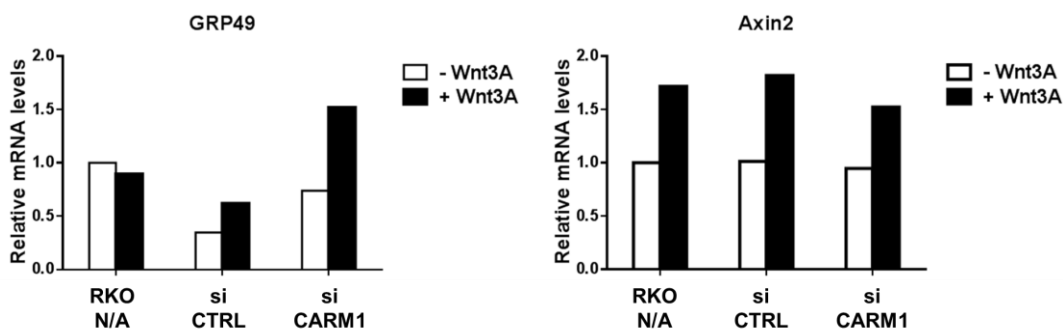


**Figure 2.7: A representative qPCR result for the randomness of the Wnt3A CM activation of downstream gene levels in RKO cells**  
cDNA 1:1 addition for qPCR. See Appendix A.6 for qPCR details.

After we looked into the detailed qPCR data, we figured the Cp value of these two genes were both over 30, indicating there would be only 5~6-fold amplification of the gene. And low amplification gene would be easily influenced by tiny contamination or pipetting differentiation, which was unavoidable. We therefore concluded that the Wnt3A pathway would not serve as the CARM1 downstream effect assay due to the undetectable level of mRNA of the downstream genes.

*c) HSP70 as CARM1 Substrate Regulating Downstream Gene RAR $\beta$ 2 Failed to Report CARM1 Cellular Activity due to Insufficient Knockdown*

HSP70 (heat-shock protein of 70 kDa), an evolutionarily conserved protein family of ATP-dependent molecular chaperone, was found to be mono-methylated (me1) by CARM1 at R469.<sup>115</sup> Literature reported that upon CARM1's methylation activity on HSP70 that regulates the controlled downstream retinoid acid (RA) regulated gene RAR $\beta$ 2, proven by siRNA knocking down CARM1 in 293T cells then re-supplement with CARM1 E267Q catalytical dead mutant failed to activate the RAR $\beta$ 2 mRNA level upon RA treatment.<sup>115</sup> Therefore, we were highly interested in setting up the HSP70 as CARM1 substrate RAR $\beta$ 2 reporting CARM1 cellular activity assay.

However, with numerous attempts, we failed to repress the RA activated RAR $\beta$ 2 mRNA level upon CARM1 siRNA knockdown, most probably due to the insufficient CARM1 knockdown, even when increasing the dosage and treatment time of CARM1 siRNA (a representative result can be seen from Figure 2.8). There were other reports indicating that cellular activities of CARM1 retained upon even 90% knockdown.<sup>116</sup> With 50% of CARM1 knockdown efficacy in our experiments (Figure 2.8), it was understandable that the downstream gene was not affected by the knockdown effect in this case.

CRISPR/Cas system knocking out CARM1 in 293T would provide a possible way to observe the downstream gene change. However, this approach would not meet our goal of evaluate small-molecule effect on the downstream gene level change since it is

impossible that small-molecule inhibition can reach the same effect of CARM1 knockout.

Therefore, we hold on the assay development on CARM1 downstream effects.

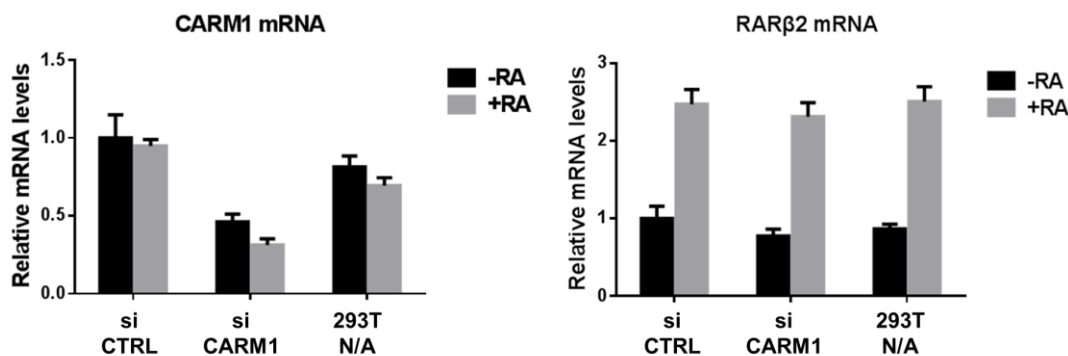


**Figure 2.8: A representative qPCR result for the no correlation between CARM1 knockdown and RARβ2 gene down regulation**  
cDNA 1:10 dilution for qPCR. See Appendix A.6 for qPCR details.

In all, the CARM1 downstream-effect assay has not been set up successfully.

Possibly, the downstream genes would not totally rely on its regulation as a co-activator.

### **2.3 Design Rationales of CARM1 Inhibitors, Computational Facilitated Structural Diversification and in silico Screening, Empirical Structural Optimization**

*(This part includes collaborative effort. The computational facilitated compound evaluations was complete by Dr. Chetan Rupakheti and Dr. Yuqi Zhang from Dr. David Beratan's Group, Duke University)*

We employed the computational modelling method for discovery of novel CARM1 inhibitors with diverse skeletons, in collaboration with the theoretical group of Dr. David Beratan. We applied the Algorithm for Chemical Space Exploration with

Stochastic Search (ACSESS) developed by the Beratan's Lab (see flow chart in Figure 2.9).<sup>117 118</sup>

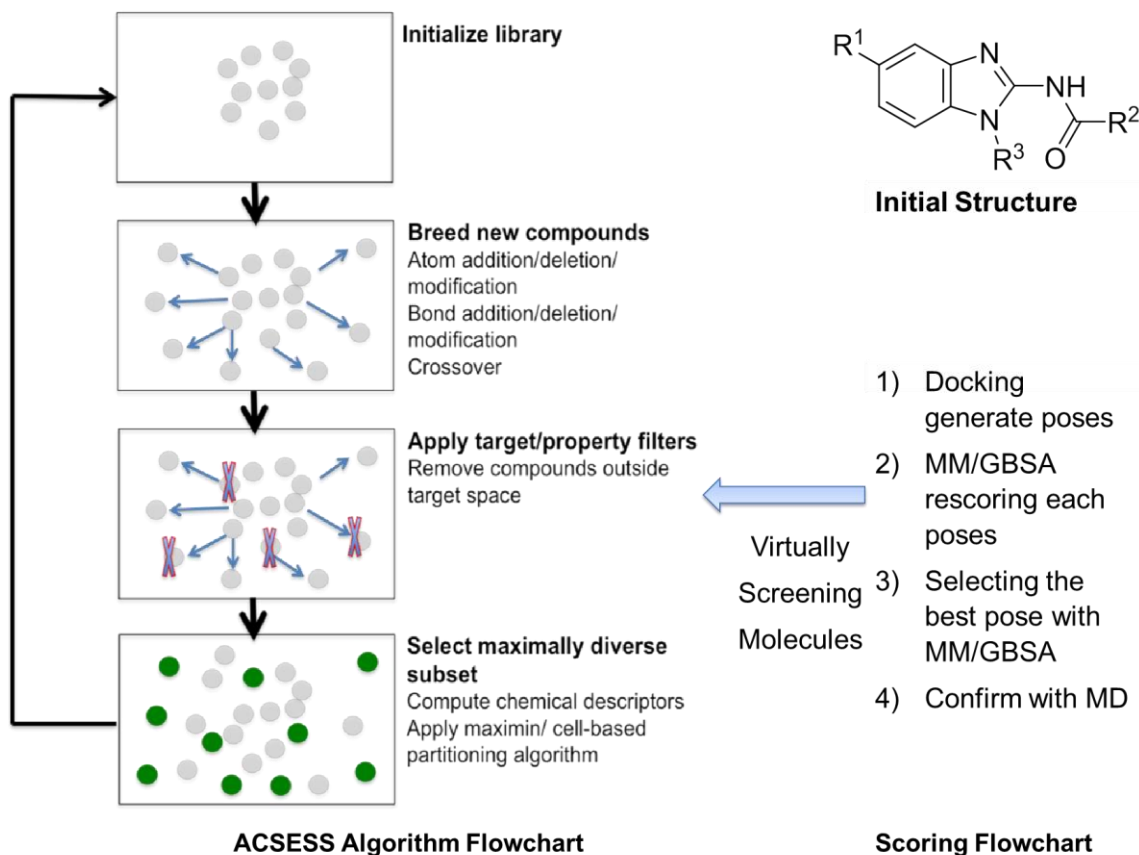


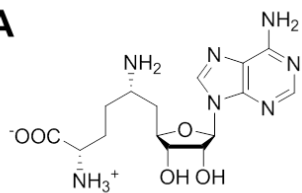
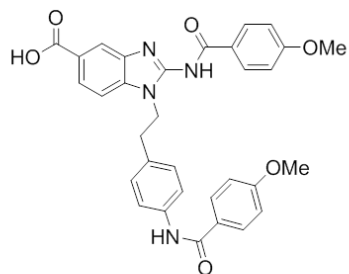
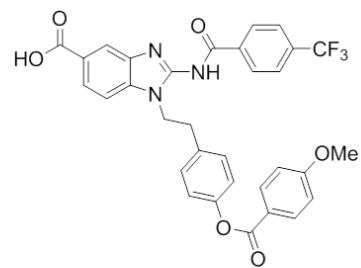
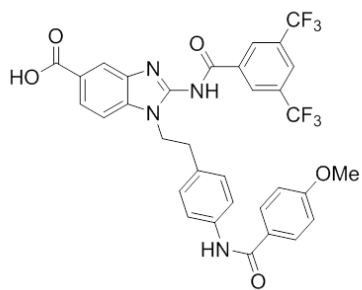
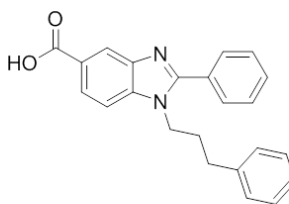
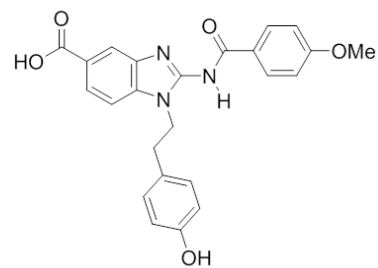
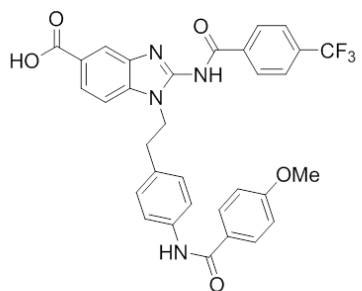
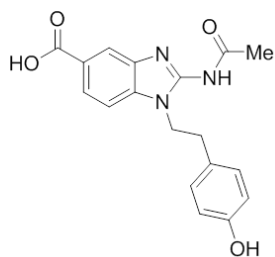
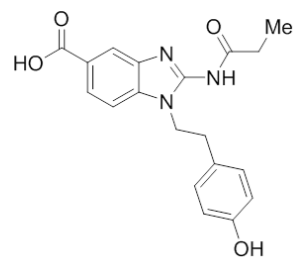
**Figure 2.9: ACSESS Algorithm Flowchart (adapted from ref <sup>118</sup>) and Docking/MMGBSA/Molecular Dynamic Scoring Flowchart**

These structure-based methods (applied as filters within ACSESS) would warrant that the compounds generated in the library would be highly diversified and had favorable activity toward the target enzyme CARM1, by the model which was set up based on its X-ray crystal structure. The created compounds by these methods would next be evaluated with molecular mechanics energies combined with the generalized

Born and surface area continuum solvation (MM-GBSA) methods. The best hits were further confirmed with molecular dynamics (MD) simulation. With the X-ray structural information of CARM1 (PDB: 5DXJ and 5DWQ)<sup>27</sup>, we coupled ACSESS with the known and tested MMGBSA method to generate a library of diverse compounds as potential SAM mimic inhibitors showing favorable binding toward CARM1 in competition with cofactor SAM. In addition, this computational framework would also be applied to significantly enhance the diversity and potency of compounds based on known scaffolds. In the development of BIX-01338(**1.2**)-based CARM1 inhibitors, we applied ACSESS to generate new benzimidazole compounds by adding various substituents R<sup>1</sup>, R<sup>2</sup>, R<sup>3</sup> (structure shown in Figure 2.9) and used the MMGBSA method to screen the compounds to be either accepted or rejected based on their computed binding score. Such computational screening would also greatly facilitate the experimental structure-activity studies to improve potency and selectivity.

*a) Benchmark of molecular dynamics computational model.*

To assess the reliability of MD as a validation tool, firstly, we compared the relative computational scoring with the experimentally measured activity of previously designed pilot library of SAM mimics. Based on a reported SAM mimic pan-methyltransferase inhibitor BIX-01338 (**1.2**, BI-50 in Figure 2.10),<sup>67</sup> a pilot library of SAM mimics (BI compounds), based on benzimidazole core, was designed and synthesized to

**A****1.1 (Sinefungin, SFG)****BI-113****BI-50****1.2 (BIX-01338)****BI-73****BI-26****BI-39****BI-71****BI-141****BI-142**

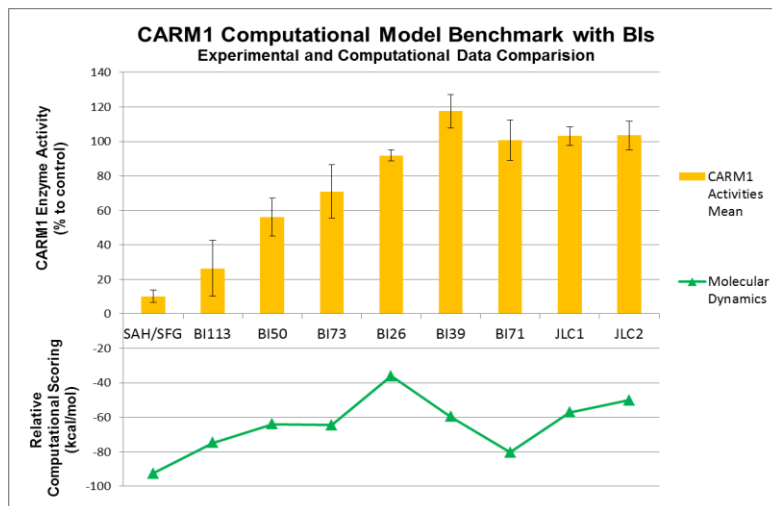


**Figure 2.10: Selective SAM mimics (BI compounds) with different level of CARM1 inhibitory effect in benchmarking of CARM1 computational model**

(A) Structures of the BI compounds. (B) Comparison of CARM1 inhibitors' effect in the antibody-based biochemical assay and molecular dynamic scoring showing the same trend, indicating the model was credible. 10  $\mu$ M of compound treatment was used. See Appendix A.1 for assay details.

verify substitution groups on the original structure. The inhibitory activity towards CARM1 of this pilot library together with SAH, the byproduct of the methylation reaction and inhibitor of the methyltransferases, were evaluated with CARM1 biochemical direct activity assay as validated in 2.2.1 and described in method section. Representative SAM mimics with different levels of CARM1 inhibitory effect, varied from up to 80% enzymatic inhibition to no inhibition, were chosen to be evaluated. (Figure 2.10) Comparing the computational data with the experimental data, we found that molecular dynamics predict the same inhibitory trend of the experimental CARM1 inhibitors: SFG, BI-113, BI-50 (BIX-01338 (**1.2**)), BI-73, as well as screened out non-active

compounds: BI-26, JLC-1, and JLC-2. However, BI-39 and BI-71, although non-active in the experimental screening, but structurally highly related to the active compounds, could not be distinguished by the computational model. The results suggested that: (1) All the active binders (SFG, BI113, BI50 and BI73) had scoring less than -60 kcal/mol; (2) Some false positive hits (e.g. BI71) indicated that binding affinity may not be the only factor that determining the scoring.

Therefore, the CARM1 computational model could predict the true positive and its trend, however, would tolerate false positive from the screening, which had been validated as the working model with certain limitations.

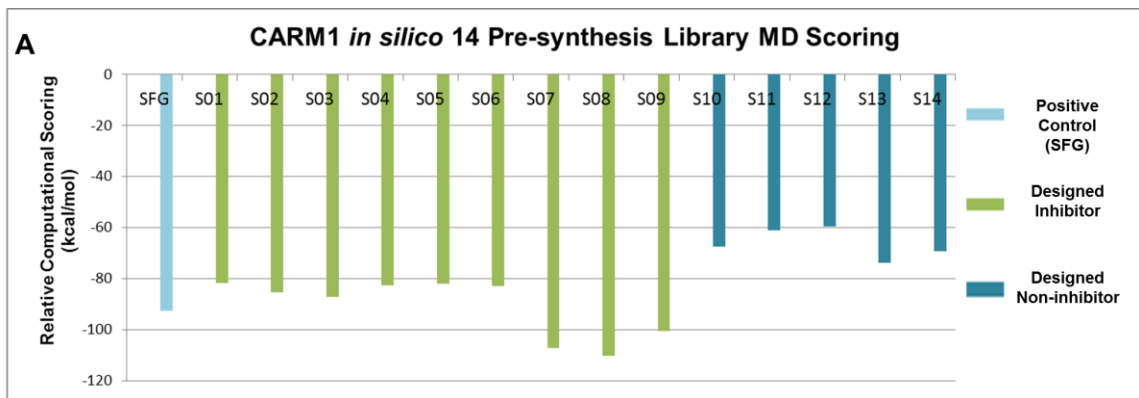
***b) The final compound from the modeling and empirical structural optimization***

Property-optimizing ACSESS (PO-ACSESS)<sup>118</sup> was able to generate a library, via diversification of the given scaffold (Figure 2.9), containing hundreds of diverse structures and having competitive binding energy scores.

The threshold for binding energy was set with SFG as reference, which shows ~-70kcal/mol MMGBSA energy as a known inhibitor of CARM1 (computed before the library generation step). The algorithm had to survey ~25,000 candidate molecules to build the library of desired molecules. The ensemble averaged MMGBSA binding free energy calculated scores of the most promising hit from the library, Compound B (Figure 2.11), was then validated using MD simulation which was then found to have a comparable binding score to SFG. By looking into the details of the structural interaction,

we also found favorable hydrogen bonding interactions between designed Compound B and the CARM1 X-ray model.

The Compound B was not readily accessible synthetically from commercial reagents. Thus, we pursued to probe structural changes of Compound B considering both starting material availability for its preparation and binding energy with empirical optimization to improve hydrogen-bond preserving, synthetic capability and with the guidance of predicted 3D protein-ligand interaction. Upon structural analysis of Compound B, we designed mutations of Compound B and used the validated MD-MMGBSA based binding energy evaluation. Then the best scoring compound was chosen to generate the next round of mutated compounds. After 4 rounds of mutate optimizations, we finally obtained a 14-compound *in silico* compound library containing the best scoring compounds and their corresponding non-active (control) compounds, which finally sum-up as the potential CARM1 14 pre-synthesis library shown in Figure 2.11B. This pilot library had all been tested with MD (Figure 2.11A) and we could see a clear energy gap between the hit compounds and control compounds.



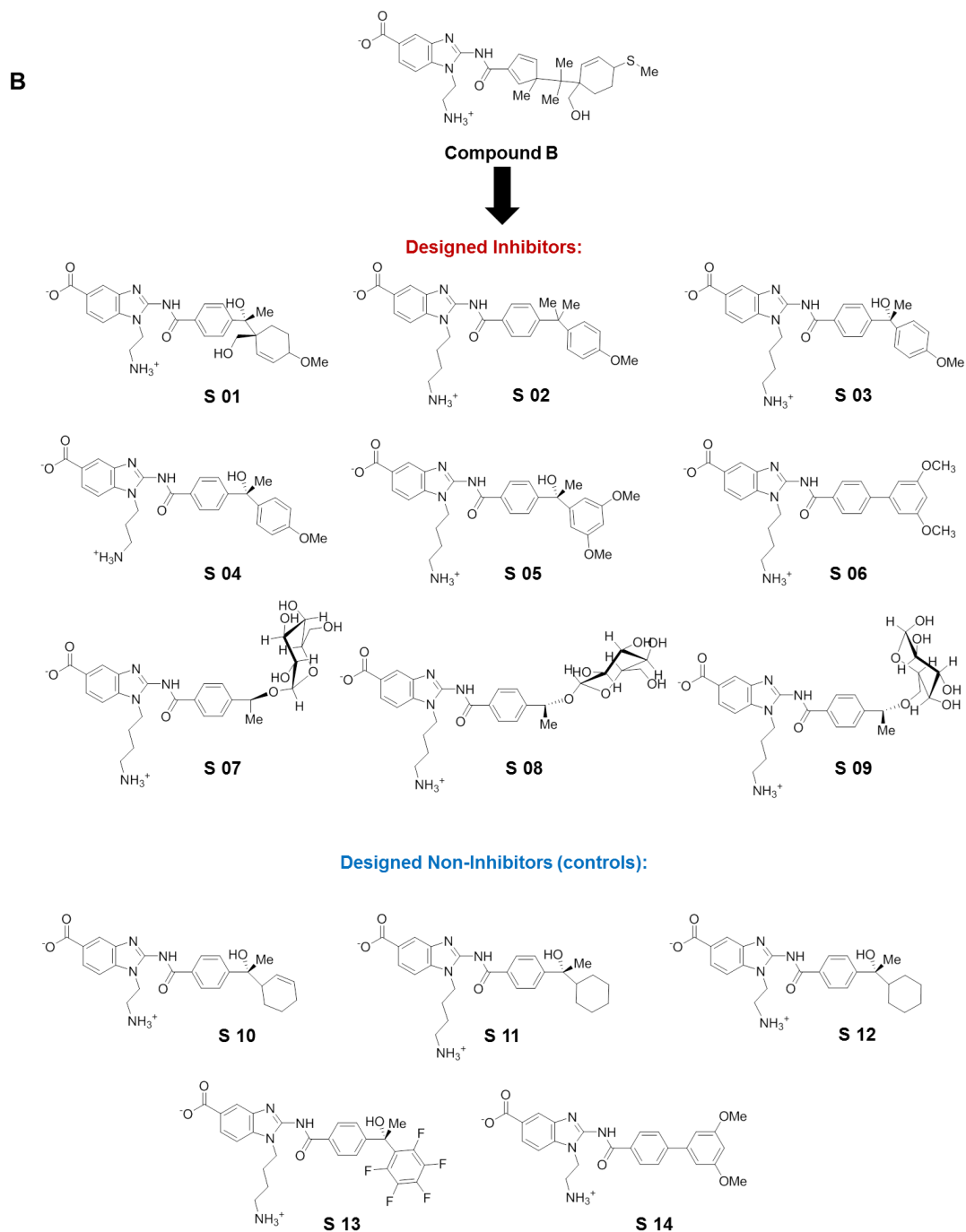


**Figure 2.11: CARM1 small molecule binder *in silico* screening and structural optimization generated 14-compound library for future synthesis**  
 (A) Molecular dynamic scoring for 14 compounds comparing with SFG. (B) Structures of the 14 compounds.

For future experiment, potential CARM1 inhibitors and their controls can be chosen from this 14 pre-synthesis pilot library and be applied to synthetic effort. This effort may diversify the biochemical CARM1 inhibitors' structure which occupied the binding pocket of co-factor SAM.

## **2.4 Conclusions and Future Plans**

In summary, we have established and validated CARM1 biochemical assays, which have been used to test in-house made hCARM1 protein. Furthermore, computational facilitated modeling has been performed toward identifying new leads of CARM1 inhibitors. These novel compounds identified from this chapter may be synthesized and be tested in the biochemical assays, providing a starting ground for future research.

Efforts toward establishing cellular downstream effect assay for CARM1 encountered unexpected difficulty associated with the insensitivity in its siRNA knockdown. Considering the co-activator nature of CARM1 in various pathways, the success of setting up the CARM1 downstream assay may require the involvement of amplified biological signals in order to be shut down to see the effect, so as the CARM1 cellular inhibitor to shown the effect. Novel CARM1 inhibitors with cellular activity require for the investigation to further understand the signaling pathways.

## **3. Potential PRMT6 Small Molecule Regulators Targeting SAM-substrate Bi-pockets**

### ***3.1 Introduction: Target of Interest – PRMT6***

#### **3.1.1 Biological Functions of PRMT6 and its Relation to Diseases**

Protein Arginine Methyltransferase 6 (PRMT6) is a nuclear-located Type I PRMT that regulates various cellular processes. It catalyzes the generation of asymmetric  $\omega$ -N(G),N(G)-dimethylarginine (Rme2a) on its protein/peptide substrates, with a preference of glycine- and arginine-rich (GAR motif) substrate. So far PRMT6 is the sole PRMT that is known to be responsible for H3R2me2a, an important epigenetic marker in regulating embryonic stem cell pluripotency,<sup>38</sup> cell cycle regulation,<sup>119</sup> and nuclear receptor-mediated gene expression(Figure 3.1A).<sup>120</sup> The H3R2me2a mark is a gene repressive outcome which is mutually exclusive to the gene activation effect of H3K4me3 marker generated by Polycomb repressive complex 2 (PRC2), demonstrating PRMT6's fundamental role in gene regulation pathways.<sup>121</sup> By methylating DNA polymerase beta, PRMT6 regulates DNA repairing process(Figure 3.1B).<sup>122</sup> Dysregulation of PRMT6 has been found in various disease conditions, including several cancers, such as melanoma,<sup>123</sup> bladder, lung,<sup>57</sup> and hormone sensitive breast and prostate cancers.<sup>53</sup> One significant mechanism is that PRMT6 transcriptionally represses the tumor suppressor gene, p21<sup>CDKN1A</sup>, leading to growth of cancer cells and their resistance to cellular toxic reagent.<sup>124</sup> Moreover, PRMT6 has also been found to be able to inhibit gene expression of human immunodeficiency virus type 1 (HIV-1) by methylating and

interfering the functions of several HIV-1 proteins, Tat, Rev and nucleocapsid (Figure 3.1C).<sup>40</sup> Therefore, perturbation of PRMT6 function with small molecule regulators may possess therapeutic potentials and the small molecule compounds may serve as useful tools for understanding the function of PRMT6 *in vitro* and *in vivo*.

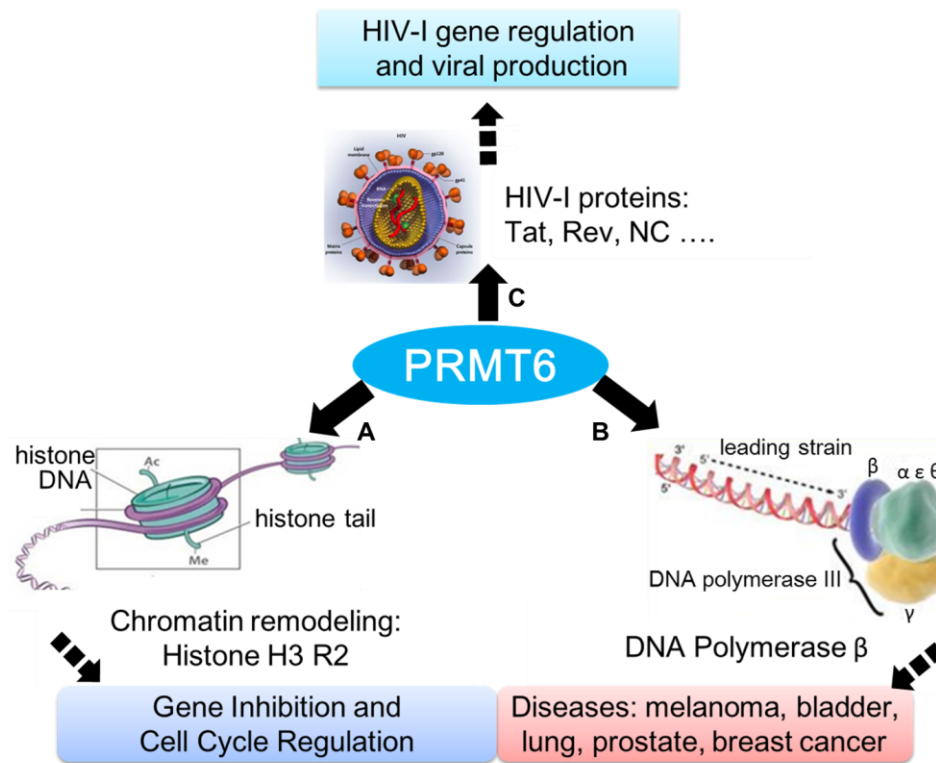


**Figure 3.1: Substrates and biological functions of PRMT6**

(A) Methylation of histone H3 Arg 2 and (B) DNA polymerase  $\beta$  by PRMT6 co-activates gene activation mediated by nuclear factors and co-relates with diseases such as cancers. (C) Methylation of non-histone substrates, such as HIV-I Tat protein, involved PRMT6 in virus infections.

### 3.1.2 Current Gap on Small Molecule Inhibitor Development towards PRMT6 and the Work of This Thesis

Although research for discovery of small-molecule regulators of PRMT6 has only been started in the recent few years, great progress has been achieved with potent biochemical and cellular PRMT6 small-molecule inhibitors have been reported.<sup>22,28,68,127</sup> Several biochemically potent Type I PRMTs inhibitor have been reported (Figure 3.2) and displayed cellular activity towards PRMT6 inhibition.<sup>22,28,68,125</sup> However, a current gap in PRMT6 small-molecule probe development is the difficulty to achieve selective inhibition of one selective PRMT due to the structural similarities among Type I PRMTs.

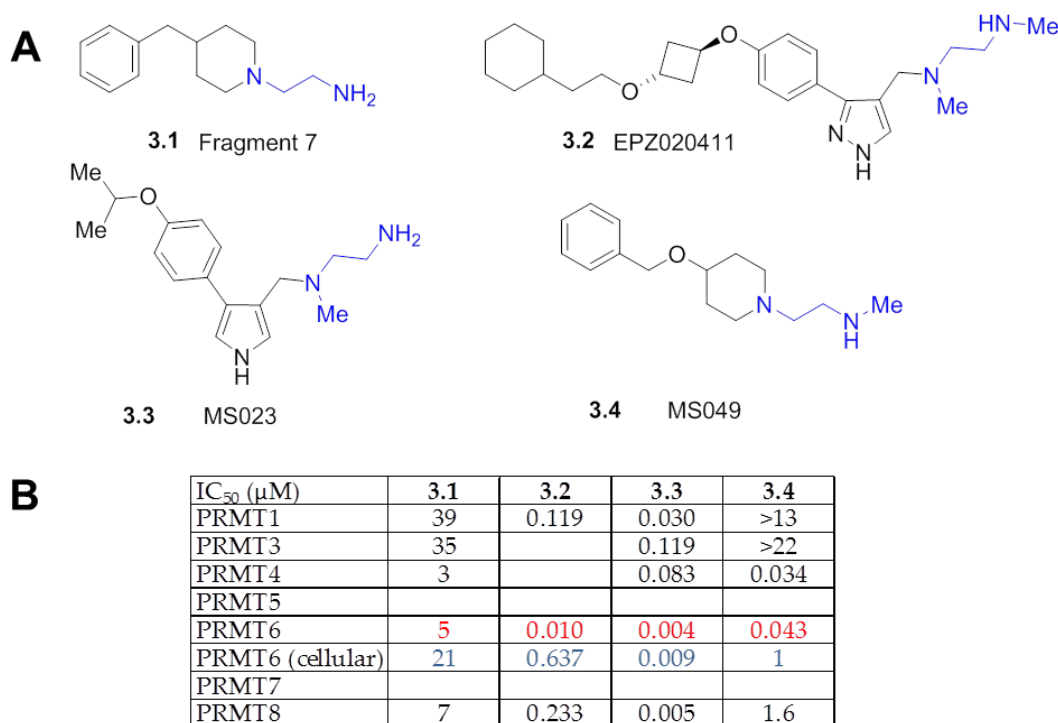


**Figure 3.2: Current Type I PRMTs inhibitors with the display of inhibition towards PRMT6**<sup>22,28,68,125</sup>

(A) Structures of inhibitors that display inhibition toward PRMT6. (B) IC<sub>50</sub> of inhibitors towards PRMTs.

Among the compounds shown in Figure 3.2, compound **3.1**, discovered in a fragment based approach, is a Type I PRMT inhibitor with most potent inhibitory effect towards CARM1 and PRMT6.<sup>68</sup> Compound **3.2** displayed more than 10-fold selectivity between PRMT6 to PRMT1,<sup>22</sup> yet its effect on CARM1 was not mentioned. Therefore it remains unclear whether **3.2** can differentiate CARM1 and PRMT6. Compound **3.3** processed same inhibitory effect towards PRMT6 and PRMT8.<sup>28</sup> Compound **3.4** was reported as a dual inhibitor towards PRMT4 and PRMT6.<sup>125</sup> Therefore, selective small-molecule regulators for PRMT6 remain in demand.

The reported Type I PRMTs inhibitors all possess a diamine side-chain (colored blue in Figure 3.2) mimicking the guanidine group of the arginine substrate, which might limit the selectivity of the small molecule. Our approach was to target both the co-factor *S*-adenosyl-methionine (SAM) binding pocket and the substrate binding pocket specifically of PRMT6, aiming to develop selective small-molecule probes of PRMT6 that can be used for cellular activity studies or potential therapeutic applications. Therefore, we proposed to develop bisubstrate mimic small molecule probes by linking the SAM mimic segment and substrate mimic segment with variable linkers, aiming to achieve higher selectivity towards PRMT6. Such a structure-based approach in designing PRMT6 probes represents a powerful and systematic strategy that was rooted in the methylation mechanisms of PRMTs. This approach combined rational design, PRMT6 structural information, modern computational modeling and chemical synthesis. To

fulfill this approach, we have established the multiple-mode screening system that includes a biochemical direct PRMT6 activity screening assay based on antibody detection of methylated peptide substrate, a cellular direct PRMT6 activity assay based on determination of endogenous H3R2me2a level, and a downstream effect assay using PRMT6 regulated gene p21 mRNA level as reporter, which would be discussed in details in the following sections.

## **3.2 Establishment and Validation of Multiple-mode Assays for Characterization of PRMT6 Inhibitors**

### **3.2.1 Validation of PRMT6 *in vitro* Biochemical Assay**

The measurement of *in vitro* PRMT6 biochemical activity was initiated with the commercially available PRMT6 direct activity assay (BPS Bioscience 52046). In this assay, the immobilized PRMT6 *in vitro* substrate histone H4 peptide substrate was incubated with the reaction mixture containing PRMT6 and the methyl donor S-adenosyl-methionine (SAM). The methylated peptide was then detected with specific anti-methylated histone arginine antibody. We then used SAH and the literature reported PRMT6 inhibitor MS023 (3.3) to validate whether the assay can show the dose responsive effect of the inhibitor treatment and calculate IC<sub>50</sub>. To be noted, the literature reported IC<sub>50</sub>=4 nM of MS023 (3.3) was determined by scintillation proximity assay (SPA),<sup>28</sup> while the IC<sub>50</sub>=0.25 μM in our studies was generated from the antibody based assay (Figure 3.3A), which reflected the difference between the assay's sensitivity. To directly validate the methylation reaction of the PRMT6 on its H4 substrate, we

purchased the H4 1-21 substrate (BPS Bioscience 52018) which was the free peptide version of the assay kit peptide and performed the reaction with the content from the assay, and successfully observed two newly formed M+14 (+ methyl) and M+28 (+ 2 methyl) peaks observed with MALDI-MS (Figure 3.3B). Methylated histone H4 peptide

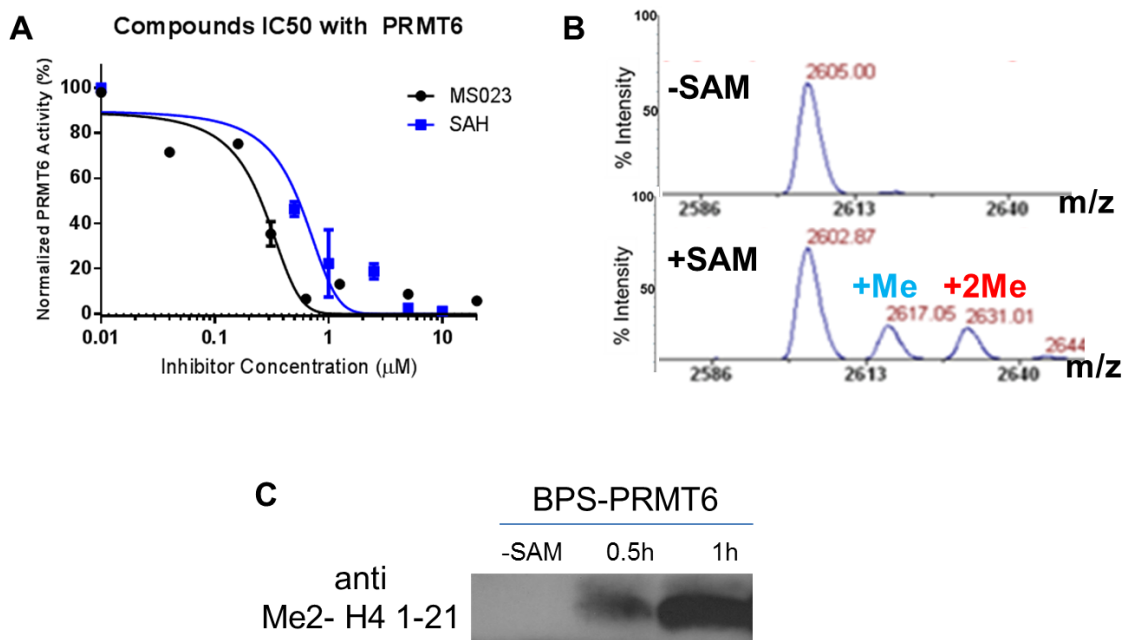


**Figure 3.3: Biochemical validation of PRMT6 methyltransferase activity**

(A) Commercial available PRMT6 antibody-based biochemical assay detected PRMT6 methyltransferase activity and determined IC<sub>50</sub> of SAH and MS023. Histone H4 substrate was immobilized on 96-well plate. Me-Arg substrate was recognized by specific anti-methylated primary antibody and signal was next produced by HRP-labeled secondary antibody. See Appendix A.1 for assay details. (B) Mono- and di-methylated histone H4 substrate generated from PRMT6 activity detected with MALDI proving methylation reaction happened in the commercial assay. See Appendix A.2 for MALDI details. (C) Methylated histone H4 substrate generated from PRMT6 activity detected by specific anti-methylated histone H4 antibody proving the signal from the commercial assay came from Me-Arg.

was also detected by immune-blotting analysis using specific anti-methylated histone arginine antibody from the assay kit (Figure 3.3C). These results suggested the PRMT6 functional biochemical assay had the capability to indicate the methylation of PRMT6 on histone H4 peptide and may serve as a tool for future screening for potential modulators of PRMT6 histone substrate methylation.

### **3.2.2 Expression and Purification of Human PRMT6-His with Insect Cell Sf9 and Determination of its Enzymatic Activity**

*(This part includes collaborative effort. The purification of hPRMT6-His was performed in collaboration with Dr. Tri Nguyen from Dr. Dewey McCafferty's group, Duke University)*

To produce adequate amount of PRMT6 for the development of scalable and robust assays and thermodynamic experiments, we expressed PRMT6 with the Bac-to-Bac Baculovirus Expression System in Sf9 insect cell.

The plasmid pFBOH-MHL-PRMT6(His) encoding hPRMT6-His was kindly provided by Dr. Masoud Vedadi.<sup>28</sup> The transfection, infection of several rounds of baculovirus and expression of hPRMT6-His in Sf9 were performed following the Bac-to-Bac manufacturer's instruction. The PRMT6-His protein was next undergone purification by Ni HisTrap column, sizing Sephacryl S200 column, and SP sepharose cation exchange column. Detailed buffer conditions were provided in the Appendix A Methods and Materials. The PRMT6-His protein we obtained reached up to 95% purity (Figure 3.4A). The expressed PRMT6 was confirmed with anti-PRMT6 antibody at each step (Figure 3.4B).

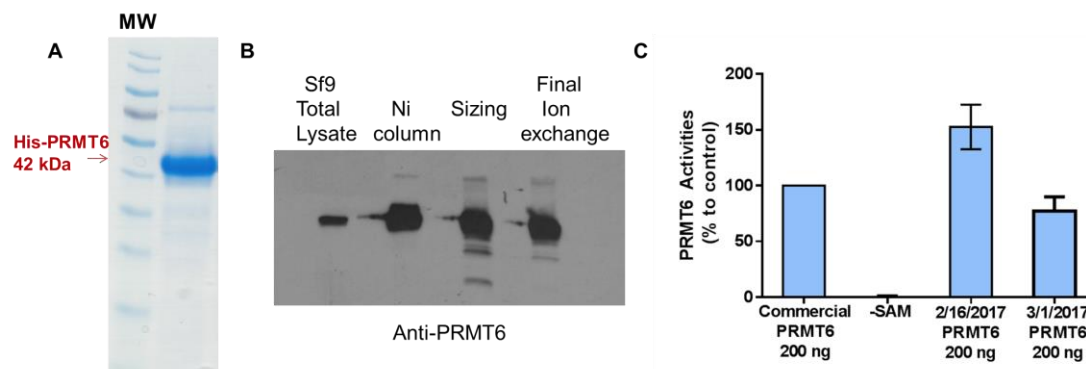


**Figure 3.4: Expression, purification and activity determination of recombinant His-PRMT6 protein**

(A) Commassie stains of SDS-PAGE with partially purified recombinant His-PRMT6 from Sf9 cells and molecular weight markers. See Appendix A.8 for His-PRMT6 purification details. (B) Western blotting confirmation of PRMT6 during its purification procedure. See Appendix A.11 for western blotting details. (C) Antibody-based direct activity assay showed the in-house PRMT6 possessed either higher activity or similar activity as the commercial PRMT6. See Appendix A.1 for assay details.

We next determined the activity of the in-house PRMT6 expressed from Sf9 by using the PRMT6 direct activity assay (validated in 3.2.1). To be noted, the BPS PRMT6 was expressed from *E.coli*. Two representative in-house batches of PRMT6 were compared with the commercial available BPS PRMT6. Figure 3.4C showed that our in-house PRMT6 protein expressed from Sf9 could achieve either similar activity or higher activity in comparison to commercial PRMT6 expressed from *E.coli*. The above experiments have shown the ability and feasibility to express active bulk hPRMT6-His in our lab for future experiment design and scale-up experiment.

### 3.2.3 Development and Validation of Direct PRMT6 Enzymatic Activity Cellular Assay and Downstream Gene Regulatory Effect Assay

Cellular direct activity of PRMT6 was known to be monitored by the methylation level of its cellular substrate H3R2 for the formation of H3R2me2a. Thus, H3R2me2a could be used as cellular indicator to report PRMT6 activity, as well as the effect of PRMT6 inhibitors or PRMT6 siRNA. On the contrary, overexpression of PRMT6 would lead to H3R2me2a accumulation in the cell. Furthermore, the catalytically inactive recombinant PRMT6 V86K/D88A (PRMT6-KLA)<sup>40</sup> was shown to not lead to H3R2me2a upregulation, thus could serve as a control for examining the effects of PRMT6 overexpression in the cells. PRMT6 and PRMT6-KLA plasmids were kindly gifted by Dr. Mark Wainberg's lab from University of McGill.<sup>40</sup>

For the PRMT6 downstream effect, gene p21 was chosen for the downstream assay development. PRMT6 transcriptionally repressed the tumor suppressor gene, cyclin-dependent kinase (CDK) inhibitor gene p21<sup>CDKN1A</sup>, in a p53-independent manner, leading to cancer cell growth and resistance to cellular toxicity reagent.<sup>124,126,127</sup> Moreover, p21 has been reported to be inversely correlated to PRMT6 level in bone osteosarcoma U2OS cell,<sup>124</sup> as well as in breast carcinoma MCF-7 and MD-MBA-231 cells.<sup>127</sup> It was reported that reduction of the PRMT6 protein level by siRNA knockdown was correlated with the accumulation of p21 mRNA.<sup>124,127</sup> Therefore, p21 seemed to be a good candidate for the downstream effect assay for PRMT6 (Figure 3.5).

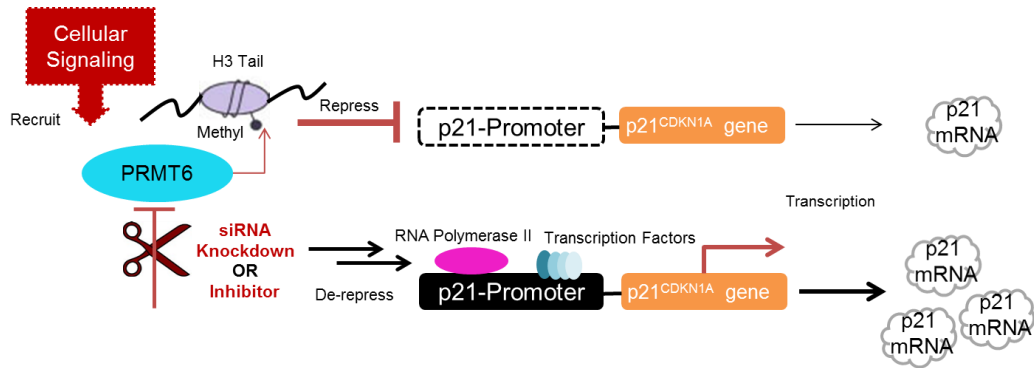


**Figure 3.5: Description of p21 downstream effect assay reporting PRMT6 cellular function**

The direct cellular assay and downstream effect assay was developed using skin malignant melanoma A375 cell line,<sup>22</sup> bone osteosarcoma U2OS cell line,<sup>124</sup> and breast carcinoma MCF-7:WS8 cell line,<sup>127</sup> all of which were previously reported to be working well for assessing cellular activity of PRMT6. A non-cancer cell line, kidney 293T was included as a control. To probe the cellular activity and downstream effect, we first performed overexpression of PRMT6-WT and PRMT6-KLA as well as siRNA knock-down of PRMT6 for initial inquiry. The direct cellular activity was determined by H3R2me2a levels using western blot and the downstream gene regulatory effect was determined by p21 mRNA levels using qPCR assay (Figure 3.6 and 3.7).

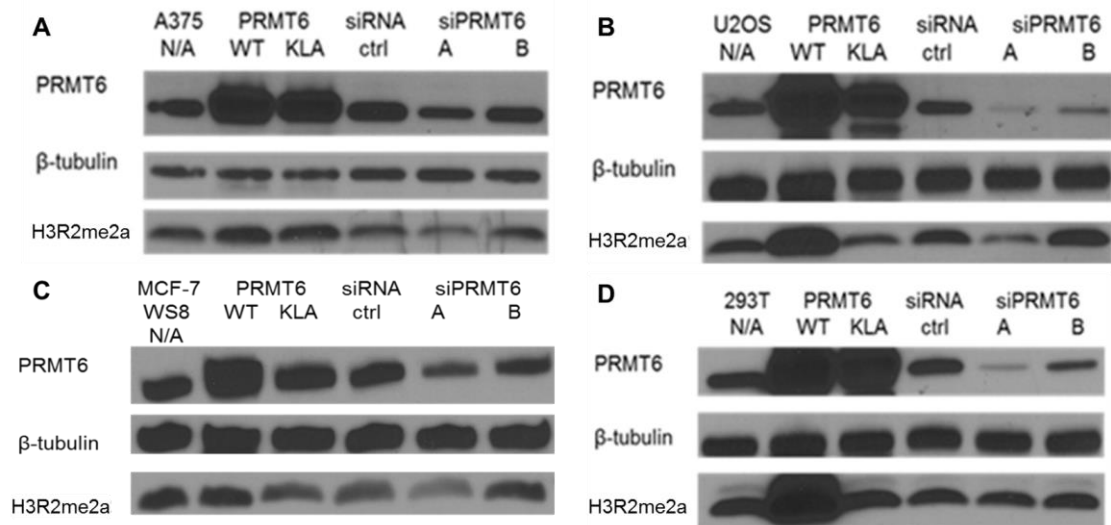


**Figure 3.6: Cellular PRMT6 direct activity assay establishment with H3R2**

Four cell lines were chosen to determine the correlation between PRMT6 level and H3R2me2a level. (A) A375 cell; (B) U2OS cell; (C) MCF-7:WS8 cell; (D) 293T cell. Immunoblotting of lane 1 from each panel shows overexpression of wild-type PRMT6 induced up-regulation of H3R2me2a shown in lane 3, but not with the catalytical disabled PRMT6-KLA mutant; successful knockdown of PRMT6 reduced H3R2me2a level showing the correlation between PRMT6 and H3R2me2a level.  $\beta$ -tubulin in lane 2 served as loading control. Among the four cell lines, U2OS showed the most significant correlation. See Appendix A.12 for PRMT6 knockdown details, Appendix A.11 for western blotting details.

As seen in Figure 3.6, the results on U2OS cell showed best correlation between the PRMT6 level and H3R2me2a level, in either overexpression or siRNA knockdown experiments. The other three cell lines had some degrees of ins and outs. U2OS cell line would be the one to set up the PRMT6 cellular direct activity assay.

From Figure 3.7, the siRNA knockdown of PRMT6 and p21 upregulation was not correlated in A375 cells. MCF-7:WS8 was the most therapeutic related cell line and also showed the correct correlation. Although the fold-upregulation in MCF-7:WS8 was not

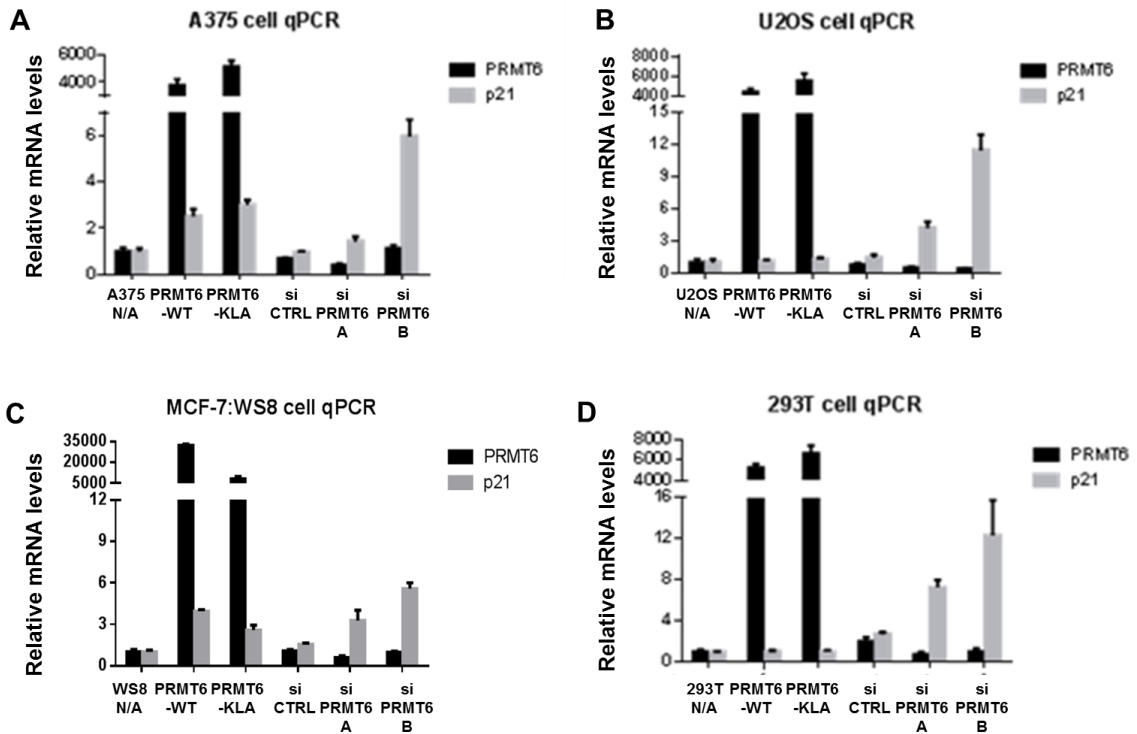


**Figure 3.7: PRMT6 downstream gene regulatory assay establishment with p21 mRNA**

Four cell lines were chosen to determine the correlation between PRMT6 level and p21 mRNA level. (A) A375 cell; (B) U2OS cell; (C) MCF-7:WS8 cell; (D) 293T cell. As repression marker, knockdown of PRMT6 should upregulate p21 mRNA level. All four cell lines showed the correlation between PRMT6 knockdown and upregulation of p21 mRNA. See Appendix A.12 for PRMT6 knockdown details, Appendix A.6 for qPCR details.

as much as in USOS, we would still like to keep this cell line for future experiment. Therefore, the final decision for establishment of the downstream gene regulatory effect assay for PRMT6 with p21 gene would be in model cell line U2OS and therapeutic related cell line MCF-7:WS8 cell line.

### **3.3 Design Rationales of Potential PRMT6 Small Molecule Regulator Targeting SAM-substrate Bi-pockets**

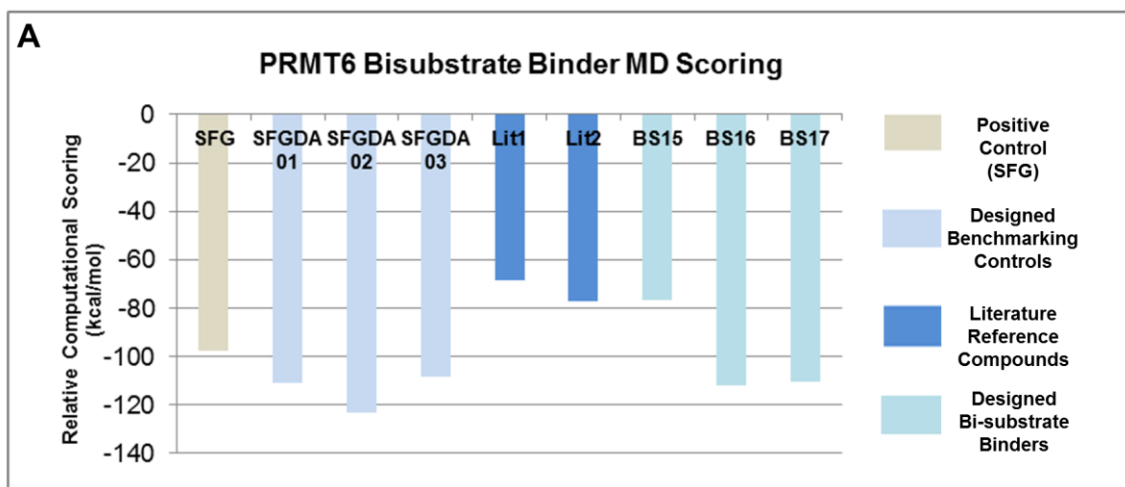
*(This part includes collaborative effort. The computational facilitated compound evaluations was complete by Dr. Yuqi Zhang from Dr. David Beratan's Group, Duke University)*

The design of the bi-pocket targeting regulators towards PRMT6 was deeply rooted in the analysis of the protein structural information. We set up the computational model of PRMT6 with the PDB 5E8R,<sup>28</sup> in which MS023 (3.3) and SAH were co-crystallized with PRMT6. All the scoring was achieved by molecular dynamics. Since there was no previous bi-pocket occupying inhibitor reported, we had no direct benchmark reference. Therefore, we designed 3 SFG-diamine (SFGDAs, Figure 3.8) by linking the bisubstrate mimic as theoretical bi-pocket occupiers for benchmarking the model. As expected, The 3 SFGDA molecules scored better than SFG in the PRMT6 bi-pocket model (Figure 3.8A).

For designing of bi-pocket targeting regulator of PRMT6, we originally started from our previous CARM1 computational small molecule backbone S02 (Figure 2.11). However, after numerous rounds of structural change, those benzimidazole based molecules all failed to have good scores in the PRMT6 model. When we looked deeply into the structural aspect, we noticed that the benzimidazole based molecules always rotate and cannot fix very well in the SAM pocket, and the arginine mimic part therefore cannot point into the substrate pocket. After several round of failures, we finally decided to discontinue on the benzimidazole based molecules.

We next followed up on the SFG-diamine structures that possessed great scores in the PRMT6 bisubstrate computational model in our previous studies. We first searched for similar structures published in literatures, and we found a 2015 paper reporting Lit 1 ( $IC_{50}$  PRMT6 = 20  $\mu$ M) and Lit 2 ( $IC_{50}$  PRMT6 = 0.7  $\mu$ M) (Figure 3.8) with similar structures as SFGDA 03.<sup>84</sup> The paper was intended to design bisubstrate PRMT inhibitor and they found certain modifications on the structure led to Lit 1 possessed selectivity towards CARM1 to PRMT1, PRMT6 and G9a.

With this inspiration, we modified the SFGDA structure aiming to achieve selectivity towards PRMT6. We designed BS 15-17 as Figure 3.8 shows, by eliminating the amino acid moiety of SFGDA to increase selectivity. The computation evaluation towards BS 15-17 was very promising. We planned to synthesize these 3 compounds, as well as SFGDA 02 as a non-selective control.



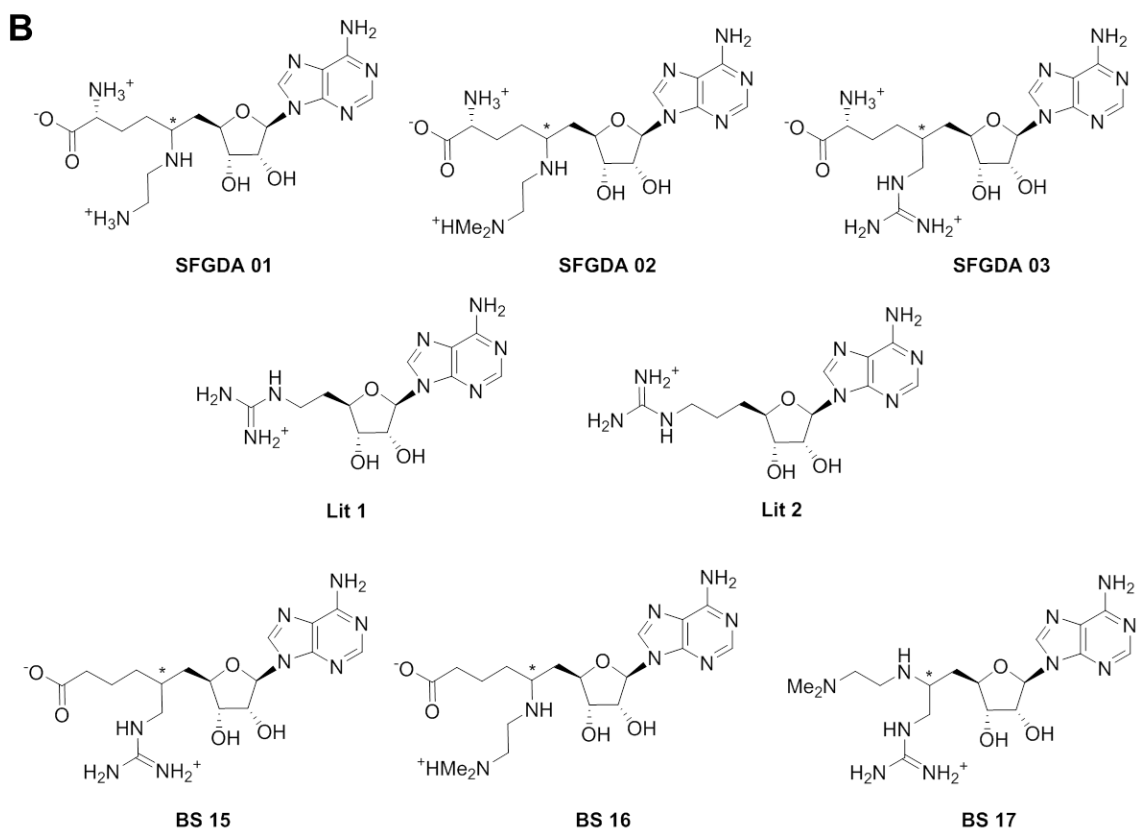


**Figure 3.8: PRMT6 empirical designed benchmarking controls, bisubstrate binders and literature reference compounds**

(A) Molecular dynamic scoring of PRMT6 bisubstrate binders comparing with SFG. All compounds were calculated in R confirmation. (B) Covalent structures of PRMT6 bisubstrate binders. Benchmarking control SFGDA 01-03, literature reference Lit 01-02<sup>84</sup>, and designed bisubstrate binders BS 15-17.

### 3.4 Conclusions and Future Plans

In summary, we have established and validated the PRMT6 biochemical assay which has been used to test the in-house produced PRMT6 protein and PRMT6 inhibitors. H3R2me2a has been validated as direct PRMT6 cellular activity reporter and

p21 mRNA level has been confirmed to show PRMT6 downstream gene regulation effect in our lab.

Four potential PRMT6 bi-pocket targeting compounds from structural facilitated designing and computational facilitated scoring have been chosen to undergo synthesis and can be further assessed through the aforementioned multiple-mode PRMT6 screening system.

## **4. Design of a Small Molecule Fluorescence Polarization (FP) Probe for Quantitative Analysis of PRMT6**

### ***4.1 Introduction: Fluorescence Polarization, Basic Principle and Current Applications in Drug Discovery***

#### **4.1.1 Fluorescence Polarization Assay is a Good Tool for Assessing Macromolecule–small Molecule Interaction**

Fluorescence polarization (FP) is a versatile solution-based technique that has been widely used to study molecular interactions and enzymatic activities. The principle of the FP assay is based on the nature of fluorophores upon being excited by plane-polarized light, about 60% of emission light would be detected in the same plane as that of the exciting light,<sup>128</sup> while the degree of polarization of the plane-polarized light excited fluorophores would be largely depolarized due to the molecular rotation driven by Brownian motions.<sup>129</sup> The theoretical basis of FP was first described by Francis Perrin in 1926,<sup>130</sup> where he used rotational correlation time ( $\theta$ ), defined as the time taken for a spherical molecule to rotate through an angle of 68.5°, to quantitatively describe the changes in FP.

$$\theta = \frac{3\eta V}{RT} \quad (1)$$

In equation (1),  $\eta$  refers to viscosity of the solution;  $V$  refers to volume of the spherical molecule;  $R$  as the universal gas constant and  $T$  as temperature. Therefore, since FP is in proportional to  $\theta$ , as dissolving and detection conditions are kept the same, the FP differences between molecules are solely dependent on the molecular size. Thus,

a small fluorophore in its bound or unbound status to a macromolecule (i.e. protein, DNA or polymer) can be differentiated by FP values.

Two decades later, in 1950s, the first instrument measuring FP was invented by Weber,<sup>131</sup> where he used parallel ( $I_{//}$ ) and perpendicular ( $I_{\perp}$ ) filters to collect the emission light and calculate the FP as difference between  $I_{//}$  and  $I_{\perp}$  normalized to the total emission intensity.

$$FP = \frac{I_{//} + I_{\perp}}{I_{//} - I_{\perp}} \quad (2)$$

This equation provides the bases of quantitative analysis of FP data and enables binding affinity dissociation constant  $K_D$  and inhibitory constant  $K_I$  determination. From the equation, it is shown that FP is a dimensionless quantity and is not correlated to concentrations of fluorophores or macromolecules that they are bound to. In literature, FP is usually reported as mille polarization ( $mP = P/1000$ ) and the actual read-out is the difference of mP ( $\Delta mP$ ) between free fluorophore and the fluorophore bound with different concentrations of macromolecules.

In conclusion, FP is a quantitative technique to analysis macromolecule – small molecule interactions. Based on equation (1), a small fluorescence molecule is likely to reorient comparing to when it's bound to a large molecule during the interval between absorbing and emitting light (Figure 4.1), which is about several nanoseconds for most

of the commonly used fluorophores.<sup>132</sup> And equation (2) provides the quantitative basis for FP measurement and calculation.

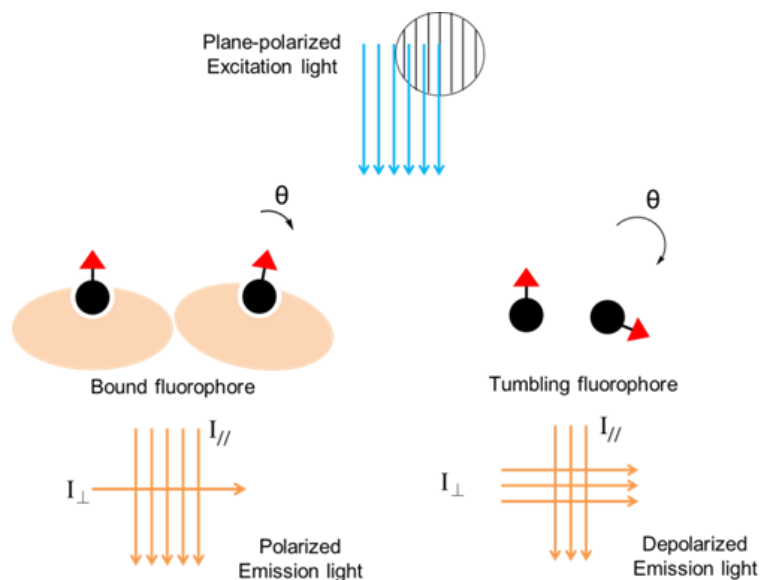


**Figure 4.1: Description of fluorescence polarization binding small fluorophores that change polarization between bound and unbound status**

#### **4.1.2 Considerations in Development of FP assay: Strengths and Drawbacks**

The versatility of FP assay enables its applications from HTS to thermodynamic constant determination such as  $K_D$ . Compared to activity based HTS assays, the mix-and-read nature of FP assay enables much more rapid preliminary screening and can be repetitively measured as the FP reading neither requires separation step nor destroys the sample.<sup>129</sup> Compared to methods measuring thermodynamic constant such as isothermal titration calorimetry (ITC) or surface plasmon resonance (SPR), the amount of expensive reagent (i.e., purified protein) needed is largely reduced. One drawback step FP assays is that it needs a fluorophore labeling step, which might be cumbersome or challenging.

The interference of protein-probe interaction after fluorophore-tagging is like a “black hole” prior to actual assay, while computation facilitated molecular modeling can facilitate the fluorophore-tagged probe design but may not be applicable to all cases.<sup>132</sup> The data of current successful and failed fluorophore labeling cases did not provide adequate evidence for prediction of the outcome.<sup>132</sup> Therefore, the risk of the labeling step is something must be born.

In the HTS FP assay, the fluorophore-tagged probe usually serves as a tracer of the protein, which is being competitively replaced by other compounds being screened. For a typical competitive assay, the tracer will be added at its  $K_D$  value,<sup>132</sup> at which the bound vs unbound population would be 1:1 when  $[\text{protein}] = [\text{tracer}]$ , and the protein concentration is kept at the level that allows 50-80% tracer to be bound. Therefore, the protein amount required for each reaction is dependent on the  $K_D$  of the tracer, that is, the affinity of the tracer to the protein. In this case, the higher the affinity is, the lower the  $K_D$  would be, and the less amount of protein would be required for the HTS screening. If the  $K_D$  of the tracer is  $> 10 \mu\text{M}$ , the problem would be limited to not only the amount of the protein required, but also potential solubility and aggregation issues of the protein. Most of the current available FP tracers possess  $K_D$  between 1 nM to 100 nM,<sup>132</sup> and FP cannot be used to study weak binding due to this limitation.

### 4.1.3 Application of FP in Drug Discovery

Since application of FP in HTS in the 1990s, FP has played an important role in drug discovery and probe development. In theory, FP can quantitatively analyze any soluble small fluorophores bound to a soluble macromolecule. And in the past few decades, some researchers used FP assay to quantify protein-ligand, DNA/RNA-ligand and protein-protein/peptide interactions, and the detection mechanism can be basically classified into 1) detection of direct binding, and 2) detection of coupled enzymatic activities.

The detection of direct binding is also called non-turnover enzymatic assay under the circumstance that the fluorophore-labeled ligand is the substrate. The non-turnover assay is especially useful for inhibitor discovery towards enzymes that requires more than one substrate with random bi-bi mechanism, and inhibitors occupying different sites can be discovered through different fluorophore labelling strategies. However, the  $K_D$  of the substrates to the enzymes often falls in the  $\mu\text{M}$  to  $\text{mM}$  range, and as aforementioned, is considered as rather weak binding thus required relatively large quantity of protein to set up the HTS assay. Therefore, under most circumstances, the direct binding detection was achieved by a high affinity fluorophore labeled small molecule inhibitor or short peptide against the target enzyme, which served as the tracer. Novel inhibitors that can replace the tracer can then be discovered. Detection of direct binding is the most straightforward application of FP in drug discovery, which has been

applied to a variety of targets including GPCRs, nuclear receptors, ion channels, epigenetic regulators, and transcription factors.<sup>132</sup>

The other class of FP assay, which couples enzymatic reactions in the process, can be classified into fluorescence polarization immunoassay (FPIA, antibody incorporated method) and antibody-free methods. These two formats share the same idea, that when a fluorophore labeled substrate is bound to its specific antibody or other affinitive large molecule, such as immobilized metal ion affinity particle (IMAP), under enzymatic activities, for example, kinase activity, that produce more antigen for the antibody which therefore competes with the affinity interactions and releases the fluorophore tracer and generates FP read-out. The assay coupled with enzymatic activities makes discovery of allosteric inhibitors possible, however, it requires the affinitive large molecules to be highly specific. This type of FP is commonly seen in applications for kinases, phosphatase, DNase, RNase and protease.<sup>132</sup>

#### **4.1.4 Emerging Applications of FP in Epigenetic Field: Meeting the Unmet Needs**

FP has caught great attention since its application in study of kinases in 2000s, and its potential application in epigenetic study has recently been more and more recognized. Similar to the study of kinases, the most representative and sensitive conventional HTS method to assay epigenetic enzymatic activities is the radiometric assay, which comes along with time-consuming assay set-up, highly costly isotopic labeled cofactors and its biohazardous affects.<sup>133</sup> To overcome these problems, efforts

have been made towards establishing antibody based ELISA-like assays. However, this has never really replaced the radiometric assay due to its limitations of non-homogeneous set-up, semi-quantitative nature, and high variations due to the specificity of antibody recognition. The most recent developed homogeneous antibody-based AlphaScreen/AlphaLISA assays fixed the problem of non-homogeneity, it still had antibody recognition problem and introduced new problem of singlet oxygen quencher intolerance due to the mechanism of Alpha assay's luminescent oxygen channeling nature.<sup>134</sup> An enzyme coupled assay developed for methyltransferases, by monitoring the by-product SAH (*S*-adenosyl-*L*-homocysteine, product of co-factor SAM removal of methyl group) of the methyltransferases activity which was further degraded by several enzymes to homocysteine and can be subsequently monitored by colorimetric or luminescent assay,<sup>135</sup> having bypassed the weakness of radiometric and antibody-based assays. However it is sensitive to pH, temperature and light due to the involvement of numerous enzymes and has high false-positive rate. Therefore, there is still a lot to do for development of reliable FP HTS assays for epigenetic enzymatic activities.

Application of FP in epigenetic studies may or may not involve small molecules. FP assays without small molecules was first developed as the non-turnover enzymatic assay as mentioned in 4.1.3, and is available for lysine methyltransferase G9a<sup>136</sup> and arginine methyltransferase PRMT1.<sup>137</sup> Other than the direct FP detection method, the SAH detection for methyltransferase activity has been developed into a competitive

FPIA assay.<sup>138</sup> A specific antibody was used to bind fluorophore-tagged SAH, and as the methyltransferase reaction going on, more SAH was produced to compete with the fluoro-SAH, which was then released, generating FP read-out. Limitations for non-turnover enzymatic assays, as mentioned also in 4.1.3, is the low affinity binding between the substrate and the enzyme, which thus limited their use in the HTS. And the antibody coupled competitive FPIA assay for SAH bears same disadvantages as all antibody coupled assays: antibody recognition specificity issues. Therefore, high affinity small molecule inhibitors/binders coupled FP assays is highly desired due to the advantages of homogeneous reaction, sensitive read-out, antibody-free nature, and less protein required for HTS.

Fluorophore tagged high affinity small molecule inhibitors have only been reported for jumonji domain-containing histone demethylases (JHDMs),<sup>81</sup> DNA hydroxylase,<sup>139</sup> histone deacetylase (HDAC)<sup>140</sup> and a commercial SAM-Screener assay including a nano-molar affinity fluorophore tagged SAM-pocket occupying probe that is available for several protein lysine methyltransferases (PKMTs), SET7/9, MLL1, and G9a.<sup>133</sup> A special case of high affinity small molecule binder coupled FP assay has been recently reported for PRMT1 and PRMT8.<sup>141</sup> In this special case, the high affinity small molecule involved was not an inhibitor, but a fluorophore tagged thiol reactive maleimide that covalently binds to a hyper-reactive cysteine residual, which directly contact with SAM in the binding pocket and is only conserved in PRMT1 and 8 but not

in other PRMTs. And small molecule hits from such assay is highly specific towards PRMT1 and 8 with the ability of interrupting the thiol binding.

The above evidence showed that high affinity small molecule inhibitor/binder coupled FP assays is of great potential use and development of reliable FP probes of target of interest is in great demand. Next, we will focus on our work for development of a PRMT6-specific FP probe.

## **4.2 FP Probe Design and Synthesis**

*(This part includes collaborative effort. The compound synthesis was complete by Dr. Kun Shen from Dr. Qiu Wang's Group, Duke University)*

To design the FP probe targeting PRMT6, we started with the current most potent inhibitor of PRMT6 reported in literature, MS023 (**3.3**). We initially tried to link a fluorescein to it to form MS023-fluoro (**4.1**), but failed to achieve. We then designed and successfully synthesized MS023-CC-flouro (**4.2**) where we inserted a two-carbon-linker and switched the end from oxygen to nitrogen to make the sulfur easier to attach. We also synthesized MS023-CC-N (**4.3**) as a negative control compound.

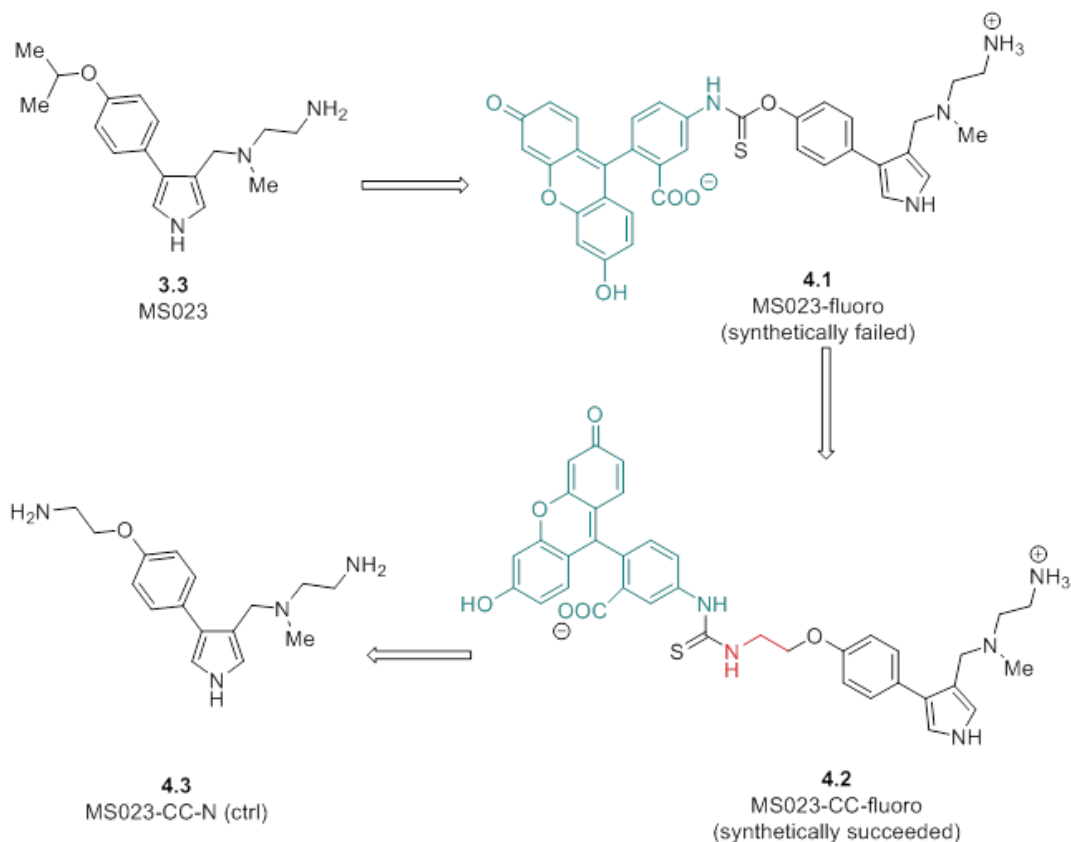
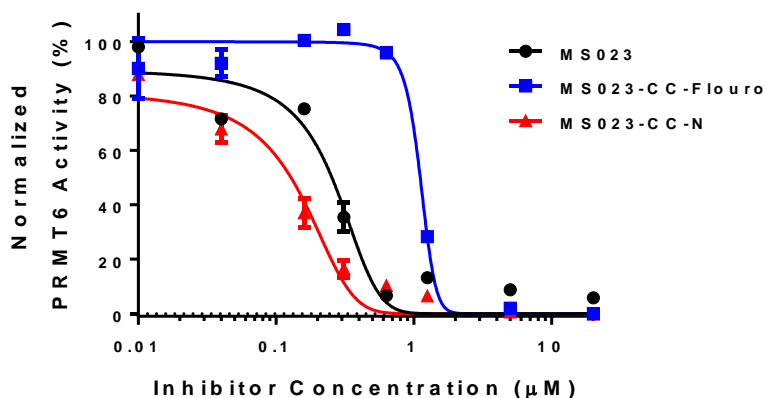


Figure 4.2: The design of PRMT6 FP probe

### 4.3 Optimization of Experimental Conditions for FP Assay by Quantitative Analysis of PRMT6 Binding

#### 4.3.1 Inhibitory Effect of Fluoro-tagged Probe against PRMT6 in Biochemical Assay

After obtaining MS023-CC-flouro (4.2) and MS023-CC-N (4.3), we tested them with the PRMT6 biochemical assay that we have validated in 3.2.1, together with MS023 (3.3).



**Figure 4.3: IC<sub>50</sub> of MS023 and derivatives with PRMT6**

The IC<sub>50</sub> was determined with the antibody-based assay validated in chapter 3.2.1. The compounds concentrations started from 20 µM and 4-fold dilution until reached 0.01 µM. See Appendix A.1 for assay details.

$$IC_{50} \text{ MS023 (3.3)} = 0.25 \pm 0.037 \mu\text{M};$$

$$IC_{50} \text{ MS023-CC-flouro (4.2)} = 1.11 \pm 0.059 \mu\text{M};$$

$$IC_{50} \text{ MS023-CC-N (4.3)} = 0.13 \pm 0.017 \mu\text{M}.$$

The IC<sub>50</sub> of 4.2 and 3.3 had ~ 5-fold difference; 4.2 and 4.3 had ~ 10-fold difference, which was quite a big gap, indicating that after the addition of the fluorescein, the affinity of the MS023 to PRMT6 may drop a lot.

### 4.3.2 ITC Determination of PRMT6 and Fluoro-tagged Probe Binding Affinity

Isothermal titration calorimetry (ITC) is the direct equipment that can detect the binding affinity ( $K_d$ ) between two molecules by measuring the heat change during the titration. The titration of MS023 to PRMT6 and MS023-CC-F to PRMT6 was performed.

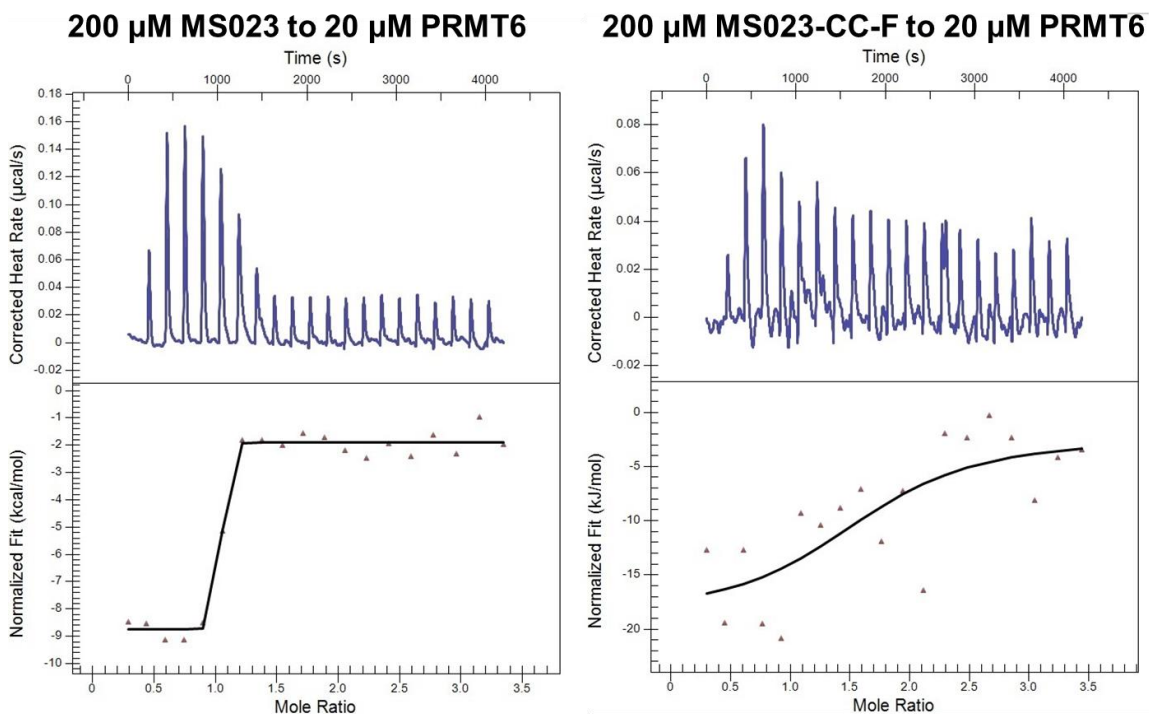


**Figure 4.4: Determination of affinity constant ( $K_d$ ) between PRMT6/MS023 and PRMT6/MS023-CC-F with ITC titration**

The ITC result showed MS023-CC-F possessed much lower affinity comparing to the parent molecule MS023 against PRMT6. See Appendix A.13 for ITC details.

The  $K_d$  of MS023 to PRMT6 was calculated as 1.6 nM, which was similar to the literature reported 6 nM.<sup>28</sup> But from Figure 4.4, we can see that the points for the regression curve of MS023-CC-F was too random which making the  $K_d$  (3.5  $\mu$ M) untrustworthy. Increasing concentration of PRMT6 might be needed for optimizing MS023-CC-F ITC experiment condition. However, we found that the highest peak from the MS023-CC-F – PRMT6 titration is about 0.08  $\mu$ cal/s which is much lower than MS023-PRMT6 titration 0.16  $\mu$ cal/s, indicating the lower affinity between the fluor-probe and PRMT6.

### 4.3.3 FP Binding Assay for PRMT6

To set up the MS023-CC-F PRMT6 FP binding assay, we chose 10 nM of MS023-CC-F based on the known minimal requirement of concentration for sufficient FP signals read-out.<sup>132</sup> Multiple rounds of experiment were performed and the least coverage and the most coverage were shown in Figure 4.5.

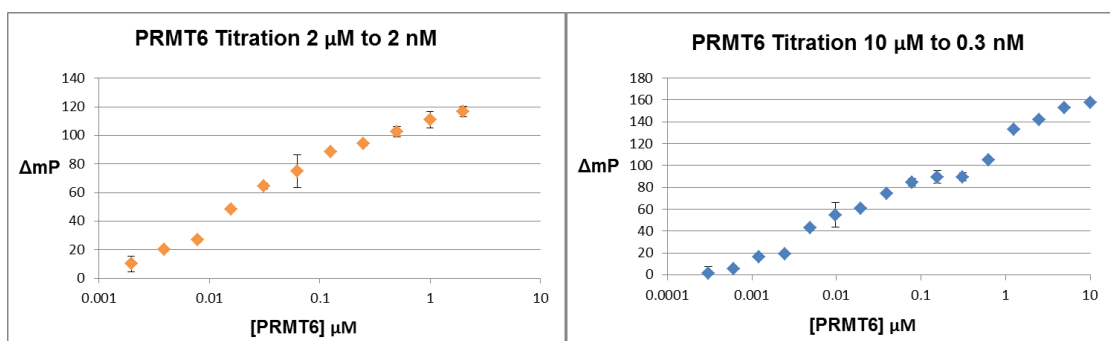


**Figure 4.5: Optimization of binding conditions for MS023-CC-F and PRMT6 in FP assay format**

10 nM of MS023-CC-F was fixed in the titration and PRMT6 concentrations were varied. Up to 10 μM of PRMT6 was tested but no signal saturation was reached indicating the affinity between MS023-CC-F and PRMT6 was low and not enough for further assay optimization. See Appendix A.14 for FP assay details.

The FP binding assay was performed with fixed concentration of fluorophore tagged small molecule and the concentrations of the protein were titrated. From Figure 4.5, we could see that, up to 10 μM PRMT6 titration, no saturation was observed, which indicated that the affinity of the MS023-CC-F to PRMT6 was very low. For protein titration, 10 μM was already a quite high concentration. A protein fluor-probe pair with high binding affinity was required since 1) in later experiment where appropriate

resolution of nonfluorescent inhibitors in an FP competition assay was needed,<sup>142</sup> and 2) less amount of total protein would be needed to set up HTS assay.

Based on the above information, our data showed that MS023-CC-F could not be a good candidate of probe for PRMT6 FP assay due to the lack of high affinity.

#### ***4.4 Conclusions and Future Plans***

As our experiment indicated, MS023-CC-F has low affinity to PRMT6 and may not be a good candidate of probe for PRMT6 FP assay.

We plan to try link other fluorophores to MS023, such as BIODIPY that contains longer carbon chains, and see how the binding affinity will change. We also plan to fluorescently label and test out the SAM pocket targeting or even SAM-substrate bi-pocket targeting inhibitors we discussed in Chapter 3 for PRMT6 FP assay.

## 5. Conclusions

CARM1 and PRMT6 have been found to have crucial roles in various diseases, most notably in cancer. Small molecule probes therefore can serve as valuable tools to study their functions under physiological or disease conditions.

In the work of this thesis, we have achieved designing novel small molecule probes toward CARM1 and PRMT6. Through computational facilitated *in silico* screening and empirical optimization, a final 14-compound library containing inhibitors and negative controls were readily for future synthesis for CARM1. And with structural-based empirical inhibitor design, 4 compounds have been finally chosen for future synthesis for PRMT6.

In order to validate these compounds, we established multiple-mode screening system including biochemical activity assays, cellular activity assay, and downstream-gene regulatory assay. All of the assays have been validated in our lab for both CARM1 and PRMT6. However, the downstream gene assay for CARM1 has been failed after numerous trails and need further assessment.

Our efforts also involved the development of a florescence probe for florescence polarization (FP) assay of PRMT6. This effort did not finally yield with a PRMT6 FP probe since after linkage the fluorescence tag to the PRMT6 small molecule inhibitor, the affinity of the probe was too low. Therefore, the fluor-probe cannot serve as the PRMT6 FP probe due to low affinity and high affinity binder is desired.

# Appendix A

## Material and Methods

**A.1 CARM1/PRMT6 direct activity assay.** The CARM1 (BPS Bioscience 52041L)/PRMT6 (BPS Bioscience 52046) direct activity assay was applied according to the manufacturer's instruction. Briefly, final volume of 50  $\mu$ L reaction mixtures contained 1x HMT assay buffer 6, 100 ng CARM1 or PRMT6 enzyme, 1  $\mu$ M SAM, with or without 10  $\mu$ M compounds in 0.2% DMSO were added to the CARM1/PRMT6 histone peptide substrate pre-coated strips and incubated for 1 hour. The strips would be washed three times TBST and in blocking buffer for 10 minutes with shaking and primary antibody for specific methylated substrate was then incubated for 1 hour in 1:100 dilution followed by the same wash and HRP-conjugated secondary antibody for 30 minutes incubation with moderate shaking in 1:1000 dilution followed by the same wash. The strips would then be added with HRP chemiluminescent substrate and read luminescence signal in a luminomitor.

**A.2 MALDI mass spectrometry confirmation of CARM1/PRMT6 methylation activity.** 1.2  $\mu$ M CARM1/PRMT6 histone peptide substrate (for CARM1, H3 substrate BPS Bioscience Biotin-H3 1-21 52011; for PRMT6, H4 substrate BPS Bioscience Biotin-H4 1-21 52018) was incubated with the reaction mixture containing 0.002  $\mu$ g/ $\mu$ L CARM1/PRMT6 enzyme, 1  $\mu$ M SAM in 1 x HMT buffer. The reactions were terminated by purification of the peptide with Ziptip C18. The Ziptip C18 was first wet with 100% acetonitrile and equilibrated with 0.1% trifluoroacetic acid. Binding of the peptide to Ziptip C18 was performed by aspirating the reaction mixture with the tip. The Ziptip C18 was next washed with 0.1% trifluoroacetic acid. The peptide was eluted by  $\alpha$ -cyano-4-hydroxycinnamic acid (HCCA) matrix solution (70% acetonitrile, 30% dH<sub>2</sub>O, 0.1% trifluoroacetic acid, 10mg/ml HCCA) and then analyzed for mass by MALDI TOF MS.

**A.3 CARM1-Myc-FLAG enzyme expression and purification.** Human kidney 293T cells were incubated in DMEM with 10% FBS and was seeded in 6x 15 cm dishes. After 48 hours of CARM1-FLAG-Myc plasmid (Origene RC217483) transfection, the cells were washed with PBS and then harvested by TBS with 1 mM EDTA lysis buffer supplied with 1% of protease inhibitor cocktail followed by 6 rounds of 10 seconds sonication and 20 seconds rest on ice. The FLAG-tagged protein was then purified with ANTI-FLAG M2 (Sigma F3165) affinity resin following the manufacture's protocol.

**A.4 CARM1 siRNA knockdown with PABP1-GFP transfection.** The CARM1 siRNA was synthesized from Qiagen: GUAACCUCCUGGAUCUGAAAdTd. In a cell culture

coated 6-well plate,  $3 \times 10^5$  of 293T was seeded. After the cell reached 60-70% confluency, 50 nM of siRNA treatment with 5  $\mu$ L of siTrans reagent per well, 56 hours of siRNA treatment followed by 48 hours of PABP1-GFP lipofectamine transfection will be treated.

**A.5 PSA-luciferase assay in LNCaP.** LNCaP cells was seeded in white 96-well plate with  $1.5 \times 10^4$  per well in phenol-red free RPMI with 10% charcoal depleted FBS. For siRNA treatment, the siRNA solution was plated in the wells first before the seeding. After 48 hours of incubation, 0.18  $\mu$ g of PSA-luc plasmid (kindly provided by Prof. McDonnell from Duke University) and 0.02  $\mu$ g of CMV-REN (Promega) plasmid were transfected to the cells for 24 hours, followed by 10 nM R1881 treatment for 24 hours. For the compound treatment,  $1.5 \times 10^4$  LNCaP cells was seeded in the 96-well plate for 24 hours and then transfected with plasmids for 8 hours followed by 24 hours of R1881 treatment. The PSA-luc signal was detected by the Dual-Luciferase Reporter Assay System (Promega) following the manufacturer's protocol, with gain at 250 for 5 seconds for PSA-luc signal and gain at 150 for 2 milliseconds for CMV-REN signal on the Biotek Synergy H1 plate reader.

**A.6 Reverse transcription PCR and qPCR.** Total cellular RNA was isolated using Trizol reagent (Invitrogen) following manufacture protocol. First strand cDNA was synthesized with oligo dT primers with iScrip cDNA Synthesis Kit (BIO-RAD) according to the manufacturer's directions and subjected to qPCR analysis in triplicate using LightCycler Multiplex DNA Master Mix (Roche). The following primer and probe sequences were used: GRP49 forward,<sup>55</sup> 5'- ACCTTGGCCCTGAACAAAATAC-3' ;GRP49 reverse,<sup>55</sup> 5'- ATGTAGAACTACCAAGCTGGAG-3'; Axin2 forward,<sup>143</sup> 5'- GGCAGCATTGAACCAGAGGAG-3'; Axin2 reverse,<sup>143</sup> 5'- GCATGAACTTGGTCACCTTCTG-3'; CARM1 forward, 5'- ACAAGCTTATGGCAGCGGC-3'; CARM1 reverse, 5'-GGAATTCGCTTAGCTCCC-3'; RAR $\beta$ 2 forward, 5'-GACTGTATGGATGTTCTGTCAG-3'; RAR $\beta$ 2 reverse, 5'- ATTTGTCCTGGCAGACGAAGCA-3'; PRMT6 forward,<sup>55</sup> 5'- AGACACGGACGTTTCAGGAG-3';PRMT6 reverse,<sup>55</sup> 5'-CCACTTTGTAGCGCAGCAG-3'; p21 forward,<sup>143</sup> 5'-GGCAGACCAGCATGACAGATTTC-3'; p21 reverse,<sup>143</sup> 5'- CGGATTAGGGCTTCTTGG-3'; GAPDH forward,<sup>50</sup> 5'- GTCATGGGTGTGAACCATGAGA-3'; GAPDH reverse,<sup>50</sup> 5'- GGTCATGAGTCCTTCCACGATAC-3'.

**A.7 SuperTopFlash (STF) luciferase assay for Wnt3A control.** STF cells was seeded in black 96-well plate clear bottom with  $1.5 \times 10^4$  per well in cultural medium. For siRNA treatment and compound treatment, the 100 nM siRNA solution or 20  $\mu$ M compound solution was added to the wells 16 hours after seeding. After 48 hours of incubation, 0.02  $\mu$ g of CMV-REN (Promega) plasmid were transfected to the cells as internal control for

24 hours, followed by Wnt3A CM treatment for 7 hours. The luciferase signal was detected by the Dual-Luciferase Reporter Assay System (Promega) following the manufacturer's protocol, with gain at 250 for 2 seconds for STF-luc signal and gain at 150 for 2 milliseconds for CMV-REN signal on the Biotek Synergy H1 plate reader.

**A.8 Expression and purification of PRMT6.** pFBOH-MHL-PRMT6(His) plasmid encoding hPRMT6-His (N-terminal 6xHis tag) was kindly provided by Dr. Masoud Vedadi.<sup>28</sup> The transfection and infection protocol was following the manufacture instruction of Bac-to-Bac Sf9 expression system (ThermoFisher). The Sf9 cells were kindly provided by Dr. Donald McDonnell's group from Department of Pharmacology and Cancer Biology, Duke University. The harvested Sf9 cells were re-suspend in 50 mM Tris-HCl (pH 7.5), 300 mM NaCl, 10% glycerol, 0.6% NP-40, 5 mM imidazole, fresh added with 2 mM beta-mecaptoethanol (BME), 0.1% protease inhibitor cocktail (Sigma), 1 mM PMSF, then pass through ice-cold cell cracker 5 times for cell lysis. Clarify the cell lysate by 45 mins high-speed centrifuge at 40,000 g, then loaded onto 1 mL HisTrap column (GE). Wash the column with FPLC with wash buffer 50 mM Tris-HCl (pH 7.5), 300 mM NaCl, 10% glycerol, 2 mM beta-mecaptoethanol (BME) and elution buffer 50 mM Tris-HCl (pH 7.5), 300 mM NaCl, 10% glycerol, 2 mM beta-mecaptoethanol (BME), 250 mM imidazole. Gradient wash the column with 0%, 30%, 55% of elution buffer for 10 column volume and final elute the PRMT6-His with 100% elution buffer. Further purify the PRMT6-His protein with sizing Sephacryl S200 column equilibrated with 50 mM NaH<sub>2</sub>PO<sub>4</sub> (adjust pH 7.5 with NaOH), 2 mM beta-mecaptoethanol (BME), then pass through 1 mL SP sepharose cation exchange column in the same buffer. Concentrate the protein down and storage in 100 mM HEPES-NaOH (pH 8.0), 200 mM NaCl, 10% glycerol, 2 mM EDTA, 2 mM beta-mecaptoethanol (BME).

**A.9 Crystallization of PRMT6.** Purified PRMT6 (5 µg/µL) dissolved in 20 mM HEPES-HCl (pH 7.5), 25 mM NaCl, 0.5 mM TCEP was crystalized with sitting drop vapor diffusion method at room temperature by mixing 0.1 µL protein solution with 0.1 µL of reservoir solution containing 0.1 M Tris-HCl (pH 7.0), 0.2 M MgCl<sub>2</sub>, 10% w/v PEG 8000.

**A.10 Cell culture.** For CARM1: 293T/17 cells, SuperTopFlash cells and Hela cells were incubated in DMEM with pyruvate and 10% FBS. RKO cells were incubated in MEM and 10% FBS. Cells were seeded in 96-well plate 24 hours before compounds treatment. All compounds were added in a final concentration of 0.1% DMSO. Detection assays were applied after 24 hours after compound addition. For Wnt3A CM and Ctrl CM preparation, L-Cells and LWnt3A-Cells were cultured in DMEM with pyruvate and 10% FBS for 72 hours then medium change for another 72 hours. Combined 2 batches of CM will be filtered with 0.22 µM filtrate and aliquot to storage at -20 °C. For continuation, LWnt3A-Cells should be cultured with 0.4 mg/ml G-418 in culture medium.

For PRMT6: 293T/17 cells and A375 cells were incubated in DMEM with pyruvate and 10% FBS. U2OS cells was incubated in McCoy's 5a and 10% FBS. MCF-7:WS8 cells was incubated in F-12/MEM 50/50 and with pyruvate and 10% FBS.

**A.11 Western blotting.** After SDS-PAGE, the transferring was performed with PVDF membrane for 1 hour with 100 V. Blocking was performed with 5% non-fat milk in TBST for 1 hour. Primary antibody was incubated under 4°C for 16 hours with 5% BSA in TBST with shaking. After 3 x 10 mins wash with TBST, secondary antibody was incubated under room temperature for 3 hours with 5 % non-fat milk in TBST. Visualization was performed with auto radiation with optimized exposure time. Most antibodies were purchase from Cell signaling, which are anti-CARM1 (#3379) [1:1000],  $\beta$ -Actin (#4970) [1:4000], Me-PABP1 (#3505) [1:4000] and from Abcam anti-GFP (ab6556) [1:4000], anti-PRMT6 (#14641) [1:1000],  $\beta$ -Tubulin (#2146) [1:2000], anti-p21 (#2947) [1:2000] and from Millipore anti-H3R2me2a (04-808) [1:1000]. Secondary anti-Rabbit (#7074) [1:2000 for CARM1, 1:4000 for the rest] and anti-Mouse (#7076) [1:4000] were purchased from Cell Signaling. The numbers in brackets are the dilutions used for the antibodies.

**A.12 PRMT6 overexpression or siRNA knockdown.** In a cell culture coated 6-well plate,  $3 \times 10^5$  of 293T and  $4 \times 10^5$  of A375, U2OS, MCF-7:WS8 was seeded. After the cell reached 60-70% confluency, siCtrl 5'-AUGAACGUGAAUUGCUCAA-3' 50 nM; siPRMT6A 5'-GCAAGACACGGACGUUUCA-3' 50 nM; siPRMT6B 5'-GGAGGGAGAGUGACUUCAU-3' 20 nM was transfected with 9 uL of Lipo RNA Max for 72 hours or PRMT6 plasmid or PRMT6-KLA plasmid 3 ug was transfected with Lipo 2000 for 72 hours, then analyzed with western blotting.

**A.13  $K_d$  determination with ITC.** MS023 was purchase from Sigma, MS023-CC-F was synthesized in our lab, SAM disulfate tosylate was purchased from Ark Pharm. Isothermal Titration Calorimetry was performed with a Nano ITC (TA instrument) at 25 °C. For ligand MS023, the cell was loaded with 21.2  $\mu$ M PRMT6 in the presence of 100  $\mu$ M SAM and 1% DMSO in 50 mM  $\text{NaH}_2\text{PO}_4$  (adjust pH to 7.5 by NaOH), 100 mM NaCl. The syringe was loaded with 200  $\mu$ M MS023, 100  $\mu$ M SAM, 1% DMSO in the same buffer. For ligand MS023-CC-F, cell was loaded with 20  $\mu$ M PRMT6, 100  $\mu$ M SAM, 2% DMSO in the buffer mentioning above and the syringe was loaded with 200  $\mu$ M MS023-CC-F, 100  $\mu$ M SAM, 2% DMSO in the same buffer. 2.5  $\mu$ L was injected for 20 times with an interval of 200 seconds. The data was fitted by Nano Analysis software supplied by TA instrument with independent one-binding site model.

**A.14 Fluorescence polarization binding assay.** FP binding was performed half-area low-binding black 96-well (Corning 3993). 80  $\mu$ L of PRMT6 by 2-fold dilution from final

concentration 10  $\mu$ M to 0.3  $\mu$ M in assay buffer (50 mM  $\text{NaH}_2\text{PO}_4$ , adjust pH to 7.5 by NaOH + 0.001% Tween) were added to each well. Then 20  $\mu$ L of MS023-CC-F (50 nM in assay buffer, making final concentration to 10 nM) were added to each buffer. Wells containing protein only were subtracted from assay wells as background. Plates were incubated at room temperature for 1 hour before reading. Each well was read 3 times.

## References

- 1 Copeland, R. A., Solomon, M. E. & Richon, V. M. Protein methyltransferases as a target class for drug discovery. *Nat. Rev. Drug Discov.* **8**, 724-732, doi:10.1038/nrd2974 (2009).
- 2 Trerotola, M., Relli, V., Simeone, P. & Alberti, S. Epigenetic inheritance and the missing heritability. *Hum. Genomics* **9**, 17, doi:10.1186/s40246-015-0041-3 (2015).
- 3 Waddington, C. H. The Epigenotype. *Endeavour*, 18-20 (1942).
- 4 Tough, D. F., Lewis, H. D., Rioja, I., Lindon, M. J. & Prinjha, R. K. Epigenetic pathway targets for the treatment of disease: accelerating progress in the development of pharmacological tools: IUPHAR Review 11. *Br. J. Pharmacol.* **171**, 4981-5010, doi:10.1111/bph.12848 (2014).
- 5 Arrowsmith, C. H., Bountra, C., Fish, P. V., Lee, K. & Schapira, M. Epigenetic protein families: a new frontier for drug discovery. *Nat. Rev. Drug Discov.* **11**, 384-400, doi:10.1038/nrd3674 (2012).
- 6 Yun, M., Wu, J., Workman, J. L. & Li, B. Readers of histone modifications. *Cell Res.* **21**, 564-578, doi:10.1038/cr.2011.42 (2011).
- 7 Luger, K., Mader, A. W., Richmond, R. K., Sargent, D. F. & Richmond, T. J. Crystal structure of the nucleosome core particle at 2.8 Å resolution. *Nature* **389**, 251 - 260 (1997).
- 8 Cedar, H. DNA methylation and gene activity. *Cell* **53**, 3-4 (1988).
- 9 Geula, S. *et al.* Stem cells. m6A mRNA methylation facilitates resolution of naive pluripotency toward differentiation. *Science* **347**, 1002-1006, doi:10.1126/science.1261417 (2015).
- 10 Strahl, B. D. & Allis, C. D. The language of covalent histone modifications. *Nature* **403**, 41-45, doi:10.1038/47412 (2000).
- 11 Tan, M. *et al.* Identification of 67 histone marks and histone lysine crotonylation as a new type of histone modification. *Cell* **146**, 1016-1028 (2011).

- 12 Huynh, J. L. & Casaccia, P. Epigenetic mechanisms in multiple sclerosis: implications for pathogenesis and treatment. *Lancet Neurol.* **12**, 195-206, doi:10.1016/S1474-4422(12)70309-5 (2013).
- 13 Morera, L., Lubbert, M. & Jung, M. Targeting histone methyltransferases and demethylases in clinical trials for cancer therapy. *Clin. Epigenetics* **8**, 57, doi:10.1186/s13148-016-0223-4 (2016).
- 14 Cuthbert, G. L. *et al.* Histone deimination antagonizes arginine methylation. *Cell* **118**, 545-553, doi:10.1016/j.cell.2004.08.020 (2004).
- 15 Hanahan, D. & Weinberg, R. A. The hallmarks of cancer. *Cell* **100**, 57-70 (2000).
- 16 Kuhn, P. & Xu, W. Protein arginine methyltransferases: nuclear receptor coregulators and beyond. *Prog. Mol. Biol. Transl. Sci.* **87**, 299-342, doi:10.1016/S1877-1173(09)87009-9 (2009).
- 17 Richon, V. M. *et al.* Chemogenetic analysis of human protein methyltransferases. *Chem. Biol. Drug Des.* **78**, 199-210, doi:10.1111/j.1747-0285.2011.01135.x (2011).
- 18 Kaniskan, H. U. *et al.* A potent, selective and cell-active allosteric inhibitor of protein arginine methyltransferase 3 (PRMT3). *Angew. Chem. Int. Edit* **54**, 5166-5170, doi:10.1002/anie.201412154 (2015).
- 19 Troffer-Charlier, N., Cura, V., Hassenboehler, P., Moras, D. & Cavarelli, J. Functional insights from structures of coactivator-associated arginine methyltransferase 1 domains. *EMBO J.* **26**, 4391-4401, doi:10.1038/sj.emboj.7601855 (2007).
- 20 Zhang, X. & Cheng, X. Structure of the predominant protein arginine methyltransferase PRMT1 and analysis of its binding to substrate peptides. *Structure* **11**, 509-520 (2003).
- 21 Schapira, M. & Ferreira de Freitas, R. Structural biology and chemistry of protein arginine methyltransferases. *Med. Chem. Comm.*, doi:10.1039/c4md00269e (2014).
- 22 Mitchell, L. H. *et al.* Aryl pyrazoles as potent inhibitors of arginine methyltransferases: identification of the first PRMT6 tool compound. *ACS Med. Chem. Lett.* **6**, 655-659, doi:10.1021/acsmchemlett.5b00071 (2015).

- 23 Cura, V. *et al.* Structural studies of protein arginine methyltransferase 2 reveal its interactions with potential substrates and inhibitors. *FEBS J.* **284**, 77-96, doi:10.1111/febs.13953 (2017).
- 24 Antonysamy, S. *et al.* Crystal structure of the human PRMT5:MEP50 complex. *Proc. Natl. Acad. Sci. USA* **109**, 17960-17965, doi:10.1073/pnas.1209814109 (2012).
- 25 Hasegawa, M., Toma-Fukai, S., Kim, J. D., Fukamizu, A. & Shimizu, T. Protein arginine methyltransferase 7 has a novel homodimer-like structure formed by tandem repeats. *FEBS Lett.* **588**, 1942-1948 (2014).
- 26 Lee, W. C. *et al.* Protein arginine methyltransferase 8: tetrameric structure and protein substrate specificity. *Biochemistry* **54**, 7514-7523, doi:10.1021/acs.biochem.5b00995 (2015).
- 27 Boriack-Sjodin, P. A. *et al.* Structural insights into ternary complex formation of human CARM1 with various substrates. *ACS Chem. Bio.* **11**, 763-771, doi:10.1021/acscchembio.5b00773 (2016).
- 28 Eram, M. S. *et al.* A potent, selective, and cell-active inhibitor of human type I protein arginine methyltransferases. *ACS Chem. Bio.* **11**, 772-781, doi:10.1021/acscchembio.5b00839 (2016).
- 29 Zhang, R. *et al.* Theoretical insights into catalytic mechanism of protein arginine methyltransferase 1. *Plos One* **8(8)**, e72424 (2013).
- 30 Rust, H. L., Zurita-Lopez, C. I., Clarke, S. & Thompson, P. R. Mechanistic studies on transcriptional coactivator protein arginine methyltransferase 1. *Biochemistry* **50**, 3332-3345, doi:10.1021/bi102022e (2011).
- 31 Obiany, O., Osborne, T. C. & Thompson, P. R. Kinetic mechanism of protein arginine methyltransferase 1. *Biochemistry* **47**, 10420-10427, doi:Doi 10.1021/Bi800904m (2008).
- 32 Wang, M., Xu, R. M. & Thompson, P. R. Substrate specificity, processivity, and kinetic mechanism of protein arginine methyltransferase 5. *Biochemistry* **52**, 5430-5440, doi:10.1021/bi4005123 (2013).
- 33 Obiany, O. & Thompson, P. R. Kinetic mechanism of protein arginine methyltransferase 6 (PRMT6). *J. Biol. Chem.* **287**, 6062-6071, doi:10.1074/jbc.M111.333609 (2012).

- 34 Yue, W. W., Hassler, M., Roe, S. M., Thompson-Vale, V. & Pearl, L. H. Insights into histone code syntax from structural and biochemical studies of CARM1 methyltransferase. *EMBO J.* **26**, 4402-4412, doi:DOI 10.1038/sj.emboj.7601856 (2007).
- 35 Gui, S. *et al.* Substrate-induced control of product formation by protein arginine methyltransferase 1. *Biochemistry* **52**, 199-209, doi:10.1021/bi301283t (2013).
- 36 Yang, Y. & Bedford, M. T. Protein arginine methyltransferases and cancer. *Nat. Rev. Cancer* **13**, 37-50, doi:10.1038/nrc3409 (2013).
- 37 Lin, Y. L. *et al.* The critical role of protein arginine methyltransferase prmt8 in zebrafish embryonic and neural development is non-redundant with its paralogue prmt1. *Plos One* **8**, e55221 (2013).
- 38 Lee, Y. H. *et al.* Protein arginine methyltransferase 6 regulates embryonic stem cell identity. *Stem Cells Dev.* **21**, 2613-2622, doi:10.1089/scd.2011.0330 (2012).
- 39 Wei, H., Mundade, R., Lange, K. C. & Lu, T. Protein arginine methylation of non-histone proteins and its role in diseases. *Cell Cycle* **13**, 32-41, doi:10.4161/cc.27353 (2014).
- 40 Boulanger, M. C. *et al.* Methylation of Tat by PRMT6 regulates human immunodeficiency virus type 1 gene expression. *J. Virol.* **79**, 124-131, doi:10.1128/JVI.79.1.124-131.2005 (2005).
- 41 Krause, C. D. *et al.* Protein arginine methyltransferases: Evolution and assessment of their pharmacological and therapeutic potential. *Pharmacol. Ther.* **113**, 50-87, doi:DOI 10.1016/j.pharmthera.2006.06.007 (2007).
- 42 Mathioudaki, K. *et al.* Clinical evaluation of PRMT1 gene expression in breast cancer. *Tumor Biol.* **32**, 575-582, doi:10.1007/s13277-010-0153-2 (2011).
- 43 Zhong, J. *et al.* Identification and expression analysis of a novel transcript of the human PRMT2 gene resulted from alternative polyadenylation in breast cancer. *Gene* **487**, 1-9, doi:10.1016/j.gene.2011.06.022 (2011).
- 44 Singh, V. *et al.* DAL-1/4.1B tumor suppressor interacts with protein arginine N-methyltransferase 3 (PRMT3) and inhibits its ability to methylate substrates in vitro and in vivo. *Oncogene* **23**, 7761-7771, doi:DOI 10.1038/sj.onc.1208057 (2004).

- 45 Heller, G. *et al.* Downregulation of TSLC1 and DAL-1 expression occurs frequently in breast cancer. *Breast Cancer Res. Treat.* **103**, 283-291, doi:10.1007/s10549-006-9377-7 (2007).
- 46 Al-Dhaheeri, M. *et al.* CARM1 is an important determinant of ER $\alpha$ -dependent breast cancer cell differentiation and proliferation in breast cancer cells. *Cancer Res.* **71**, 2118-2128 (2011).
- 47 Sun, Y., Chung, H. H., Woo, A. R. & Lin, V. C. Protein arginine methyltransferase 6 enhances ligand-dependent and -independent activity of estrogen receptor  $\alpha$  via distinct mechanisms. *Biochim. Biophys. Acta* **1843**, 2067-2078, doi:10.1016/j.bbamcr.2014.04.008 (2014).
- 48 Thomassen, M., Tan, Q. & Kruse, T. A. Gene expression meta-analysis identifies chromosomal regions and candidate genes involved in breast cancer metastasis. *Breast Cancer Res. Treat.* **113**, 239-249, doi:10.1007/s10549-008-9927-2 (2009).
- 49 Seligson, D. B. *et al.* Global histone modification patterns predict risk of prostate cancer recurrence. *Nature* **435**, 1262-1266, doi:10.1038/nature03672 (2005).
- 50 Majumder, S., Liu, Y., Ford, O. H., 3rd, Mohler, J. L. & Whang, Y. E. Involvement of arginine methyltransferase CARM1 in androgen receptor function and prostate cancer cell viability. *Prostate* **66**, 1292-1301, doi:10.1002/pros.20438 (2006).
- 51 Hong, H. *et al.* Aberrant expression of CARM1, a transcriptional coactivator of androgen receptor, in the development of prostate carcinoma and androgen-independent status. *Cancer* **101**, 83-89, doi:10.1002/cncr.20327 (2004).
- 52 Kim, Y. R. *et al.* Differential CARM1 expression in prostate and colorectal cancers. *BMC Cancer* **10**, 197, doi:10.1186/1471-2407-10-197 (2010).
- 53 Almeida-Rios, D. *et al.* Histone methyltransferase PRMT6 plays an oncogenic role of in prostate cancer. *Oncotarget* **7**, 53018-53028, doi:10.18632/oncotarget.10061 (2016).
- 54 Cha, B. *et al.* Methylation by protein arginine methyltransferase 1 increases stability of Axin, a negative regulator of Wnt signaling. *Oncogene* **30**, 2379-2389, doi:10.1038/onc.2010.610 (2011).
- 55 Ou, C. Y. *et al.* A coactivator role of CARM1 in the dysregulation of  $\beta$ -catenin activity in colorectal cancer cell growth and gene expression. *Mol. Cancer Res.* **9**, 660-670, doi:10.1158/1541-7786.MCR-10-0223 (2011).

- 56 Zhang, B. *et al.* Targeting protein arginine methyltransferase 5 inhibits colorectal cancer growth by decreasing arginine methylation of eIF4E and FGFR3. *Oncotarget* **6**, 22799-22811, doi:10.18632/oncotarget.4332 (2015).
- 57 Yoshimatsu, M. *et al.* Dysregulation of PRMT1 and PRMT6, type I arginine methyltransferases, is involved in various types of human cancers. *Int. J. Cancer* **128**, 562-573, doi:10.1002/ijc.25366 (2011).
- 58 Elakoum, R. *et al.* CARM1 and PRMT1 are dysregulated in lung cancer without hierarchical features. *Biochimie* **97**, 210-218 (2014).
- 59 Gu, Z. *et al.* Protein arginine methyltransferase 5 is essential for growth of lung cancer cells. *Biochem. J.* **446**, 235-241 (2012).
- 60 Cheung, N. *et al.* Targeting aberrant epigenetic networks mediated by PRMT1 and KDM4C in acute myeloid leukemia. *Cancer Cell* **29**, 32-48, doi:10.1016/j.ccell.2015.12.007 (2016).
- 61 Lui, W. C., Chan, Y. F. & Ng, R. PRMT1 activates leukemic stem cell program in MLL-rearranged leukemia. *Blood* **124**, 3493 (2014).
- 62 Jin, Y. *et al.* Targeting methyltransferase PRMT5 eliminates leukemia stem cells in chronic myelogenous leukemia. *J. Clin. Invest.* **126**, 3961-3980, doi:10.1172/JCI85239 (2016).
- 63 Wang, L., Pal, S. & Sif, S. Protein arginine methyltransferase 5 suppresses the transcription of the RB family of tumor suppressors in leukemia and lymphoma cells. *Mol. Cell. Biol.* **28**, 6262-6277, doi:10.1128/MCB.00923-08 (2008).
- 64 Pal, S. *et al.* Low levels of miR-92b/96 induce PRMT5 translation and H3R8/H4R3 methylation in mantle cell lymphoma. *EMBO J.* **26**, 3558-3569, doi:10.1038/sj.emboj.7601794 (2007).
- 65 Hu, H., Qian, K., Ho, M. C. & Zheng, Y. G. Small molecule inhibitors of protein arginine methyltransferases. *Expert Opin. Inv. Drug* **25**, 335-358, doi:10.1517/13543784.2016.1144747 (2016).
- 66 Vedel, M., Lawrence, F., Robert-Gero, M. & Lederer, E. The antifungal antibiotic sinefungin as a very active inhibitor of methyltransferases and of the transformation of chick embryo fibroblasts by rous sarcoma virus. *Biochem. Biophys. Res. Commun.* **85**, 371-376 (1978).

- 67 Kubicek, S. *et al.* Reversal of H3K9me2 by a small-molecule inhibitor for the G9a histone methyltransferase. *Mol. Cell* **25**, 473-481, doi:10.1016/j.molcel.2007.01.017 (2007).
- 68 Ferreira de Freitas, R. *et al.* Discovery of a potent class I protein arginine methyltransferase fragment inhibitor. *J. Med. Chem.* **59**, 1176-1183, doi:10.1021/acs.jmedchem.5b01772 (2016).
- 69 Smil, D. *et al.* Discovery of a dual PRMT5-PRMT7 inhibitor. *ACS Med. Chem. Lett.* **6**, 408-412, doi:10.1021/ml500467h (2015).
- 70 Cheng, D. *et al.* Small molecule regulators of protein arginine methyltransferases. *J. Biol. Chem.* **279**, 23892-23899, doi:10.1074/jbc.M401853200 (2004).
- 71 Feng, Y., Li, M., Wang, B. & Zheng, Y. G. Discovery and mechanistic study of a class of protein arginine methylation inhibitors. *J. Med. Chem.* **53**, 6028-6039, doi:10.1021/jm100416n (2010).
- 72 Spannhoff, A. *et al.* A novel arginine methyltransferase inhibitor with cellular activity. *Bioorg. Med. Chem. Lett.* **17**, 4150-4153, doi:10.1016/j.bmcl.2007.05.088 (2007).
- 73 Sinha, S. H. *et al.* Synthesis and evaluation of carbocyanine dyes as PRMT inhibitors and imaging agents. *Eur. J. Med. Chem.* **54**, 647-659 (2012).
- 74 Hu, H. *et al.* Exploration of cyanine compounds as selective inhibitors of protein arginine methyltransferases: synthesis and biological evaluation. *J. Med. Chem.* **58**, 1228-1243 (2015).
- 75 Spannhoff, A. *et al.* Target-based approach to inhibitors of histone arginine methyltransferases. *J. Med. Chem.* **50**, 2319-2325, doi:10.1021/jm061250e (2007).
- 76 Yu, X. R. *et al.* Discovery and structure-activity analysis of 4-((5-nitropyrimidin-4-yl)amino)benzimidamide derivatives as novel protein arginine methyltransferase 1 (PRMT1) inhibitors. *Bioorg. Med. Chem. Lett.* **25**, 5449-5453 (2015).
- 77 Yan, L. *et al.* Diamidine compounds for selective inhibition of protein arginine methyltransferase 1. *J. Med. Chem.* **57**, 2611-2622, doi:10.1021/jm401884z (2014).
- 78 Xie, Y. *et al.* Virtual screening and biological evaluation of novel small molecular inhibitors against protein arginine methyltransferase 1 (PRMT1). *Org. Biomol. Chem.* **12**, 9665-9673, doi:10.1039/c4ob01591f (2014).

- 79 Chan-Penebre, E. *et al.* A selective inhibitor of PRMT5 with in vivo and in vitro potency in MCL models. *Nat. Chem. Biol.* **11**, 432-437, doi:10.1038/nchembio.1810 (2015).
- 80 Lavogina, D., Enkvist, E. & Uri, A. Bisubstrate inhibitors of protein kinases: from principle to practical applications. *ChemMedChem* **5**, 23-34, doi:10.1002/cmdc.200900252 (2010).
- 81 Xu, W. Q. *et al.* Quantitative analysis of histone demethylase probes using fluorescence polarization. *J. Med. Chem.* **56**, 5198-5202, doi:Doi 10.1021/Jm3018628 (2013).
- 82 Dowden, J., Hong, W., Parry, R. V., Pike, R. A. & Ward, S. G. Toward the development of potent and selective bisubstrate inhibitors of protein arginine methyltransferases. *Bioorg. Med. Chem. Lett.* **20**, 2103-2105, doi:10.1016/j.bmcl.2010.02.069 (2010).
- 83 Dowden, J. *et al.* Small molecule inhibitors that discriminate between protein arginine N-methyltransferases PRMT1 and CARM1. *Org. Biomol. Chem.* **9**, 7814-7821 (2011).
- 84 van Haren, M., van Ufford, L. Q., Moret, E. E. & Martin, N. I. Synthesis and evaluation of protein arginine N-methyltransferase inhibitors designed to simultaneously occupy both substrate binding sites. *Org. Biomol. Chem.* **13**, 549-560, doi:10.1039/c4ob01734j (2015).
- 85 Chen, D. *et al.* Regulation of transcription by a protein methyltransferase. *Science* **284**, 2174-2177 (1999).
- 86 Bedford, M. T. Arginine methylation at a glance. *J. Cell Sci.* **120**, 4243-4246, doi:10.1242/jcs.019885 (2007).
- 87 El Messaoudi, S. *et al.* Coactivator-associated arginine methyltransferase 1 (CARM1) is a positive regulator of the Cyclin E1 gene. *Proc. Natl. Acad. Sci. USA* **103**, 13351-13356, doi:DOI 10.1073/pnas.0605692103 (2006).
- 88 Ma, H. *et al.* Hormone-dependent, CARM1-directed, arginine-specific methylation of histone H3 on a steroid-regulated promoter. *Curr. Biol.* **11**, 1981-1985 (2001).

- 89 Bauer, U. M., Daujat, S., Nielsen, S. J., Nightingale, K. & Kouzarides, T. Methylation at arginine 17 of histone H3 is linked to gene activation. *EMBO Rep.* **3**, 39-44, doi:DOI 10.1093/embo-reports/kvf013 (2002).
- 90 Covic, M. *et al.* Arginine methyltransferase CARM1 is a promoter- specific regulator of NF- $\kappa$ B-dependent gene expression. *EMBO J.* **24**, 85-96, doi:10.1038/ (2005).
- 91 An, W., Kim, J. & Roeder, R. G. Ordered cooperative functions of PRMT1, p300, and CARM1 in transcriptional activation by p53. *Cell* **117**, 735-748, doi:10.1016/j.cell.2004.05.009 (2004).
- 92 Xu, W. *et al.* A transcriptional switch mediated by cofactor methylation. *Science* **294**, 2507-2511, doi:10.1126/science.1065961 (2001).
- 93 Lee, Y. H. & Stallcup, M. R. Roles of protein arginine methylation in DNA damage signaling pathways is CARM1 a life-or-death decision point? *Cell Cycle* **10**, 1343-1344, doi:10.4161/cc.10.9.15379 (2011).
- 94 Lee, J. & Bedford, M. T. PABP1 identified as substrate of CARM1 using array. *EMBO Rep.* (2001).
- 95 Li, H. *et al.* Lipopolysaccharide-induced methylation of HuR, an mRNA-stabilizing protein, by CARM1. Coactivator-associated arginine methyltransferase. *J. Biol. Chem.* **277**, 44623-44630, doi:10.1074/jbc.M206187200 (2002).
- 96 Fujiwara, T. *et al.* CARM1 regulates proliferation of PC12 cells by methylating HuD. *Mol. Cell. Biol.* **26**, 2273-2285, doi:10.1128/MCB.26.6.2273-2285.2006 (2006).
- 97 Cheng, D., Cote, J., Shaaban, S. & Bedford, M. T. The arginine methyltransferase CARM1 regulates the coupling of transcription and mRNA processing. *Mol. Cell* **25**, 71-83, doi:10.1016/j.molcel.2006.11.019 (2007).
- 98 Sims, R. J. The C-terminal domain of RNA polymerase II is modified by site-specific methylation. *Science* **332**, 99-103 (2011).
- 99 Chen, S. L., Loffler, K. A., Chen, D. G., Stallcup, M. R. & Muscat, G. E. O. The coactivator-associated arginine methyltransferase is necessary for muscle differentiation - CARM1 coactivates myocyte enhancer factor-2. *J. Biol. Chem.* **277**, 4324-4333, doi:DOI 10.1074/jbc.M109835200 (2002).

- 100 Frieze, S., Lupien, M., Silver, P. A. & Brown, M. CARM1 regulates estrogen-stimulated breast cancer growth through up-regulation of E2F1. *Cancer Res.* **68**, 301-306, doi:Doi 10.1158/0008-5472.Can-07-1983 (2008).
- 101 Purandare, A. V. *et al.* Pyrazole inhibitors of coactivator associated arginine methyltransferase 1 (CARM1). *Bioorg. Med. Chem. Lett.* **18**, 4438-4441, doi:10.1016/j.bmcl.2008.06.026 (2008).
- 102 Huynh, T. *et al.* Optimization of pyrazole inhibitors of coactivator associated arginine methyltransferase 1 (CARM1). *Bioorg. Med. Chem. Lett.* **19**, 2924-2927, doi:10.1016/j.bmcl.2009.04.075 (2009).
- 103 Allan, M. *et al.* N-Benzyl-1-heteroaryl-3-(trifluoromethyl)-1H-pyrazole-5-carboxamides as inhibitors of co-activator associated arginine methyltransferase 1 (CARM1). *Bioorg. Med. Chem. Lett.* **19**, 1218-1223, doi:DOI 10.1016/j.bmcl.2008.12.075 (2009).
- 104 Therrien, E. *et al.* 1,2-Diamines as inhibitors of co-activator associated arginine methyltransferase 1 (CARM1). *Bioorg. Med. Chem. Lett.* **19**, 6725-6732 (2009).
- 105 Wan, H. *et al.* Benzo[d]imidazole inhibitors of coactivator associated arginine methyltransferase 1 (CARM1)--hit to lead studies. *Bioorg. Med. Chem. Lett.* **19**, 5063-5066, doi:10.1016/j.bmcl.2009.07.040 (2009).
- 106 Selvi, B. R. *et al.* Identification of a novel inhibitor of coactivator-associated arginine methyltransferase 1 (CARM1)-mediated methylation of histone H3 Arg-17. *J. Biol. Chem.* **285**, 7143-7152, doi:10.1074/jbc.M109.063933 (2010).
- 107 Cheng, D. H. *et al.* Novel 3,5-bis(bromohydroxybenzylidene)piperidin-4-ones as coactivator-associated arginine methyltransferase 1 Inhibitors: enzyme selectivity and cellular activity. *J. Med. Chem.* **54**, 4928-4932, doi:Doi 10.1021/Jm200453n (2011).
- 108 Sack, J. S. *et al.* Structural basis for CARM1 inhibition by indole and pyrazole inhibitors. *Biochem. J.* **436**, 331-339, doi:10.1042/BJ20102161 (2011).
- 109 Ferreira de Freitas, R. *et al.* Discovery of a potent and selective coactivator associated arginine methyltransferase 1 (CARM1) inhibitor by virtual screening. *J. Med. Chem.* **59**, 6838-6847, doi:10.1021/acs.jmedchem.6b00668 (2016).

- 110 Kaniskan, H. U. *et al.* Design and synthesis of selective, small molecule inhibitors of coactivator-associated arginine methyltransferase 1 (CARM1). *Med. Chem. Comm.* **7**, 1793-1796, doi:10.1039/C6MD00342G (2016).
- 111 Lee, J. & Bedford, M. T. PABP1 identified as an arginine methyltransferase substrate using high-density protein arrays. *EMBO Reports* **3**, 268-273, doi:10.1093/embo-reports/kvf052 (2002).
- 112 Zambon, C. F. *et al.* Effectiveness of the combined evaluation of KLK3 genetics and free-to-total prostate specific antigen ratio for prostate cancer diagnosis. *J. Urol.* **188**, 1124-1130, doi:10.1016/j.juro.2012.06.030 (2012).
- 113 Kohli, M. *et al.* Exploratory study of a KLK2 polymorphism as a prognostic marker in prostate cancer. *Cancer Biomarkers* **7**, 101-108 (2010).
- 114 Clevers, H. & Nusse, R. Wnt/ $\beta$ -catenin signaling and disease. *Cell* **149**, 1192-1205, doi:10.1016/j.cell.2012.05.012 (2012).
- 115 Gao, W. W. *et al.* Arginine methylation of HSP70 regulates retinoid acid-mediated RARbeta2 gene activation. *Proc. Natl. Acad. Sci. USA* **112**, E3327-3336, doi:10.1073/pnas.1509658112 (2015).
- 116 Wang, L. *et al.* CARM1 methylates chromatin remodeling factor BAF155 to enhance tumor progression and metastasis. *Cancer Cell* **25**, 21-36, doi:10.1016/j.ccr.2013.12.007 (2014).
- 117 Virshup, A. M., Contreras-García, J., Wipf, P., Yang, W. & Beratan, D. N. Stochastic voyages into uncharted chemical space produce a representative library of all possible drug-like compounds. *J. Am. Chem. Soc.* **135**, 7296-7303 (2013).
- 118 Rupakheti, C., Virshup, A., Yang, W. & Beratan, D. N. Strategy to discover diverse optimal molecules in the small molecule universe. *J. Chem. Inf. Model.* **55**, 529-537, doi:10.1021/ci500749q (2015).
- 119 Kleinschmidt, M. A., de Graaf, P., van Teeffelen, H. A. A. M. & Timmers, H. T. M. Cell cycle regulation by the PRMT6 arginine methyltransferase through repression of cyclin-dependent kinase inhibitors. *Plos One* **7**, doi:ARTN e4144610.1371/journal.pone.0041446 (2012).

- 120 Harrison, M. J., Tang, Y. H. & Dowhan, D. H. Protein arginine methyltransferase 6 regulates multiple aspects of gene expression. *Nucleic Acids Res.* **38**, 2201-2216, doi:10.1093/nar/gkp1203 (2010).
- 121 Guccione, E. *et al.* Methylation of histone H3R2 by PRMT6 and H3K4 by an MLL complex are mutually exclusive. *Nature* **449**, 933-937, doi:10.1038/nature06166 (2007).
- 122 El-Andaloussi, N. *et al.* Arginine methylation regulates DNA polymerase beta. *Mol. Cell* **22**, 51-62, doi:10.1016/j.molcel.2006.02.013 (2006).
- 123 Limm, K. *et al.* Deregulation of protein methylation in melanoma. *Eur. J. Cancer* **49**, 1305-1313, doi:10.1016/j.ejca.2012.11.026 (2013).
- 124 Stein, C., Riedl, S., Ruthnick, D., Notzold, R. R. & Bauer, U. M. The arginine methyltransferase PRMT6 regulates cell proliferation and senescence through transcriptional repression of tumor suppressor genes. *Nucleic Acids Res.* **40**, 9522-9533, doi:10.1093/nar/gks767 (2012).
- 125 Shen, Y. *et al.* Discovery of a potent, selective, and cell-active dual inhibitor of protein arginine methyltransferase 4 and protein arginine methyltransferase 6. *J. Med. Chem.* **59**, 9124-9139, doi:10.1021/acs.jmedchem.6b01033 (2016).
- 126 Nakakido, M. *et al.* PRMT6 increases cytoplasmic localization of p21CDKN1A in cancer cells through arginine methylation and makes more resistant to cytotoxic agents. *Oncotarget* **6**, 30957-30967, doi:10.18632/oncotarget.5143 (2015).
- 127 Phalke, S. *et al.* p53-Independent regulation of p21Waf1/Cip1 expression and senescence by PRMT6. *Nucleic Acids Res.* **40**, 9534-9542, doi:10.1093/nar/gks858 (2012).
- 128 Rossi, A. M. & Taylor, C. W. Analysis of protein-ligand interactions by fluorescence polarization. *Nat. Protoc.* **6**, 365-387, doi:10.1038/nprot.2011.305 (2011).
- 129 Lea, W. A. & Simeonov, A. Fluorescence polarization assays in small molecule screening. *Expert Opin. Drug Discov.* **6**, 17-32, doi:10.1517/17460441.2011.537322 (2011).
- 130 Perrin, F. The polarisation of fluorescence light. Average life of molecules in their excited state. *J. Phys.*, 390-401 (1926).

- 131 Weber, G. Polarization of the fluorescence of macromolecules. *Biochem. J.*, 145-167 (1952).
- 132 Hall, M. D. *et al.* Fluorescence polarization assays in high-throughput screening and drug discovery: a review. *Methods Appl. Fluoresc.* **4**, 022001, doi:10.1088/2050-6120/4/2/022001 (2016).
- 133 Zeng, H. & Xu, W. in *Epigenetic Technological Applications* (ed Yujun George Zheng) (Elsevier Inc, 2015).
- 134 Eglen, R. M. *et al.* The use of AlphaScreen rechnology in HTS: current status. *Curr. Chem. Genomics* **1**, 2 - 10 (2008).
- 135 Hendricks, C. L., Ross, J. R., Pichersky, E., Noel, J. P. & Zhou, Z. S. An enzyme-coupled colorimetric assay for S-adenosylmethionine-dependent methyltransferases. *Anal. Biochem.* **326**, 100-105, doi:10.1016/j.ab.2003.11.014 (2004).
- 136 Liu, F. *et al.* Discovery of a 2,4-diamino-7-aminoalkoxyquinazoline as a potent and selective inhibitor of histone lysine methyltransferase G9a. *J. Med. Chem.* **52**, 7950-7953, doi:10.1021/jm901543m (2009).
- 137 Feng, Y., Xie, N., Wu, J., Yang, C. & Zheng, Y. G. Inhibitory study of protein arginine methyltransferase 1 using a fluorescent approach. *Biochem. Biophys. Res. Commun.* **379**, 567-572, doi:10.1016/j.bbrc.2008.12.119 (2009).
- 138 Graves, T. L., Zhang, Y. & Scott, J. E. A universal competitive fluorescence polarization activity assay for S-adenosylmethionine utilizing methyltransferases. *Anal. Biochem.* **373**, 296-306, doi:10.1016/j.ab.2007.09.025 (2008).
- 139 Marholz, L. J., Wang, W., Zheng, Y. & Wang, X. A fluorescence polarization biophysical assay for the naegleria DNA hydroxylase Tet1. *ACS Med. Chem. Lett.* **7**, 167-171, doi:10.1021/acsmchemlett.5b00366 (2016).
- 140 Mazitschek, R., Patel, V., Wirth, D. F. & Clardy, J. Development of a fluorescence polarization based assay for histone deacetylase ligand discovery. *Bioorg. Med. Chem. Lett.* **18**, 2809-2812, doi:10.1016/j.bmcl.2008.04.007 (2008).
- 141 Dillon, M. B. C. *et al.* Novel inhibitors for PRMT1 discovered by high-throughput screening using activity-based fluorescence polarization. *ACS Chem. Bio.* **7**, 1198-1204, doi:10.1021/cb300024c (2012).

- 142 Huang, X. Y. Fluorescence polarization competition assay: The range of resolvable inhibitor potency is limited by the affinity of the fluorescent ligand. *J. Biomol. Screen.* **8**, 34-38, doi:10.1177/1087057102239666 (2003).
- 143 Ou, C. Y., Kim, J. H., Yang, C. K. & Stallcup, M. R. Requirement of cell cycle and apoptosis regulator 1 for target gene activation by Wnt and beta-catenin and for anchorage-independent growth of human colon carcinoma cells. *J. Biol. Chem.* **284**, 20629-20637, doi:10.1074/jbc.M109.014332 (2009).